SIMULTANEOUS PROCESS AND MOLECULAR DESIGN/SELECTION THROUGH PROPERTY INTEGRATION

A Dissertation

by

XIAOYUN QIN

Submitted to the Office of Graduate Studies of
Texas A&M University
in partial fulfillment of the requirements for the degree of

DOCTOR OF PHILOSOPHY

December 2006

Major Subject: Chemical Engineering

SIMULTANEOUS PROCESS AND MOLECULAR DESIGN/SELECTION THROUGH PROPERTY INTEGRATION

A Dissertation

by

XIAOYUN QIN

Submitted to the Office of Graduate Studies of
Texas A&M University
in partial fulfillment of the requirements for the degree of

DOCTOR OF PHILOSOPHY

Approved by:

Chair of Committee, Mahmoud M. El-Halwagi
Committee Members, M. Sam Mannan
John T. Baldwin
Bruce McCarl
Head of Department, Nagamangala K. Anand

December 2006

Major Subject: Chemical Engineering

ABSTRACT

Simultaneous Process and Molecular Design/Selection
Through Property Integration. (December 2006)
Xiaoyun Qin, B.S., Nanjing University of Science and Technology;
M.S., Chinese Academy of Forestry Science
Chair of Advisory Committee: Dr. Mahmoud M. El-Halwagi

The overall purpose of this work is to develop systematic methodology for the simultaneous design and selection of processes and molecules (materials). A property-based approach is used to develop an interface between process and molecular design/selection. In particular, we focus on the problem of designing/selecting materials that are used in the context of a recycle/reuse system of process streams and for energy applications. Fresh and recycled resources (e.g., process streams, biomass, solvents, etc.) are integrated with the process to satisfy property-based constraints for the process units and to optimize the usage of the resources and the design of the process. For molecular design, property operators for mixing streams and group contribution methods (GCM) are used to consistently represent process sources, sinks, and different functional groups on the same property-base. For material selection, property based criteria (e.g., heat rate, high heating value, etc.) are used to bridge the process with material. This consistent representation enables the definition of the optimization problem formulation for product design while taking into consideration the recycle/reuse of process streams. In particular, this dissertation addresses four integrated topics. First, a new graphical approach for material targeting and substitution is presented. This graphical approach offers initial solutions and valuable insights that can be effectively used for conceptual design and for initializing mathematical programming techniques. Second, a mathematical optimization approach is developed along with a decomposition-based global solution procedure for material targeting and substitution using property integration. Third, an implementation approach is developed to synthesize the details of a recycle/reuse process network design

based on the targets identified through the graphical and/or the mathematical approaches. Finally, property integration techniques are extended to a broader scope which deals with the lifecycle analysis of biomass utilization for energy generation. A generic model is developed to optimize the types and quantities of the feedstocks used to optimize power generation with biomass-fossil fuel co-fed system. Important issues of biomass growth, harvesting, transportation, processing, and disposal are included. Property-based tracking and constraints are included in the analysis. Also, the issues associated with greenhouse gas (GHG) emissions are incorporated in the analysis. Case studies are solved throughout the dissertation to demonstrate the applicability of the developed procedures.

ACKNOWLEDGMENTS

I would like to express my sincere thanks to a number of people who have been and will continue to be the source of my knowledge and success. First, I am very grateful to Dr. Mahmoud El-Halwagi, my advisor, who has been the beacon light that guided and supported me throughout my graduate studies. His professional experience, profound knowledge, and noble character always inspire and help me to pursue my goal.

I wish to express my gratitude to Dr. Bruce McCarl whose invaluable advice and insightful suggestions have brought me great strength in understanding and analysis in this new area of research. I wish to thank Dr. Mannan whose advice and help have been priceless to my research. I wish to thank Dr. Baldwin whose experience and knowledge have greatly helped my study and research.

I wish to thank all the members of my group for their constant cooperation and support. I would like to especially thank Dr. Gerald Cornforth, Ben, Abdullah, Nasser, Vasiliki and Daniel who have helped me better understand many things.

I am thankful to the US Department of Energy and the US Department of Agriculture and the National Resources Conservation Service for funding my research.

Above all, I am deeply indebted to my parents, Qin Jinfu and Xiao Xuezhu, my wife, Wang Yu, and my son, Qin Jiasheng for their encouragement, support and inspiration. With their endless love and support, I can continue to pursue my dreams and achieve success.

TABLE OF CONTENTS

CHAPTER Page

LIST OF FIGURES

FIGURE Page

LIST OF TABLES

NOMENCLATURE

AT	Algebraic techniques
C	Cost in economical evaluation or symbol of carbon atom
$C1$	Group contribution of first order group
$C2$	Group contribution of second order group
$C3$	Group contribution of third order group
C_g	Group contribution of group g
CAMD	Computer-aided molecular design
CAP	Effective power generator capacity
CO_2-Eq.	Carbon dioxide equivalent
d	Characteristic value in Eq. (3.30)
DEG	Diethylene glycol
DGA	Diglycolamine
E	Emission
F	Process source flowrate
f	fresh source index
$f_{i,j}$	flowrate of source i entering sink j
Fr	Fresh source flowrate
G	Sink flowrate
g'	Index of first order group
g''	Index of second order group
g'''	Index of third order group
GT	Graphical techniques
GCM	Group contribution method
genN	N^{th} power generator
GHG	Greenhouse gas
HHV	High heating value
H_{fus}	Heat of fusion

H_v	Heat of vaporization
i	Source index or generator index in Chapter V
IPCC	Intergovernmental Panel on Climate Change
j	Sink index or month index in Chapter V
k	Property index or the feedstock index in Chapter V
l	Index of position in a molecule or low limit
L	Distance
MEA	Monoethanolamine
MDEA	Methyldiethanolamine
MINLP	Mixed integer nonlinear programming
MILP	Mixed integer linear programming
MPT	Mathematical programming techniques
m	Number of sources or mass quantity in Chapter V
M	Mass quantity in Table 5.4
Max	Maximum
Min	Minimum
m_{LAS}	Last active source
m_{proxy}	Proxy source
n	number of sinks
$N1$	Occurrence of first order group in a molecule
$N2$	Occurrence of second order group in a molecule
$N3$	Occurrence of third order group in a molecule
N_g	Occurrence of group g in a molecule
$N_{biomass}$	number of biomass
N_{sinks}	Number of sinks
$N_{sources}$	Number of process sources
p	Property value
P	Parameter in Eq. (4.22) or power generator capacity in Chapter V
QBFR	Quasi-boundaries of the feasibility region

R	Co-firing ratio
RREF	Reduced row echelon form
sw	Switchgrass
S	Symbol of source
$SINKS$	Set of sinks
$SOURCES$	Set of sources
Su	Supply of feedstock
T_b	Boiling temperature
T_c	Critical temperature
T_m	Melting temperature
u	Upper limit
U	Symbol of sink
w	number of non-zero rows in the RREF
W	Waste flowrate
W_T	Targeted waste discharge
$x_{i,j}$	allocation fraction of source i entering sink j
Y	Yield
z	Dominant property (concentration) in Chapter IV
z''	Binary weight factor for second order group
z'''	Binary weight factor for third order group
$\phi(p)$	Group contribution function of property p
η	Thermal efficiency
υ	Valency of the first order group
$\psi(p)$	Property operator of property p

CHAPTER I
INTRODUCTION

Processing operations feature the use of enormous amounts of material resources. Consequently, process design received extensive studies over the last two decades in order to develop cost-effective and pollution-mitigated processes. Material (molecular) design and selection are important activities in optimizing the performance of processing facilities. Hence, they have become one of the most important considerations associated with process design. Conventional chemical processes are chemo-centric and component dependent. However, in assessing the performance of a material utility (e.g., a solvent), one should not only rely on its chemical constituents, but rather on their characteristics and effectiveness for the particular system. These characteristics involve a wide variety of properties such as equilibrium distribution coefficient, critical point, volatility, solubility, density, GHG (greenhouse gas) equivalence, heat of combustion, etc. Since properties form the basis and constraints of the performance of many units, they can be primarily considered in order to select material, design and optimize a process system. Several papers have addressed the problem of property-based process design using graphical tools that guided the synthesis and analysis tasks (Shelley and El-Halwagi, 2000; El-Halwagi et al., 2004; Kazantzi and El-Halwagi, 2005). Moreover, algebraic techniques were developed and employed for property-based integration of systems with more than three properties of interest (Qin et al., 2004). These process design methodologies have been developed through commitment to the available process and external resources which were selected through material screening. Screening of commonly used and already known products is the prevailing way to select materials for process operation to achieve better process design. This method mainly includes two aspects: determining existing materials that should be used for particular applications and allocating the selected materials to process units to acquire optimal process

---

This dissertation follows the style and format of Chemical Engineering Science.

objectives. Notwithstanding its great impact on process optimization, there are certain limitations with this method. For a given application, there are typically numerous potential candidate materials leading to a selection task that is tedious and expensive. In addition, streams may be mixed in an infinite number of ways, thus increasing the dimensionality of the problem. For each combination of process streams, there is an optimum material utility to be mixed with these streams. Considering all blending possibilities, there are numerous material utilities to be screened before an optimum selection is made. Additionally, screening among existing material could hinder the identification of new material structures and/or material blends that could achieve a better performance of the system, i.e. selection of existing materials can lead to sub-optimal solutions. Therefore, material selection needs to be considered as a task of selecting a set of properties to target a process performance, and has to be addressed simultaneously through synthesis at the material- and systems- level. Thus, there is a need for incorporating proper design criteria and constraints into molecular design and selection. This has to be done while systematically identifying the optimum set of properties and consequently the optimum material (molecular) structures or mixtures. Eden et al., (2002, 2004) and Gani and Pistikopoulos, (2002) employed property models to address simultaneous process and product design problems. However, they only considered screening solvent molecules and not generating them. Furthermore, their analysis was limited to individual-unit performance rather than the network system operation in the chemical process. It is important to examine synthesis aspects at the molecular levels and carry out molecular design at the same time while observing the process system characteristics and performing process design. This will provide useful information about all important features and interactions between process and molecular design. Another important issue in process and material (molecular) design is the need to accurately estimate properties of molecules before conducting expensive experimental activities. In addition, it is not always possible to find experimental data in literature that are needed for identifying potentially new molecules. This literature gap suggests the use of theoretical and computational approaches for property estimation. Based on this

consideration, the group contribution method (GCM) is widely applied in molecular design area, which is also adopted in this work. These limitations will be addressed by this work. The overall objective is to develop systematic and generally applicable procedures for conserving natural resources used in industry. Specifically, process design, molecular (material) design/selection, and scheduling techniques will be developed and used to address the following four integrated topics:

1. A graphical targeting approach for simultaneous molecular and process design: This problem focuses on material recycle/reuse with property constraints. In addition to the process sources, fresh streams may be purchased and used in process units. Molecular design is used to screen potential fresh streams. This graphical approach offers initial solutions and valuable insights that can be effectively used for conceptual design and for initializing mathematical programming techniques.
2. A mathematical programming approach is developed to address the similar but more complicated problem mentioned under the graphical approach. An optimization formulation is developed to embed potential solutions and to select the optimum one. A decomposition approach is used for the global solution procedure for material targeting and substitution using property integration.
3. A network synthesis implementation approach is developed to synthesize the details of a recycle/reuse process network design based on the targets identified through the graphical and/or the mathematical approaches.
4. A holistic approach is developed to analyze biomass-to-energy systems. The property integration techniques are extended to a broader scope which deals with the lifecycle analysis of biomass utilization for energy generation. A generic model is developed to optimize the types and quantities of the feedstocks used to optimize power generation with biomass-fossil fuel co-fed feedstocks. Important issues of biomass growth, harvesting, transportation, processing, and disposal are included. Property-based tracking and constraints

are included in the analysis. Also, the issues associated with greenhouse gas (GHG) emissions are incorporated in the analysis.

CHAPTER II
SIMULTANEOUS PROCESS AND MOLECULAR DESIGN THROUGH PROPERTY INTEGRATION – A GRAPHICAL APPROACH

2.1 Introduction

Molecular design and selection are important activities in optimizing the performance of processing facilities. Numerous contributions have been made in this field. In spite of their great achievements, they have a common limitation: the targeted properties for the molecules are pre-set based on specific requirements of a certain unit. In so doing, conventional molecular design fails to account for the important input resulting from integrating the process. On the other hand, conventional process design is based on the using of existing materials without considering synthesizing new molecules which could lead to suboptimal process design. So it is very desirable for simultaneous process and molecular design.

The objective of simultaneously designing integrated processes and molecules can be greatly facilitated by invoking the recently developed area of property integration and componentless design. Property integration is a "functionality-based, holistic approach to the allocation and manipulation of streams and processing units, which is based on the tracking, adjustment, assignment, and matching of functionalities throughout the process" (El-Halwagi et al., 2004). Since properties (or functionalities) are critical factors in determining performance of many processing units, process design techniques should keep track of the important properties throughout the process. Recent work done by Shelley and El-Halwagi (2000) has shown that it is possible to tailor conserved quantities, called clusters that act as surrogate properties and enable the conserved tracking of functionalities instead of components. With the property-integration framework posing the process design problem in the property domain, there is a natural interface with molecular design which driven by targeted properties.

This chapter introduces a new, process-centered molecular design graphical approach for material substitution through property-based integration and GCM. In this procedure, the process is first optimized using property integration techniques. This optimization leads to obtaining process information that are primarily considered in identifying a set of potential candidate molecules with desired properties and selecting the best molecules among this set. Two process-based attainable regions are obtained by considering certain process objectives and constraints characterizing the process: the improvement region and the feasibility region for molecular design of all candidate molecules with the desired properties. In this particular work, the solvent molecules are chosen to support the recycle/reuse of process streams so as to reduce the waste discharge to a certain desirable extent. Several molecular groups that are of particular utility for a given process (they provide either the required chemistry for the specific performance or the physical characteristics necessary for a certain process task) were considered and graphically represented as unit vectors. The number of occurrences of the groups in the molecule dictates the magnitude of the vector. Through the new "molecular" pinch approach developed in this paper, both the process design and the molecular design problems are represented on the same consistent basis and are solved without iterations.

2.2 Selective Literature Review

In this section, two relevant literature topics are reviewed: group contribution methods (GCMs) and property-based material-recovery pinch analysis. Both topics are key building blocks for the new approach to be developed in this chapter.

2.2.1 Group Contribution Methods

Group contribution methods have been widely used for the quick estimation of properties of pure compounds alone or in conjunction with other computational methods to obtain more accurate predictions of properties (Horvath, 1992; Jensen, 1999; Achenie, et al, 2003). The group contribution method for solvent design was first introduced by

Gani and Brignole (1983), whereas many other methodologies for solvent design (Odele and S. Macchietto, 1993; Pretel et al., 1994; Pistikopoulos and Stefanis, 1998; Giovanoglou et al., 2003; Marcoulaki and Kokossis, 2000) with various applications, polymer design (Derringer and Markham, 1985; Vaidyanathan and El-Halwagi, 1994; Venkatasubramanian et al., 1994), refrigerant design (Joback and Stephanopoulos, 1989; Sahinidis et al., 2003; Lehmann and Maranas, 2004) and the design of environmentally benign species (Hostrup et al., 1999; Buxton et al., 1999) were later found in literature. In all these methodologies, the approaches were driven by formulating and globally solving an optimization-based problem with different optimization methods.

The basic model used in GCM is the one presented by Constantinou and Gani (1994). If C_g is the contribution of the first order group of type g, which occurs N_g times in a compound, and $\phi(p)$ is a simple function of the property p, the property estimation model takes the form of Eq. 2.1.

$$\phi(p) = \sum_g N_g C_g \tag{2.1}$$

The selection of the function $\phi(p)$ depends on the following factors: (1) The function must be additive in the contributions of C_g ; (2) it has to demonstrate the best possible fit of the experimental data; and (3) the expressions should be able to provide sufficient extrapolating behavior and, therefore, a wide range of applicability.

2.2.2 Property-Based Graphical Approach for Waste Reduction

Recently, Kazantzi and El-Halwagi (2005) introduced a property-based material-recovery pinch analysis and rigorous visualization technique for a process with a given number of process sinks and sources. Process sinks require certain flowrate values and impose certain property constraints for their acceptable feed. Each process source has a given flowrate and property value. Kazantzi and El-Halwagi assumed the pre-selection of a single fresh resource with a known property value. The objective was to develop a non-iterative graphical procedure to determine the target for minimum usage of the

fresh, maximum material reuse, and minimum discharge to waste. Consider the property resulting by mixing several sources (Shelley and El-Halwagi, 2000):

$$\overline{F} * \psi(\bar{p}) = \sum_{i}^{N_{sources}} F_i * \psi(p_i) \tag{2.2}$$

where $\psi(p_i)$ is the property mixing operator and $\overline{F}$ is the total flowrate of the mixture which is given by:

$$\overline{F} = \sum_{i}^{N_{sources}} F_i \tag{2.3}$$

Two different categories of fresh feed were considered; in the first one the fresh property corresponds to the minimum property operator value with respect to the process sources, i.e.

$$\psi^{Fresh} \leq \psi_i \tag{2.4a}$$

whereas the second one deals with fresh that has property operator larger than those of the process sources, i.e.

$$\psi^{Fresh} \geq \psi_i \tag{2.4b}$$

For the first case, the sink constraints on properties take the following form:

$$\psi^{Fresh} \leq \psi_j^{in} \leq \psi_j^{\max} \tag{2.5a}$$

whereas for the second case the maximum acceptable feed operator to sink *j* is limited by the fresh operator, i.e:

$$\psi_j^{\min} \leq \psi_j^{in} \leq \psi^{Fresh} \tag{2.5b}$$

The targeting procedure, which is described in detail by Kazantzi and El-Halwagi (2005) involves the following steps. First the maximum value of property operator $\psi_j^{\max}$ for each sink is calculated based on its acceptable range of property (property constraints). Then, a composite curve for the sinks is constructed by plotting the maximum admissible property loads ($G_j * \psi_j^{\max}$) versus their flowrate G_j in ascending order of $\psi_j^{\max}$ and using superposition (Figure 2.1). Similarly, a source composite curve is constructed in ascending order of property operators. For a pre-selected fresh source

with a given property operator (ψ^{Fresh}), the source composite curve is slid on the fresh line until the two composites touch at the pinch point with the source composite completely below the sink composite in the overlapped region. The pinch analysis determines the targets for minimum consumption of fresh resource (Fr1) and the minimum discharge of the waste (*W*) as shown by the pinch diagram (Figure 2.1).

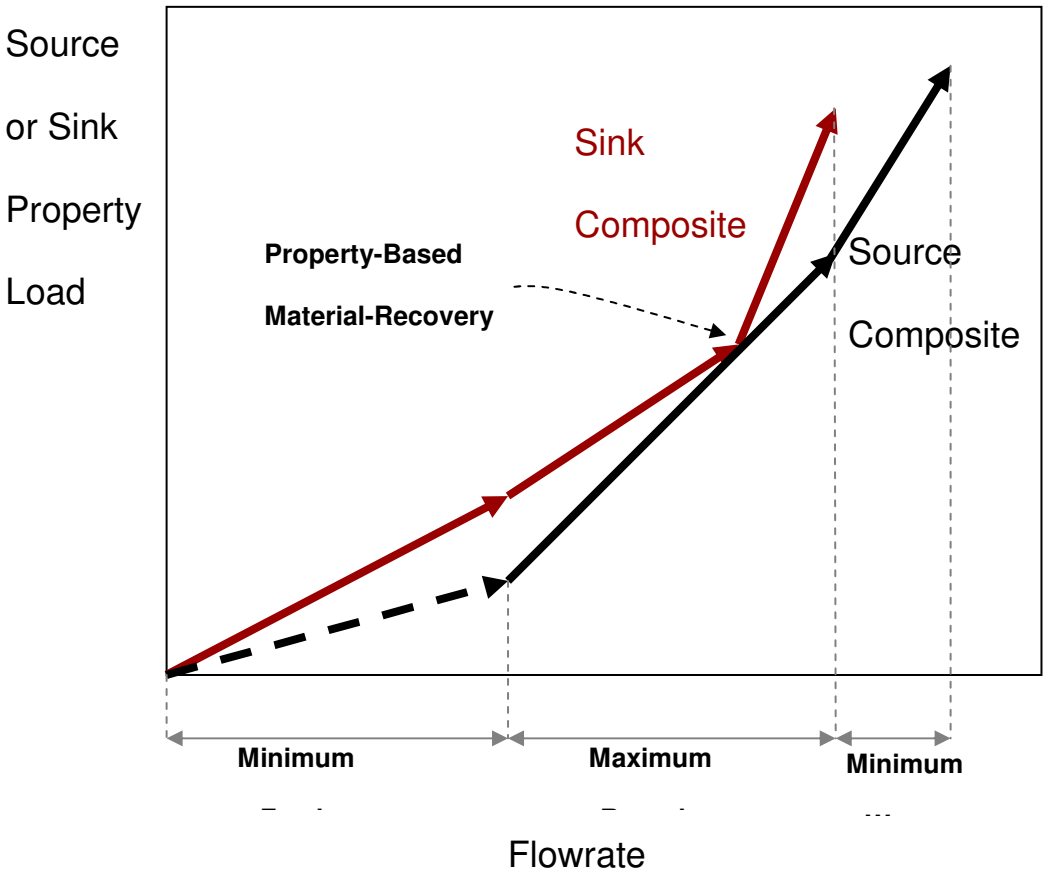

Figure 2.1 Property-based material-recovery pinch diagram (Kazantzi and El-Halwagi, 2005)

2.3 Problem Statement

The general problem statement considered in this chapter is stated as follows:

Given is a process with a number, N_{Sinks}, of processing units (or sinks), which accept streams with certain flowrates, G_j, and property values that need to satisfy the following constraints:

$$p_j^l \le p_j^{\text{sink}} \le p_j^u \qquad , \qquad j=1, 2,\ldots, N_{Sinks} \tag{2.6}$$

where, p_j^{sink} is the property of a stream entering sink *j*. The feed to each sink may involve one or more streams (sources) that satisfy the property-based requirements given by inequality constraint (2.6). These streams may be process streams and/or external (fresh) sources. A number, $N_{Sources}$, of process streams are available for recycle. Each process source has a given flowrate, F_i, and property value, p_i^{source}. The fresh (external) sources are unknown and are to be selected or synthesized from a combination of *N* functional groups. Each functional group, *g*, has a known property contribution C_g. Unused process sources are discharged as wastes. The current discharge of the process is referred to as W_o. In order to optimize the use of process sources and reduce environmental impact, the objective is to reduce the waste discharge to a targeted level (W_T). To reach this objective, it is desired to develop a systematic procedure that determines the following:

- What materials should be selected as fresh sources to achieve the target of waste discharge? These materials are to be synthesized from the given functional groups.
- Allocation of process sources to sinks (what flowrate of each source should be directed to each sink? Any segregation or mixing?)

Because of the strong interaction between the process design (source recycle, source-sink allocation, waste discharge) and the molecular design and allocation problems, it is critically important to develop a systematic approach which can consistently and simultaneously address both the process and the (material) molecular aspects of the problem.

The problem can be schematically represented as Figure 2.2.

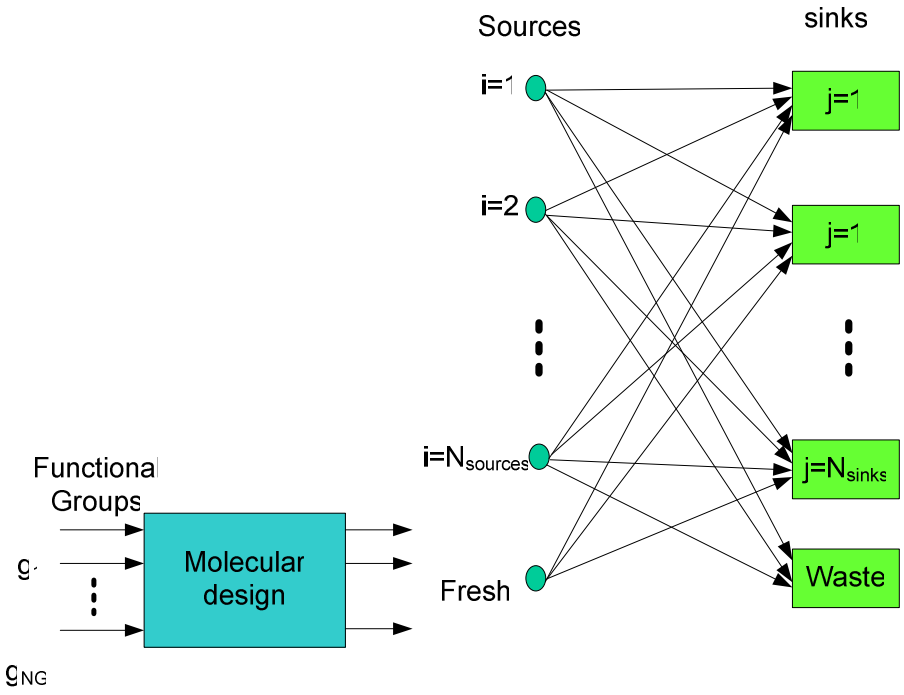

Figure 2.2 Schematic representation of the stated problem

2.4 Graphical Design Approach for the Stated Problem

In order to simultaneously consider the process and molecular design problems, we initiate the design from process targeting. It is possible to determine the feasibility region for the molecular design problem through insights from the process design problem. In our specific problem, we propose a new procedure based on the following elements:

1. For the given target of waste discharge (W_T), use the property-based material-recovery pinch analysis to (a) determine optimal allocation of process sources to sinks and (b) to derive the boundaries of the feasibility region for the molecular design problem. These boundaries of the feasibility region will define the attainable region for the candidate molecules through *targeting* and without infringing upon the degrees of freedom for the process or molecular design problems.

2. Exploit additive similarities between property-based mixing rules for streams and functional groups (although the property operators may be different) to represent process streams, sinks, and functional groups on the same pinch diagram. Use molecular design techniques to generate molecules (fresh sources) that are synthesized from the given functional groups while lying within the attainable region for the candidate molecules. This can be done through the new concept of a molecular pinch diagram.
3. Use the common representation of the property-based material-recovery pinch diagram (for process sources and sinks) and the molecular pinch diagram (for functional groups and fresh molecules) to determine the allocation of process and fresh sources to the sinks.

Figure 2.3 is a schematic representation of the devised approach for the interaction of the process design (source-sink allocation) and the material design (molecular design and allocation) through the common interface of the attainable region for candidate molecules obtained by targeting the process design problem.

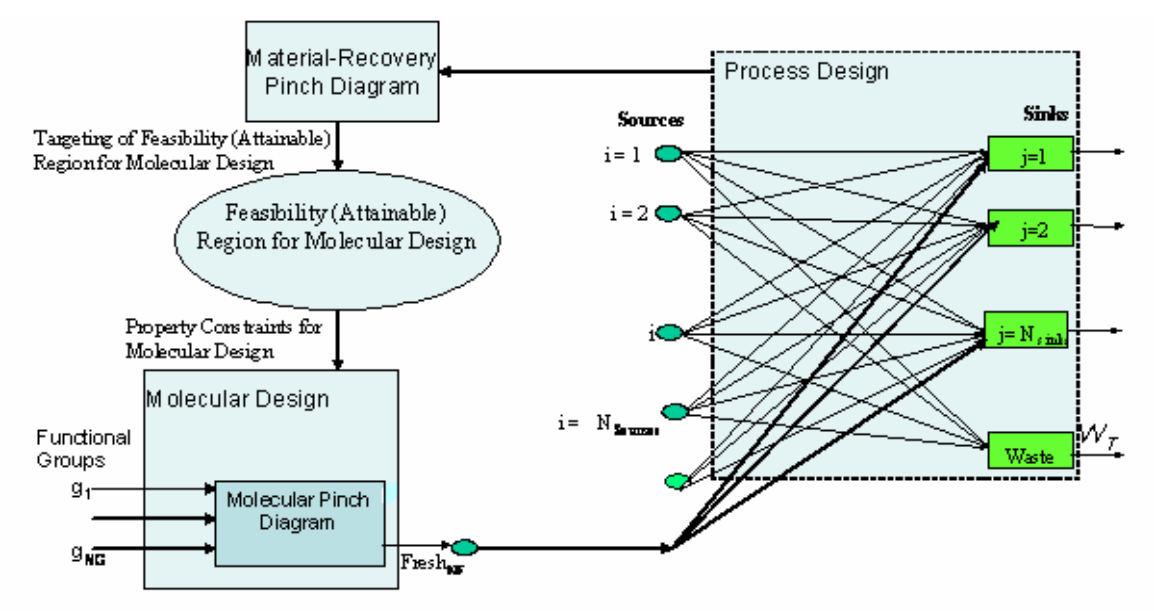

Figure 2.3 Property-based process and molecular design approach

2.5 Details of the Graphical Design Approach

The first step in the design procedure is to determine targets for the allocation of process sources and for the properties of the fresh molecules to be synthesized. Consider a system characterized by a single key property with the conditions described by Eqs. (2.5a) and (2.6a). For a given extent of waste discharge, W_T, a vertical line is drawn with a horizontal distance of W_T from the end of the sink composite curve. The source composite curve is constructed using superposition of all recyclable process sources. The source composite curve is slid on the vertical line until it touches the sink composite curve while lying below it. As a result, the maximum slope of the fresh molecule as well as the feasibility region for the molecular design problem is determined as shown by Figure 2.4 (process part).

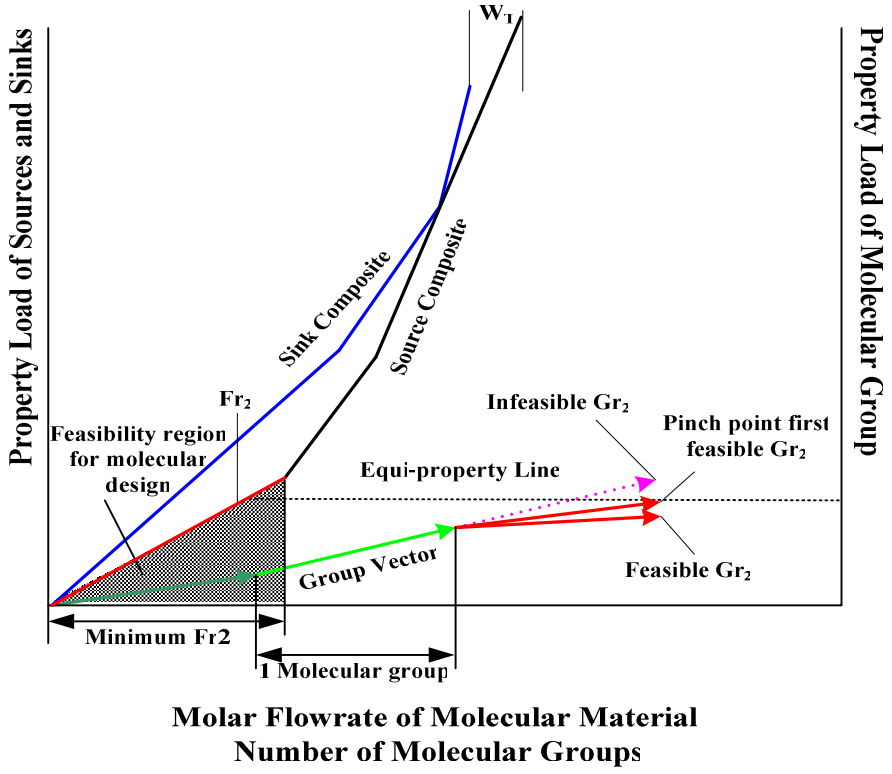

Figure 2.4 Group-contribution molecular pinch diagram

This feasibility region is determined as a target and incorporates the optimal recycle strategies for process sources to process sinks without infringing on the degrees of freedom for the molecular design problem. This is a key accomplishment towards the integration of process and molecular design. The feasibility region can be expressed as:

$$\psi^{fresh} \le \psi^{fresh\max} \tag{2.7}$$

It can also be shown that to maximize the slope of the fresh molecule that defines the feasibility region for molecular design, $\psi^{fresh\max}$, it is favored that to discharge the waste in the sequence from process source with higher property operator ψ_H^{source} to those with lower property operators ψ_L^{source} (subscripts H and L denote the stream with higher and lower property operator). Otherwise, it may lead a smaller feasibility region for the candidate fresh molecules and not the maximum one.

Since the fresh source is only involved in the subsystem below the process pinch point (the closed system), we focus on this subsystem to justify the above statement. Let ψ_H^{fresh} and Fr_H be the property operator and the flowrate of the fresh resulting from discharging the process source *H* respectively, and ψ_L^{fresh} and Fr_L the property operator and flowrate of the fresh resulting from discharging process source *L* respectively. For this closed system, total load of the process sources and the fresh is equal to the total load required by the sinks:

$$Fr_H\psi_H^{fresh} + \sum_{i=1}^{n-1} F_i\,\psi_i^{source} + F_L\psi_L^{source} = \sum_{j=\text{sink}\,sofclosedsystem} G_j\psi_j^{\text{sink}} \tag{2.8}$$

where F_i^{source} and ψ_i^{source} are the flowrates and property operators of any process source below the pinch point except for process source *L* (*i*=1,…,*n-1*). Eq. (2.8) holds for the case of discharging the process source with the higher property operator.

For this closed system, instead of using process source with lower property operator, we use same amount of process source with higher property operator ($F_H = F_L$), i.e. discharge any the process source L, then there is:

$$Fr_L\psi_L^{fresh} + \sum_{i=1}^{n-1} F_i\,\psi_i^{source} + F_H\psi_H^{source} = \sum_{j=\text{sink}\,sofclosedsystem} G_j\psi_j^{\text{sink}} \tag{2.9}$$

The right hand sides of Eq. (2.8) and (2.9) are equal and thus:

$$Fr_H \psi_H^{fresh} + F_L \psi_L^{source} = Fr_L \psi_L^{fresh} + F_H \psi_H^{source} \tag{2.10}$$

At a given extent of targeted waste discharge, W_T, since $F_L = F_H$, we have $Fr_H = Fr_L$. Thus, Eq. (2.10) becomes:

$$Fr_H (\psi_H^{fresh} - \psi_L^{fresh}) = F_H (\psi_H^{source} - \psi_L^{source}) \tag{2.11}$$

Because $\psi_H^{source} \geq \psi_L^{source}$, Eq. (2.11) gives:

$$\psi_H^{fresh} \geq \psi_L^{source} \tag{2.12}$$

which means that discharging the process source with the higher property operator yields higher slope for the fresh representing higher feasibility region for the design of new candidate molecules. Therefore, discharging process source from the one with the highest property operator will guarantee to get maximum feasibility property region.

Since the stream mixing operator (ψ) may differ from the GCM operator (ϕ), Eq. (2.7) is transformed to the property domain by inverting the property operator:

$$p^{fresh} \leq p^{fresh\max} = [\psi^{fresh\max}]^{-1} \tag{2.13}$$

Where $[\ ]^{-1}$ is the inverse of the function. Eq. (2.13) is the case when the property operator is monotonically increasing as function of the property values. If the property operator is monotonically decreasing as a function of the property values, then the less than or equal sign should be substituted with a greater than or equal sign and the maximum superscript should be substituted with a minimum superscript. Next, the property constraint is transformed to a GCM constraint using the functional form of the GCM expression:

$$\phi^{fresh} \leq \phi^{fresh\max} \tag{2.14}$$

Combining Eqs. (2.1) and (2.14), we get

$$\sum_g N_g C_g \leq \phi^{fresh\max} \tag{2.15}$$

The left-hand side of inequality (2.15) enjoys an additive attribute: it can be graphically represented through superposition of the contributions of the functional groups. This new representation is referred to as the group-contribution molecular pinch

diagram and can be shown in the molecule design part of Figure 2.4. To construct this diagram, a vertical scale (on the right-hand side of the diagram) is developed for the group-contribution load (ϕ). The horizontal axis represents the number (or ratio of numbers) of the functional groups existing in the molecule to be synthesized. Next, each functional group is represented by a vector whose slope is the group contribution to the property C_g. Linear superposition is used to add the group contributions. To insure soundness of the molecule, structural feasibility rules for combining functional groups are followed (e.g., Vaidyanathan and El-Halwagi, 1994, 1996; Gani and Constantinou, 1996). Additionally, there may be a constraint imposed on the maximum number of functional groups in the molecule or the maximum allowable molecular weight of the molecule. Search is limited to molecules lying within the feasibility region described by inequality (2.14).

Therefore, the group contribution molecular pinch diagram is used to directly identify feasible functional groups of a molecule that meets certain process objectives, and limits the search space for this identification.

In the case described by equation (2.5b) and (2.6b), following the aforementioned procedure, one can construct the combined process and molecular pinch diagram shown as Figure 2.5, from which, a simultaneous process and molecule design was also achieved.

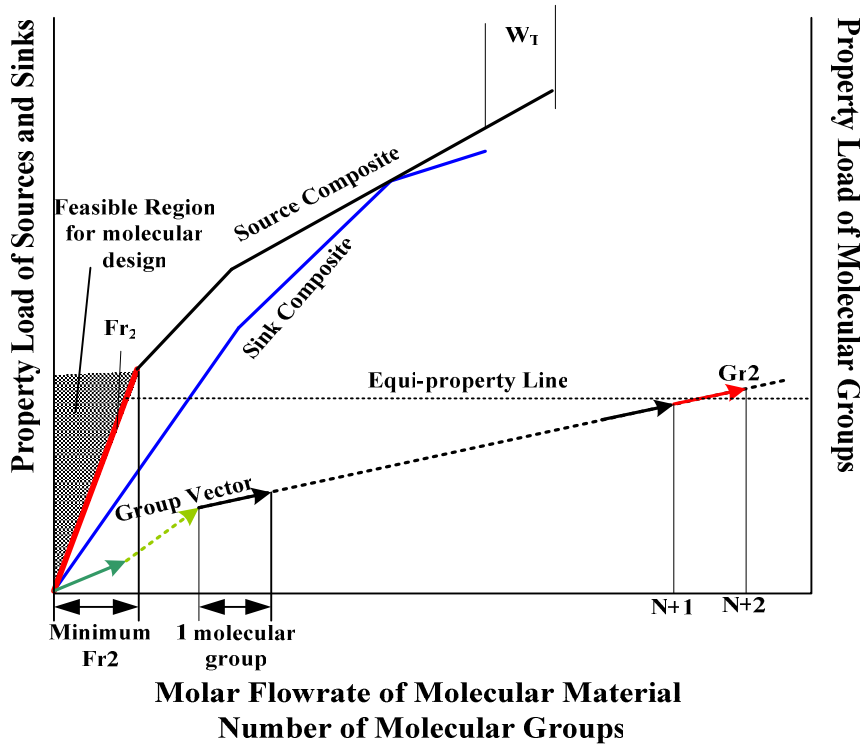

Figure 2.5 Process and molecular design for the case of Eq. (2.4b) and (2.5b)

To show the validation of the introduced approach, a case study of acid gas removal process is addressed in the following section.

2.6 Case Study

A gas purification facility is considered in this case study. It employs three operating units Unit 1 (U1), Unit 2 (U2) and Unit 3 (U3) to purify a gas mixture that contains significant amounts of acidic gases. In an existing gas treatment facility, two process sources diethylene glycol (DEG) (S1) and monoethanolamine (MEA) (S2) are used with a fresh stream of methyldiethanolamine (MDEA) (F1) to make up the solvent loss (Kohl and Nielsen, 1997).

Operating experience in gas treatment facilities show that the ideal heat of vaporization required for the solvent mixture (which can be obtained by a simple linear mixing rule $\overline{Hv} = \sum x_i * Hv_i$) should be higher than 75kJ/mole for Unit 1, 80kJ/mole for

Unit 2, and 70kJ/mole for Unit 3. It has been found that below this range, solvent loss is appreciable. The available molar flowrates for S1 and S2 in the existing facility are 180kmole/month and 160kmole/month respectively. In order to minimize solvent use and the discharge of process source for treatment, the plant has been integrated with the solution being a solvent mixture of 130kmole/month MDEA, 180kmole/month DEG and 120 kmole/month MEA for gas purification, and an additional 40kmole/month MEA (process source) that is to be sent for treatment without being used in this process (Table 2.1 provides the specific data for this system). This result can be observed from the pinch analysis illustrated as the dashed lines in Figure 2.6.

Table 2.1 Case study data

Process Data	Source1 (DEG)	Source 2 (MEA)	Fresh 1 (MDEA)	Sink 1 (U1)	Sink 2 (U2)	Sink 3 (U3)
Flowrate (kmole/month)	180	160	130	150	150	130
H_v (kJ/mole)	77.3	56.9	89.3	≥75	≥80	≥70
Adjustable Parameters and Constants: Hv_0 = 11.7 kJ/mole $\phi(Hv) = Hv - Hv_0 = \sum_g N_g Hv_g^{group}$ Group contribution of $N(CH_3)$ and CH_2 are 9.5 and 4.9 respectively.						

The problem in the case study is how to eliminate the discharge of MEA sent for treatment without being used in this process, i.e. $W_T=0$. To solve this problem, it is necessary to either find or design new solvents that can substitute MDEA in the process. The new solvent needs to have properties that are similar to MDEA, in order to meet process requirements. As a result, solvents that are homologous to MDEA are preferred, which means that molecules with the basic structure of MDEA, and the addition of a

specified number of the two free bond intermediate groups $-CH_2-$ and $-N(CH_3)-$ present in MDEA should be examined. The two primary objectives of the case study are:

1. To identify the feasible property values (*Hv*) of new solvents designed to eliminate the direct discharge of MEA.
2. To find or design feasible solvent molecules based on Group Contribution Method (GCM) that satisfy the first objective.

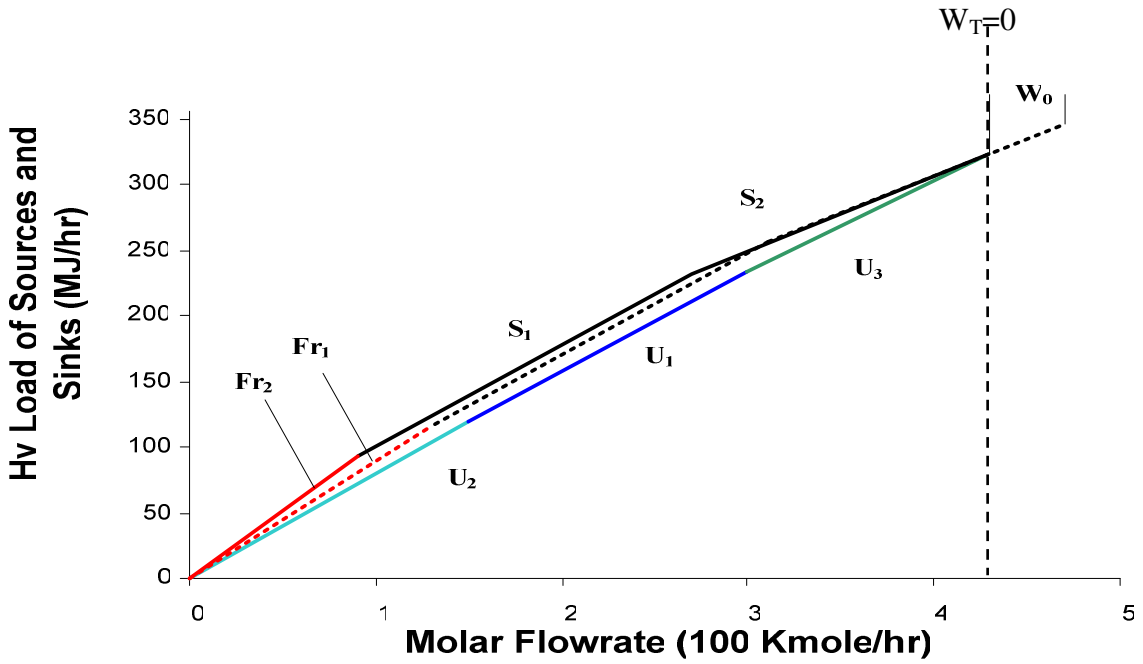

Figure 2.6 Pinch analysis for identifying feasible regions of possible solvents

Upon the developed approach, to achieve the targets described earlier in the case study, we first construct the sink composite curve of U_1, U_2, and U_3 and source composite curve of S_1 and S_2; then move the source composite curve down along the vertical line which represent zero waste discharge until it touches the sink composite curve; connect the origin point and the head point of S_1 to form the new fresh source whose slope found with a value of 103.8kJ/mole represents the minimum heat of vaporization for all feasible freshes. If without any other constraints, all sources with slopes larger than this value are feasible new fresh sources and yield zero waste

discharge. However, solvents with property (*Hv*) close to that of the first feasible solvent, Fr2, are preferred, since they render the system less disturbed. The graphical solution is shown in Figure 2.7.

Once the first process-based feasible solvent has been identified, the feasibility of designing this solvent molecule is explored. A novel approach is employed, which maps the feasible property of the solvent molecules in a molecular design diagram. This procedure uses the heat of vaporization relationship (H_v-H_{v0} = Group contribution), which is based on the Group Contribution Method (Marrero J. and Gani R., 2001). Through this approach, the preferred feasible group can be found as discussed in the previous section, and the corresponding new solvent that completely eliminates MEA discharge can also be identified. For simplicity, the groups in MDEA are considered as existing molecular groups that are to be incorporated in the molecular search (Figure 2.7). From group vector addition, it can be identified that the preferred new solvents should be structured from the previous homologue (MDEA) with the addition of the obtained feasible groups shown below:

MDEA+2N(CH_3), MDEA+1N(CH_3)+1CH_2 and MDEA+3CH_2, which can completely eliminate the excess process source discharge. In addition, it is observed from the group contribution molecular pinch diagram (Figure2.7) that MDEA + CH_2, MDEA+2CH_2 and MDEA+1N(CH_3) are candidates that partially reduce MEA discharge.

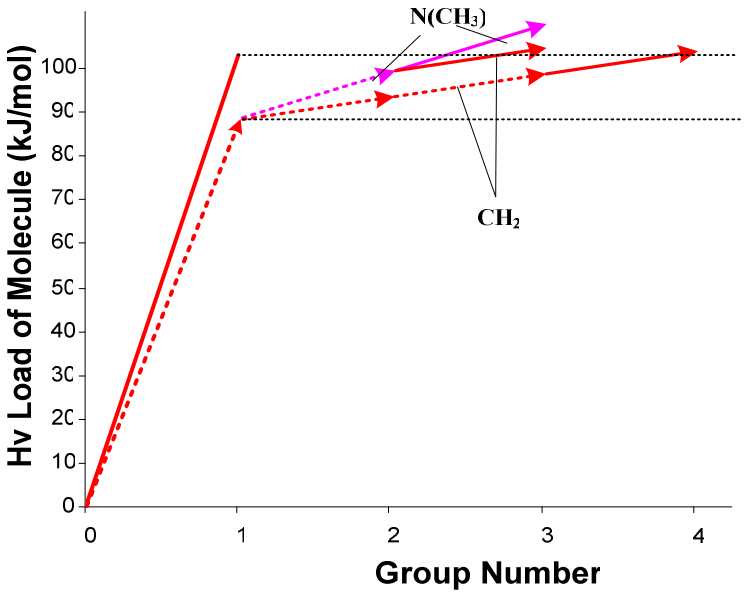

Figure 2.7 Group-contribution molecular diagram for the identification of new molecules

The solvents discussed above, are the preferred new solvents that satisfy the objectives of the case study. However, a further evaluation of the relative advantages in the synthesis of these candidate solvent molecules is required, before they can be produced and used for the process.

Consequently, based on the process and molecular design graphical approach developed for the current case study, one of the optimal solutions and configurations of the material usage are generated and shown in Figure 2.8 (values in parenthesis are the integrated configuration for the old system using MDEA).

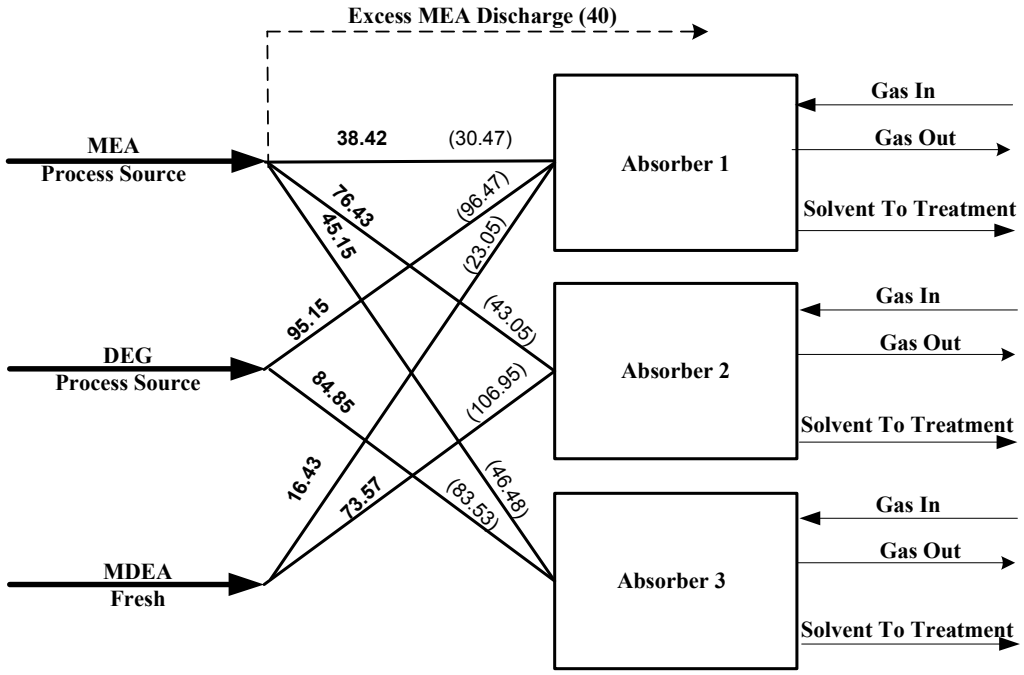

Figure 2.8 One of the optimal configuration of the gas purification system

2.7 Conclusions

In this chapter, a new property-based pinch approach to integrate process and molecular design has been introduced. A visualization technique, in which properties were used to represent process and material characteristics, was first developed and different categories for fresh material properties were explored. Process requirements and objectives, as well as molecular group properties were interrelated and integrated to simultaneously target process and material design. The new methodology employs property integration tools, along with group contribution methods (GCM) to map the system from the process- level to the molecule- and molecular group- levels, and vice versa. As a result, the current procedure defines a general framework for generating a set of candidate materials that meet the process objective, and can be next evaluated through various performance criteria. It also provides a starting point for addressing problems in

integrated process and material design/selection, in which important interrelated features are simultaneously taken into consideration.

CHAPTER III
SIMULTANEOUS PROCESS AND MOLECULAR DESIGN THROUGH PROPERTY INTEGRATION – A GLOBAL OPTIMIZATION APPROACH

3.1 Introduction

Notwithstanding the intuitive and illustrative effect of the graphical approach for simultaneous process and material design, it has limitations pertaining to the number of properties it can handle and the impracticality for a large number of streams. To overcome these limitations, a mathematical programming formulation is warranted to address the simultaneous process and material (molecule) design problem.

So far, based on GCM numerous contributions have been made in the field of computer-aided molecular design (CAMD). A recent survey of the CAMD field is given by Achenie et al. (2003). The new GCM proposed by Constantinou and Gani (1994) showed that improved accuracy can be achieved by using more structural information for the molecules. This method performs the estimation at two levels: the basic level uses contributions from first-order simple groups, while the second level takes into consideration the proximity effects by using a set of second order groups having first order groups as building blocks. Next, this new method was extended to include third order groups, thus being capable of describing more complex species such as large polycyclic compounds, and improve the accuracy of the predictions (Marrero and Gani, 2001). Their basic property estimation model takes the form of Eq. (3.1)

$$\phi(p_k) = \sum_{g'} N1_{g'} C1_k + z'' \sum_{g''} N2_{g''} C2_{g'',k} + z''' \sum_{g'''} N3_{g'''} C3_{g''',k} \tag{3.1}$$

where $C1_{g',k}$, $C2_{g'',k}$, and $C3_{g''',k}$ are property k related contributions of first-order group *g'*, second-order group *g''* and third-order group *g'''* respectively; $N1_{g'}$, $N2_{g''}$, and $N3_{g'''}$ are their corresponding occurrence in the molecule; *z''* and *z'''* are binary weight factors.

Based on various group contribution models, CAMD is widely used for designing molecules with different applications, such as design of solvent, polymer, refrigerant and environmentally benign species, but most of the design only use first order groups. The use of second- and third-order groups poses much complexity in CAMD models.

The CAMD models are typically formulated as mixed integer nonlinear programming (MINLP) problems. Much attention has been given to developing solution approaches to the MINLPs. These approaches include enumeration techniques, gradient-based optimization algorithms, stochastic search methods, and several global optimization algorithms. A brief review can be found in Karunanithi et al. (2005) in which a decomposition-based methodology were introduced.

This chapter introduces a new process-centered molecular design mathematical approach for material substitution through property-based integration and GCM. In this procedure, the process is first targeted using global optimization techniques. This optimization leads to obtaining process information that are primarily considered in identifying a set of potential candidate molecules with desired properties and selecting the best molecules among this set. To design the molecules, several groups that are of particular utility for a given process (they provide either the required chemical function for the specific performance or the physical characteristics for a certain process task) as well as some generic groups were selected for configure molecular structures. Both lower level group contribution and high level group contribution are considered in the same model. Through this work, the process design and the molecular design problems are simultaneously addressed with the global optimization method.

3.2 Problem Statement

The general problem statement is very similar to that of Chapter II. The main difference is that there are N_p governing properties other than only one involving in this problem. Therefore, the kth property constraint of sink j is expressed as:

$$p_{j,k}^{\text{sinkl}} \le p_{j,k}^{\text{sink}} \le p_{j,k}^{\text{sink}u} \quad , j = 1, 2,\ldots, N_{sinks} \text{ and } k=1, 2,\ldots, N_p \tag{3.2}$$

where, $p_{j,k}^{\text{sink}}$ is the property k of a stream entering sink *j*, and the superscript of *l* and *u* represent the lower and upper limit respectively. The feed to each sink may involve one or more streams (sources) that satisfy the flowrate constraints and property-based requirements given by inequality (3.2). These streams may be process streams and/or fresh sources. A number, $N_{Sources}$, of process streams are available for recycle. Each process source, *i*, has a given flowrate, F_i , and property values, $p_{i,k}^{source}$. The fresh (external) source, *f*, is unknown and is to be synthesized from a combination of N functional groups. Each functional group, g', has the known property contributions $C1_{g',k}$. Property contributions of second order groups and third order groups which may occur in synthesized molecules are also given, i.e. $C2_{g'',k}$ and $C3_{g''',k}$.

The mixing rule for the k[th] property is described by:

$$\overline{F} * \psi_k(\bar{p}_k) = \sum_{i}^{N_{sources}} F_i * \psi_k(p_{i,k}^{source}) \tag{3.3}$$

where $\psi_k(p_{i,k}^{source})$ is the property mixing operator for the *k*th property, *i* is the source index, and $\overline{F}$ is the total flowrate of the mixture.

The objectives of this problem are similar to those mentioned in Chapter II. In particular, the mathematical optimization procedure should determine the following:

- What materials should be selected as fresh sources to achieve the target of waste discharge? These materials are to be synthesized from the given functional groups.
- Which material (molecule) and/or a set of molecules are optimal among multiple candidates?
- Allocation of process sources to sinks (what flowrate of each source should be directed to each sink? Any segregation or mixing?)

3.3 Design Approach

Because of the strong interaction between the process design problem (source recycle, source-sink allocation, waste discharge) and the molecular design problem, the

mathematical approach should provide a framework for interfacing the two problems and for handling multiple properties. The mathematical programming model for the entire problem is an MINLP. To solve this model and get global optimal solution, the stated problem is decomposed into several subproblems generating a new "looping" problem formulation. The basic idea is to create an iterative loop which involves the global solution of interconnected subproblems. The solution results are passed from one subproblem to the next until convergence is achieved. First, process considerations and integration opportunities are transformed into property-based constraints which form a feasibility region for molecular design. This is essentially a targeting step which generates an "attainable region" for the molecular design problem based on incorporating all relevant process constraints. Based on the identified property-based attainable region for feasible molecules, a CAMD is formulated and solved to synthesize a set of candidate molecules. Finally, the process design task of assigning sources to sinks is solved using the synthesized candidates. Once the loop is completed, the solution results provide sufficient details on the process and molecular design problems. The loop at the core of the overall solution approach is illustrated by Figure 3.1. If no feasible solution is found, a new loop should be initiated by either relaxing previous process constraints or modifying process objectives. The looping is repeated until a feasible solution is found. In the case of multiple new molecular candidates, the cost criterion can be used to identify the global optimal new molecule or molecular set. Finally process design based on the global optimal new molecule or molecular set is optimized. The flowchart of the overall design approach is represented by Figure 3.2.

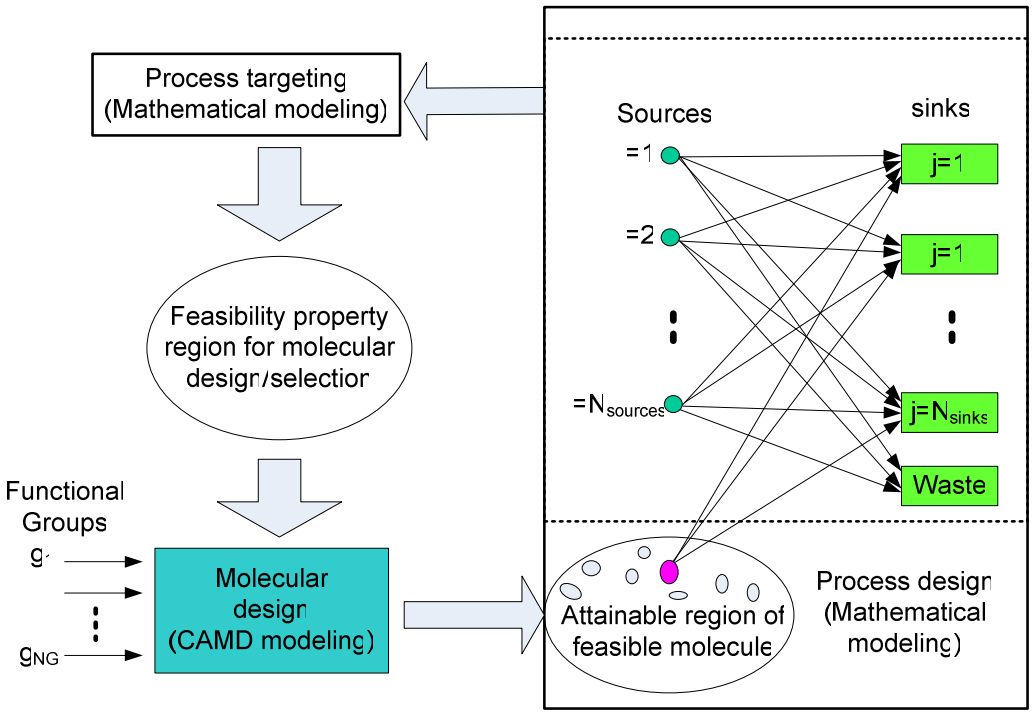

Figure 3.1 Schematic representation of the single loop of solution

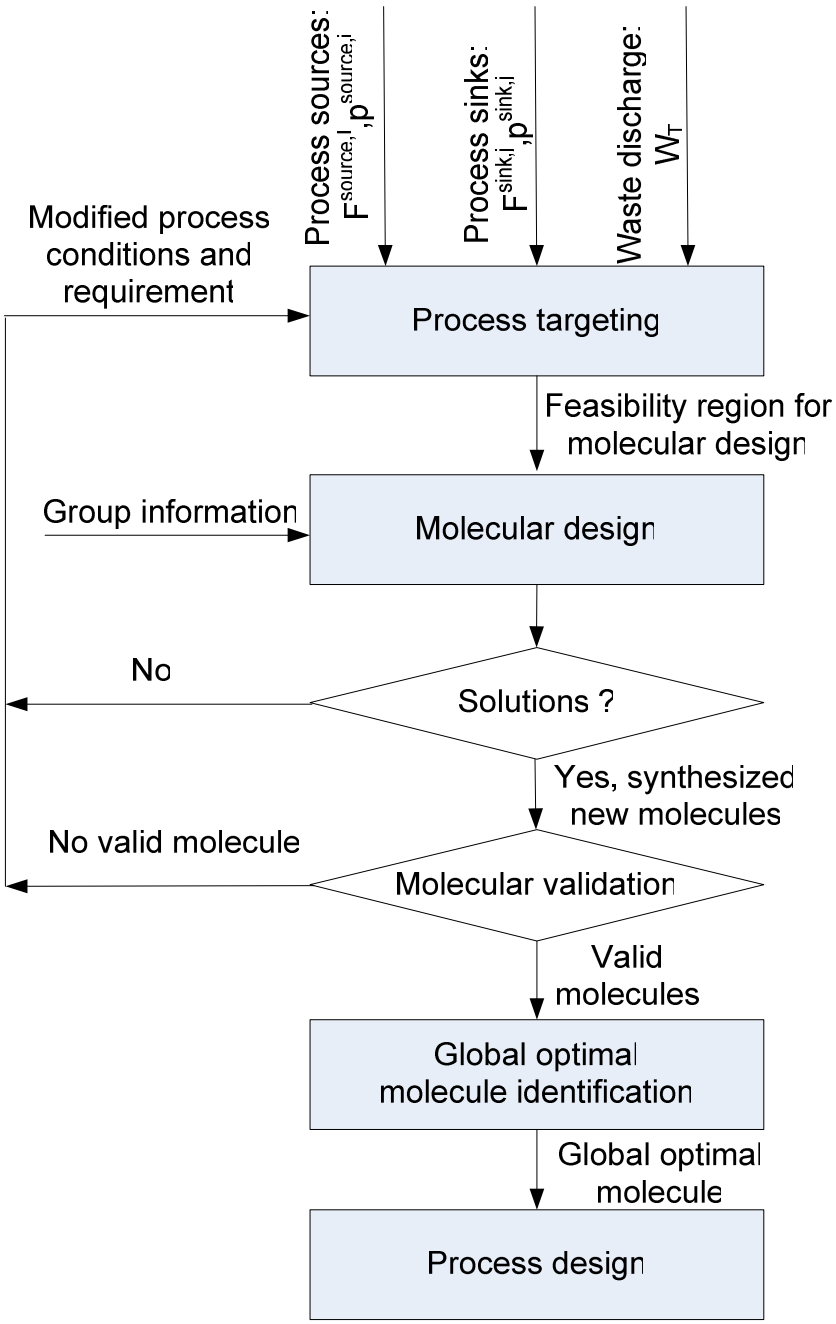

Figure 3.2 Overall design flowchart

The details of the various steps in the proposed approach are described in the following sections.

3.3.1 Process Targeting: Identifying the Feasibility Property Region for Molecular Design

The first step of the design procedure is to identify the property-based feasibility (or attainable) region for molecular design. This targeting is to be performed ahead of detailing the process or molecular design problems. The idea is to identify property-based bounds that capture the process constraints without committing to the selection of a process or a molecular solution. For each property, *k*, two optimization problems are solved: one for identifying the lower bound for the property and one for the upper bound. The mathematical formulation is given by:

$$\min or \max = p_k^{fresh} \tag{3.4}$$

Subject to

Flowrate balance

$$F_i = \sum_{j=1}^{N_{\text{sinks}}} f_{i,j} + f_{i,waste} \qquad i=1, 2, ..., N_{sources} \tag{3.5}$$

$$Fr_f = \sum_{j=1}^{N_{\text{sinks}}} Fr_{f,j} \tag{3.6}$$

$$G_j = \sum_{i=1}^{N_{sources}} f_{\text{i,j}} + Fr_{f,j} \qquad j=1, 2, \ldots, N_{sinks} \tag{3.7}$$

$$W = \sum_{i=1}^{N_{sources}} f_{i,waste} \le W_T \qquad \text{for waste disposal} \tag{3.8}$$

Property *k* constraints for process sink *j*:

$$p_{j,k}^{\text{sinkl}} \le p_{\text{j,k}}^{\text{sink}} \le p_{j,k}^{\text{sinku}} \qquad j=1, 2, \ldots, N_{sinks}; \tag{3.9}$$

Where

$$p_{j,k}^{\text{sink}} = f(f_{1,\text{j}},..., f_{\text{i,j}},..., f_{N_{sources},j}, Fr_{f,j}, p_{1,k}^{source},..., p_{i,k}^{source},..., p_{N_{sources},k}^{source}, p_{f,k}^{fresh}) \tag{3.10}$$

$f_{i,j}$ is the flowrate of source *i* flowing into mixture for sink *j*, $f_{i,waste}$ is the flowrate of source *i* discharged as waste, *Fr* is the fresh flowrate, *W* is the total flowrate of discharged waste. $f_{i,j}$ can be further expressed in the function of $x_{i,j}$, the allocation fraction of source *i* entering sink *j* as follows:

$$f_{i,j} = x_{i,j} F_i \tag{3.11}$$

By introducing the mixing rule in form of Eq. (3.3), the property-based model can be converted to property operator-based model, with the objective function change to

$$\min or \max = \psi_k(p_k^{fresh}) \tag{3.12}$$

and property constraints converted to property operator constraints, i.e.

For the case ψ monotonically increases with p increasing (category A of property operators), there is

$$G_j \psi_k(p_{j,k}^{\text{sink}l}) \le \sum_{i=1}^{N_{sources}} f_{i,j} \psi_k(p_{i,k}^{source}) + Fr_{f,j} \psi_k(p_k^{fresh}) \le G_j \psi_k(p_{j,k}^{\text{sink}u}) \tag{3.13a}$$

For the case ψ monotonically increases with p decreasing (category B of property operators), there is

$$G_j \psi_k(p_{j,k}^{\text{sink}u}) \le \sum_{i=1}^{N_{sources}} f_{i,j} \psi_k(p_{i,k}^{source}) + Fr_{f,j} \psi_k(p_k^{fresh}) \le G_j \psi_k(p_{j,k}^{\text{sink}l}) \tag{3.13b}$$

Although the nonlinearity of the property operator-based process targeting model is greatly reduced, it is still a nonlinear programming model because of the existence of bilinear terms $Fr_{f,j} \psi_k(p_k^{fresh})$ which in general is not globally solvable. However, following demonstration shows that the objective function $\psi_k(p_k^{fresh})$, which is also variable in the model, is confined in closed intervals. Additionally, since all other variables are confined obviously, global optimization technique based on interval analysis can be employed for pursuing global optimal solutions.

Taking summation of inequality (3.13a) over the process sinks for property *k*, we have

$$\sum_{j=1}^{N_{\text{sinks}}} G_j \psi_k(p_{j,k}^{\text{sink}l}) \le \sum_{j=1}^{N_{\text{sinks}}} \sum_{i=1}^{N_{sources}} f_{i,j} \psi_k(p_{i,k}^{source}) + Fr_f \psi_k(p_k^{fresh}) \le \sum_{j=1}^{N_{\text{sinks}}} G_j \psi_k(p_{j,k}^{\text{sink}u}) \tag{3.14}$$

For term $\sum_{j=1}^{N_{\text{sinks}}} \sum_{i=1}^{N_{sources}} f_{i,j} \psi_k(p_{i,k}^{source})$, we have following constraints

$$\sum_{j=1}^{N_{\text{sinks}}}\sum_{i=1}^{N_{sources}} f_{i,j}\psi_k^{source\min} \le \sum_{j=1}^{N_{\text{sinks}}}\sum_{i=1}^{N_{sources}} f_{i,j}\psi_k(p_{i,k}^{source}) \le \sum_{j=1}^{N_{\text{sinks}}}\sum_{i=1}^{N_{sources}} f_{i,j}\psi_k^{source\max} \tag{3.15}$$

Furthermore,

$$\sum_{j=1}^{N_{\text{sinks}}}\sum_{i=1}^{N_{sources}} f_{i,j}\psi_k^{source\min} = \psi_k^{source\min}\sum_{j=1}^{N_{\text{sinks}}}\sum_{i=1}^{N_{sources}} f_{i,j} = \psi_k^{source\min}(\sum_{j=1}^{N_{\text{sinks}}} G_j - Fr_f) \tag{3.16}$$

and

$$\sum_{j=1}^{N_{\text{sinks}}}\sum_{i=1}^{N_{sources}} f_{i,j}\psi_k^{source\max} = \psi_k^{source\max}\sum_{j=1}^{N_{\text{sinks}}}\sum_{i=1}^{N_{sources}} f_{i,j} = \psi_k^{source\max}(\sum_{j=1}^{N_{\text{sinks}}} G_j - Fr_f) \tag{3.17}$$

Therefore, inequality (3.15) turns to

$$\sum_{j=1}^{N_{\text{sinks}}}\sum_{i=1}^{N_{sources}} f_{i,j}\psi_k^{source\min} \le \sum_{j=1}^{N_{\text{sinks}}}\sum_{i=1}^{N_{sources}} f_{i,j}\psi_k(p_{i,k}^{source}) \le \psi_k^{source\max}(\sum_{j=1}^{N_{\text{sinks}}} G_j - Fr_f) \tag{3.18}$$

By adding $Fr_f\psi_k(p_k^{fresh})$, inequality (3.18) becomes

$$\begin{aligned}\psi_k^{source\min}(\sum_{j=1}^{N_{\text{sinks}}} G_j - Fr_f) + Fr_f\psi_k(p_k^{fresh}) &\le \sum_{j=1}^{N_{\text{sinks}}}\sum_{i=1}^{N_{sources}} f_{i,j}\psi_k(p_{i,k}^{source}) + Fr_f\psi_k(p_k^{fresh}) \\ &\le \psi_k^{source\max}(\sum_{j=1}^{N_{\text{sinks}}} G_j - Fr_f) + Fr_f\psi_k(p_k^{fresh})\end{aligned} \tag{3.19}$$

Combining inequality (3.19) and inequality (3.14), we have

$$\begin{aligned}(\sum_{j=1}^{N_{\text{sinks}}} G_j\psi_k(p_{j,k}^{\text{sink}l}) - \psi_k^{source\max}(\sum_{j=1}^{N_{\text{sinks}}} G_j - Fr_f))/Fr_f &\le \psi_k(p_k^{fresh}) \\ &\le (\sum_{j=1}^{N_{\text{sinks}}} G_j\psi_k(p_{j,k}^{\text{sink}u}) - \psi_k^{source\min}(\sum_{j=1}^{N_{\text{sinks}}} G_j - Fr_f))/Fr_f\end{aligned} \tag{3.20}$$

i.e.

$$\begin{aligned}p_k^{fresh} \in [&\psi_k^{-1}((\sum_{j=1}^{N_{\text{sinks}}} G_j\psi_k(p_{j,k}^{\text{sink}l}) - \psi_k^{source\max}(\sum_{j=1}^{N_{\text{sinks}}} G_j - Fr_f))/Fr_f), \\ &\psi_k^{-1}((\sum_{j=1}^{N_{\text{sinks}}} G_j\psi_k(p_{j,k}^{\text{sink}u}) - \psi_k^{source\min}(\sum_{j=1}^{N_{\text{sinks}}} G_j - Fr_f))/Fr_f)]\end{aligned} \tag{3.21a}$$

Similarly, we can get the closed interval for category B of property operator, i.e.

$$p_k^{fresh} \in [\psi_k^{-1}((\sum_{j=1}^{N_{sinks}} G_j \psi_k(p_{j,k}^{sink u}) - \psi_k^{source\max}(\sum_{j=1}^{N_{sinks}} G_j - Fr_f))/Fr_f), \\ \psi_k^{-1}((\sum_{j=1}^{N_{sinks}} G_j \psi_k(p_{j,k}^{sink l}) - \psi_k^{source\min}(\sum_{j=1}^{N_{sinks}} G_j - Fr_f))/Fr_f)] \quad (3.21b)$$

where $\psi_k^{source\max}$ and $\psi_k^{source\min}$ are maximum and minimum of *k* property operator among process sources, and ψ^{-1} is the inverse function of function ψ.

With the identification of the interval bounding the value of objective function, it is possible to use the interval-based technique of Vaiydanathan and El-Halwagi (1998) to identify the global minimum. This technique involves several methods such as the discretization procedure for performing shifted partitioning around local optima (feasible point in our case). This procedure is intended to accelerate the identification of the global optimum with the help of a local optimizer. To find both the global maximum and the global minimum, two direction searches need to be carried out. To partition subintervals containing feasible value of $\psi_k(p_k^{fresh})$, the bisection method is used here because of its simple implementation.

After getting the global minimum and maximum values of each property operator, the next step is to convert the property operator feasibility range to raw property feasibility range with the inverse relation:

$p_k^{fresh\max} = [\psi_k^{\max}]^{-1}$ and $p_k^{fresh\min} = [\psi_k^{\min}]^{-1}$ for category A of monotonically increasing property operators; (3.22a)

$p_k^{fresh\min} = [\psi_k^{\max}]^{-1}$ and $p_k^{fresh\max} = [\psi_k^{\min}]^{-1}$ for category B of monotonically decreasing property operators. (3.22b)

It is worth noting that the range $[p_k^{fresh\min}, p_k^{fresh\max}]$ does not have to be exact. Overestimation of the boundaries of the feasibility region (BFR) is allowable. The overestimated is referred to as the quasi-boundaries of the feasibility region (QBFR). Clearly, the tighter the QBFR, the less the computations needed for the global solution.

3.3.2 Molecular Design

For effective solution, the molecular design problem is decomposed into two steps. First, finding the first order groups (block building groups) and their occurrence as well as the occurrence of second order groups and third order groups, which satisfying the constraints of QBFR. We name this step "feasible group set identification". Second, "molecule structure configuration". In this step molecules are configured based on the 'feasible group set' as well as some restrictions from the viewpoint of chemistry and chemical process.

Process requirements and molecular characteristics are used to narrow down the type and number of candidate functional groups. As mentioned before, the GCM may involve the use of first-, second-, and third-order groups. We propose to initially pre-screen the first-order groups. The pre-selected first-order groups as well as the generic first-order groups will form the set of candidates serving as the building blocks of the molecules. By inspection of the selected first-order groups, second- and third-order groups may be screened out from database.

We start the modeling with the consideration of process requirements for certain functional groups. For example, when designing a solvent for acid gas removal, the amino group may be required for the purpose of providing the necessary alkalinity in water solutions. However, too many occurrences of the amino group in the molecule may cause a corrosion problem. Therefore, a constraint is imposed on the number of occurrence of this specific group. In general, such constraints are described as follows:

$$N1_{g'}^{\min} \le \sum_{l} N1_{g',l} \le N1_{g'}^{\max} \tag{3.23}$$

where l is the position of first order group g' in the molecule, and $N1_{g'}^{\min}$ and $N1_{g'}^{\max}$ are the minimum and maximum number of occurrences of group g', and $N1_{g',l}$ is a binary variable.

Although a molecule may be designed based on first-order groups only, the use of second- and third-order groups help in developing appropriate constraints for structural feasibility and provide more accuracy in predicting the molecular properties.

Since second- and third-order group are constructed based on first-order groups, the following constraints can be added to limit the search space:

$$b1_{g''}N2_{g''} \le \sum_{l} a1_{g'}N1_{g',l} \tag{3.24}$$

for individual second order group *g''* with the first order group *g'* in its structure, and

$$\sum_{g''} b2_{g''}N2_{g''} \le \sum_{l} a2_{g'}N1_{g',l} \tag{3.25}$$

for second order groups which share same first order group *g'* in their structures;
Similarly for third order group we have

$$b3_{g'''}N3_{g'''} \le \sum_{l} a3_{g'}N1_{g',l} \tag{3.26}$$

and

$$\sum_{g'''} b4_{g'''}N3_{g'''} \le \sum_{l} a4_{g'}N1_{g',l} \tag{3.27}$$

where *a1, b1, a2, b2, a3, b3, a4*and *b4* are coefficient need to be carefully explored. After setting up the first two sets of constraints, we come to the third set of constraints

$$\phi(p_k^{fresh\min}) \le \sum_{g'}\sum_{l} N1_{g',l}\ C1_{g',k} + \sum_{g''} N2_{g''}\ C2_{g'',k} + \sum_{g'''} N3_{g'''}\ C3_{g''',k} \le \phi(p_k^{fresh\max}) \tag{3.28}$$

This constraint is based on the targeted boundaries of the feasibility region ($QBFR_{fresh}$).

The fourth set of constraints of our CAMD model is

$$\sum_{g'} N1_{g',l} = 1 \text{ for all } l, \tag{3.29}$$

where $N1_{g',l}$ is a binary variable. Eq. (3.29) insures that one position only can be occupied by one group.

To make sure that a molecule has no free bonds, the octet rule of structural feasibility is used:

$$\sum_{g'}\sum_{l} N1_{g',l}(2 - \upsilon_{g'}) = 2d \tag{3.30}$$

Where $v_{g'}$ is the valency of the first order group g' and d is 1, 0, -1 or -2 for acyclic, monocyclic, bicyclic and tricyclic compounds respectively.

The resulting formulation is a mixed-integer linear program (MILP) which can be globally solved to determine the molecular design including the type and number of selected functional groups.

3.3.3 Process Design

This section involves two tasks: final validity verification of the designed molecule and process optimization.

1. Validation of Molecular Feasibility

As pointed early, the quasi-boundaries of the feasibility region (QBFR) is an overestimation of the actual property-based feasibility region. Therefore, some of the designed molecules may be located in the overestimated part. Therefore, it is important to check on the feasibility of the designed molecule with respect to the actual feasibility region. This can be achieved by checking the feasibility of all the constraints in the aforementioned process targeting model. If all the constraints are satisfied, then the valid solution has been identified. Otherwise, if a single constraint is violated then no feasible solution has been identified. In this case, there is a need to iterate by relaxing the original process constraints. The process is repeated until a feasible solution is found.

2. Identification of Optimal Molecule or Molecular Set and Corresponding Optimal Process Design

The identified feasible molecules can fulfill the process requirement of reducing the waste discharge from T_0 to no more than W_T, while satisfying all process constraints. Next, the optimal molecule should be selected from the identified list based on economic issues. The cost of new fresh source (feasible molecules) (C^{fresh}), the cost of waste discharge (process source discharged as waste) (C^{source}) and the cost of piping and fitting (C^{piping}) are the main operating costs of the recycle/reuse network design in consideration. As we stated before, process design will accept individual feasible

molecule candidate as well as the molecular sets which are the combinations of valid individual candidates. So the overall cost can be expressed as:

$$C = \sum_{i=1}^{N_{sources}} C_i^{source} f_{i,waste} + \sum_{f=1}^{N_{fresh}} C_f^{fresh} Fr_f + \sum_{i=1}^{N_{sources}} \sum_{j=1}^{N_{sinks}} C_{i,j}^{piping} f_{i,j} + \sum_{f=1}^{N_{fresh}} \sum_{j=1}^{N_{sinks}} C_{f,j}^{piping} Fr_{f,j} \quad (3.31)$$

The model to select the optimal molecule or molecular set is expressed as follows:

$$\min \; C = \sum_{i=1}^{N_{sources}} C_i^{source} f_{i,waste} + \sum_{f=1}^{N_{fresh}} C_f^{fresh} Fr_f + \sum_{i=1}^{N_{sources}} \sum_{j=1}^{N_{sinks}} C_{i,j}^{piping} f_{i,j} + \sum_{f=1}^{N_{fresh}} \sum_{j=1}^{N_{sinks}} C_{f,j}^{piping} Fr_{f,j} \quad (3.32)$$

subject to:

$$F_i = \sum_{j=1}^{N_{sinks}} f_{i,j} + f_{i,waste} \qquad i=1, 2, \ldots, N_{sources} \quad (3.5)$$

$$Fr_f = \sum_{j=1}^{N_{sinks}} Fr_{f,j} \quad (3.6)$$

$$G_j = \sum_{i=1}^{N_{sources}} f_{i,j} + \sum_{f=1}^{N_{fresh}} Fr_{f,j} \qquad j=1, 2, \ldots, N_{sinks} \quad (3.33)$$

$$W = \sum_{i=1}^{N_{sources}} f_{i,waste} \le W_T \qquad \text{for waste disposal} \quad (3.8)$$

$$G_j \psi_k(p_{j,k}^{sink l}) \le \sum_{i=1}^{N_{sources}} f_{i,j} \psi_k(p_{i,k}^{source}) + \sum_{f=1}^{N_{fresh}} Fr_{f,j} \psi_k(p_{f,k}^{fresh}) \le G_j \psi_k(p_{j,k}^{sink u}) \quad \text{for category A} \quad (3.34a)$$

or

$$G_j \psi_k(p_{j,k}^{sink u}) \le \sum_{i=1}^{N_{sources}} f_{i,j} \psi_k(p_{i,k}^{source}) + \sum_{f=1}^{N_{fresh}} Fr_{f,j} \psi_k(p_{f,k}^{fresh}) \le G_j \psi_k(p_{j,k}^{sink l}) \quad \text{for category B} \quad (3.34b)$$

With the known properties of all given fresh candidates, this is a linear programming model and global minimum of *C* is guaranteed. The molecule or a set of molecules with the minimum total cost while satisfying process constraints is selected. The solution also identifies the optimal flowrate of the fresh and the recycle configuration.

3.4 Case Study

Let us consider an acid gas removal process (e.g., Kohl and Nielsen, 1997). It involves five units (sink1 to sink5: U1 to U5) to purify a gaseous mixture that contains significant amounts of acid gases (primarily CO_2 and H_2S). Currently, the process has four process sources: methyldiethanolamine "MDEA" (S1), Monoethanolamine "MEA" (S2), Diethanolamine "DEA" (S3), and Diglycolamine "DGA" (S4). These four sources are considered to be used along with a fresh stream (Fr) to make up the solvent losses.

The objective of this case study is to design/select an acyclic amine molecule, which can be mixed with process sources to meet the property criteria of makeup solvents for each process unit. It is also desired to determine the process design aspects of the solution such as flowrate of the solvent and allocation from sources to sinks.

For solvent makeup, the following three properties are considered: heat of vaporization (H_v), heat of fusion (H_{fus}), and critical temperature (T_c). The acceptable property ranges of the makeup solvents as well as their flowrates for each process unit are listed in Table 3.1. Additionally, two thermal constraints are imposed on the synthesized molecule. It must have a melting point (T_m) less than or equal to 293.15 K and a boiling point (T_b) greater than or equal to 480 K (to prevent excessive solvent losses via vaporization). To insure water solubility and to reduce vapor pressure, the amine must have two or more –OH groups. To limit the extent of corrosion, only one amino group is allowed to be in the amine (N in the amino group either connect with H or C). Finally, to limit detrimental effects of direct exposure to the solvent, tertiary amines are ruled out in this case study. The properties and flowrate of each process stream are also given. The mixing rules of all three properties are taken to be linear relations.

Table 3.1 Data for case study

Source and sink	T_c (K)	H_v (kJ/mol)	H_{fus} (kJ/mole)	Flowrate (kmol/month)
S1 (MDEA)	678	95.0	23.0	60
S2 (MEA)	670	64.0	18.4	90
S3 (DEA)	715	85.0	22.1	70
S4 (DGA)	699	82.0	21.7	60
U1	[685, 705]	[67.5, 80.0]	[15.0, 19.0]	200
U2	[690, 705]	[67.5,82.5]	[15.0, 19.5]	210
U3	[690, 710]	[70.0, 82.5]	[16.0, 19.5]	230
U4	[695, 710]	[70.0, 85.0]	[16.0, 20.0]	190
U5	[695, 715]	[72.5, 85.0]	[17.0, 20.0]	170

A key criterion for a useful GCM is the proper balance between accuracy and computation intensity. Towards this end, several GCM methods may be employed. In this case study, we use the GCM of Marrero and Gani (2004) since it has been shown to provide reliable estimations of various molecules with a reasonable computational requirement.

In this work, the commercial optimization software Hyper LINGO release 8.0 (9 May 03) Copyright© 2003 was used to solve our established model.

Following the developed design approach, we provide case study solution in three major steps.

1. Process targeting to identify the QBFR

First, the process targeting model is formulated to determine the QBFR. Although the property targeting model is a nonlinear programming, the global optimum solution may be determined using the global solver of LINGO. The targeted QBFR is listed in Table 3.2.

Table 3.2 Targeted QBFR for molecular design

	T_c (k)	H_v (kJ/mole)	H_{fus} (kJ/mole)
minimum	691.34	65.375	13.720
maximum	716.43	84.125	20.410

However, if a nonlinear variable is beyond the default limit of LINGO, the introduced global optimization approach based on interval analysis can be employed. To illustrate this method, we take H_v as an example. From the given data in Table 3.1, we have $H_v^{sourcemax}$ =95kJ/mole; $H_v^{sourcemin}$ =64kJ/mole. From formula (3.21a), we have $H_v^{fresh} \in [59.444,90.250]$, where H_v^{fresh} is the H_v of fresh (new molecule). Starting with the half point, using bisection method to partition H_v^{fresh} value, then checking its feasibility (table 3.3), we obtain the same global optima identified by LINGO.

Table 3.3 Global optimal minimum and maximum value based on interval analysis

Hvl bottom	*Hvl* top	Half point	Feasibility check	*Hvu* bottom	*Hvu* top	Half point	Feasibility check
59.444	90.250	74.847	Yes	59.444	90.250	74.847	Yes
59.444	74.847	67.146	Yes	74.847	90.250	82.549	Yes
59.444	67.146	63.295	No	82.549	90.250	86.399	No
63.295	67.146	65.220	No	82.549	86.399	84.474	No
65.220	67.146	66.183	Yes	82.549	84.474	83.511	Yes
65.220	66.183	65.702	Yes	83.511	84.474	83.993	Yes
65.220	65.702	65.461	Yes	83.993	84.474	84.233	No
65.220	65.461	65.341	No	83.993	84.233	84.113	Yes
65.341	65.461	65.401	Yes	84.113	84.233	84.173	No
65.341	65.401	65.371	No	84.113	84.173	84.143	No
65.371	65.401	65.386	Yes	84.113	84.143	84.128	No
65.371	65.386	65.378	Yes	84.113	84.128	84.120	Yes
65.371	65.378	65.375	Yes	84.120	84.128	84.124	Yes

2. Molecular design

Based on the problem data and constraints, 15 first-order groups are pre-selected from the group table in Marrero and Gani (2004). Furthermore, nine second-order groups and four third-order groups were screened out. The results are listed in Table 3.4.

Table 3.4 Numbered preselected groups

1st Order Group					2nd Order group	
Group	No.	Group	No.		Group	No.
CH_3	1	$CHNH_2$	9		$(CH_3)_2CH$	21
CH_2	2	CH_3NH	10		$(CH_3)_3C$	22
CH	3	CH_2NH-	11		$CH(CH_3)CH(CH_3)$	23
OH	4	CHNH	12		$CH(CH_3)C(CH_3)_2$	24
CH_3-O-	5	C	13		$C(CH_3)_2C(CH_3)_2$	25
CH_2-O-	6	C-O-	14		CHOH	26
CH-O-	7	-OCH_2CH_2OH	15		COH	27
CH_2NH_2	8	g^e (Empty group)	16		$CH_m(OH)CH_n(OH)$ (m,n, 0..2)	28
					$CH_m(OH)CH_n(NH_p)$ (m,n,p, 0..2)	29

3rd Order Group	No.
$NH_2(CHn)_mOH$ (m>2, n in 0..2)	31
$HO(CH_n)_mOH$ (m>2, n in 0..2)	32
$HO(CH_p)_k$-O-$(CH_n)_mOH$ (m,k>0, p,n in 0..2)	33
$HO(CH_p)_k$-NH_x-$(CH_n)_m$-OH (m,k>0, p,n,x in 0..2)	34

The corresponding functions of left hand side expressions of Eq. (3.1) are

$$\phi_1(T_m) = \exp(T_m / T_{m0}) \tag{3.35}$$

$$\phi_2(T_b) = \exp(T_b / T_{b0}) \tag{3.36}$$

$$\phi_3(T_c) = \exp(T_c / T_{c0}) \tag{3.37}$$

$$\phi_4(H_v) = H_v - H_{v0} \tag{3.38}$$

$$\phi_5(H_{fus}) = H_{fus} - H_{fus0} \tag{3.39}$$

where T_{m0}, T_{b0}, T_{c0}, H_{v0} and H_{fus0} are constants with the values of 147.450K, 222.543K, 231.239K, 11.733kJ/mol and -2.806kJ/mol respectively. Based on these functions, the converted QBFR values for Eq. (3.1) are listed in table 3.5.

Table 3.5 QBFR conversion for group contribution function

	$\phi_1(T_m)$	$\phi_2(T_b)$	$\phi_3(T_c)$	$\phi_4(H_v)$	$\phi_5(H_{fus})$
Minimum	-	8.64	19.88	72.392	22.006
Maximum	7.30	-	22.16	53.642	16.520

Since, multiple solutions (feasible group sets) can be found, integer cuts are used to generate all feasible molecules. Each time a solution is found, an integer cut is added to restrict the solution from generating the solution again. The process is continued until no feasible solution is found which indicates that all integer solutions have been identified. Following the proposed procedure, one feasible molecule was identified. Its molecular structure is given by: $C_4H_{11}NO_2$. It is worth noting that two isomers may be generated for the molecules. Both isomers are given by Fig. 3.3. The two isomers may be named as N-Methyl-2,3-dihydroxyethylamine and N-Ethyl-1,2-dihydroxyethylamine respectively.

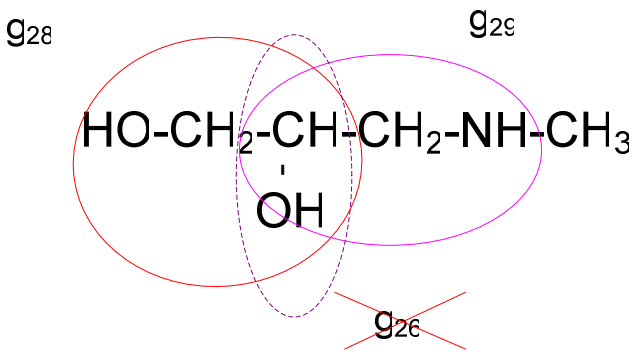

(a)

and

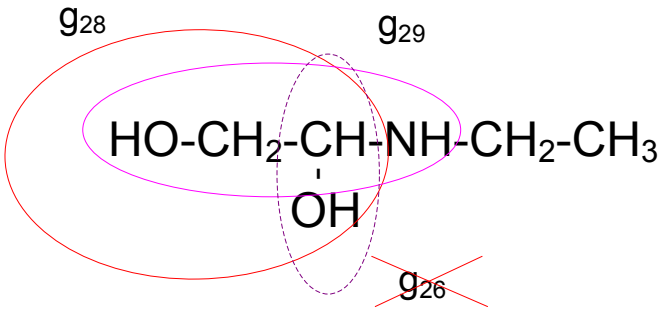

(b)

Figure 3.3 Structures of synthesized isomers.
(a) N-Methyl-2,3-dihydroxyethylamine
(b) N-Ethyl-1,2-dihydroxyethylamine

As we mentioned before, the QBFR is an overestimation of the actual feasibility region. Therefore, it is important to insure that the synthesized molecule satisfy the original set of constraints. By using Eq. (3.35) – (3.39), the group contribution values of these molecules are converted into the raw property values listed in Table 3.6. These values are indeed feasible with respect to the original constraints of the problem.

Table 3.6 Properties of $C_4H_{11}NO_2$

$C_4H_{11}NO_2$	T_m (K)	T_b(K)	T_c(K)	H_v(kJ/mol)	H_{fus} (kJ/mol)
	292.92	518.10	698.81	79.76	18.56

3. Process design

Finally, the synthesized molecule is used in the optimization formulation for the source-sink allocation. No economic data were found for the synthesized molecule. Therefore, the objective function was selected to minimize the flowrate of the fresh solvent. The mathematical formulation is a linear program which can be solved globally to get the following solution.

$Fr_{f,1}$=153.9814; $Fr_{f,2}$=85.38791; $Fr_{f,3}$=187.8055; $Fr_{f,4}$=122.8251; $Fr_{f,5}$=170.0000; $f_{1,1}$ =20.63066; $f_{1,4}$ =39.36934; $f_{2,1}$ =25.38791; $f_{2,2}$=64.61209; $f_{3,3}$ =42.19445; $f_{3,4}$=27.80555; $f_{4,2}$=60.00000. The results are shown graphically using Figure 3.4.

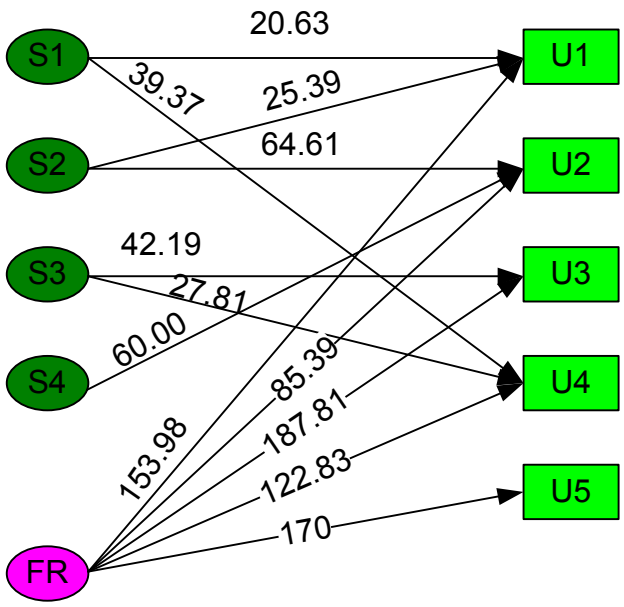

Figure 3.4 Optimal source-sink allocation

3.5 Conclusions

This chapter introduced a new property-based mathematical programming technique to integrate process and molecular design. This approach decomposed the process and molecular design tasks. Feasibility-region targeting for molecular design is obtained by solving optimization programs based on the process constraints and a framework for recycling process sources to sinks. As a result, the boundaries of the feasibility region in the property domain are determined. Next, molecular design techniques are used to generate a set of candidate molecules. Group contribution methods are used to relate properties to structures. Initially, first-order groups are used to tighten the search space. Next, second- and third-order groups are used to provide more accurate estimates of the properties. The synthesized molecules are returned back to the process design problem where a linear program is globally solved to determined the minimum cost of the system, the type and flowrate of the fresh resources (external molecules), and the allocation of fresh and process sources to sinks. Various insights are used to accelerate the computational scheme and gear it towards the global solution.

CHAPTER IV
GENERAL IMPLEMENTATION APPROACH FOR DIRECT-RECYCLE NETWORKS DESIGN WITH ONE DOMINANT PROPERTY

4.1 Introduction

In direct-recycle problems (such as the one addressed in Chapter II), the first step is typically to identify the target for minimum fresh usage, maximum recycle, and minimum waste discharge. It is worth noting that for a given target, there are normally multiple implementations (infinite in many cases) that can reach the target. Therefore, it is important to develop an approach for identifying the various implementations of a target. Considering the source-sink mapping representation intended to minimize the usage of fresh or valuable resources for the system with one dominant property, a special case of this problem is material recycle problems with one limiting component where the composition serves as the special case of property.

In general, the targeting techniques are categorized into three groups of methods: graphical techniques (GT), algebraic techniques (AT), and mathematical programming techniques (MPT). The GT is mainly applied to systems with one dominant property. This case is encountered when satisfying the constraints for one (key or limiting) property implies the satisfaction of constraints for other properties. Another case is when multiple components are lumped into one property such as total organic carbon (TOC), biochemical oxygen demand (BOD), and the chemical oxygen demands (COD). El-Halwagi and Manousiouthakis (1989) introduced a GT pinch analysis to the problem of synthesizing mass exchange networks (MENs) that seeks to transfer certain species from a set of rich streams to a set of lean streams. By extending the MEN pinch analysis to water networks, Wang and Smith (1994) proposed a graphical approach to effectively target minimum freshwater use and wastewater discharge. Following that work, several methods were proposed to locate the pinch points for recycle/reuse networks and to target minimum fresh usage ad minimum wastewater discharge. Examples include the

material recovery pinch analysis for targeting for recycle/ reuse networks developed by El-Halwagi et al (2003). This approach provides a non-iterative, systematic and graphical targeting technique. Other examples include the work of Aly et al. (2005) which used the load problem table for water network design, and the work of Vasilik and El-Halwagi (2005) which successfully extended the application of graphical techniques into property based system design. Generally, a GT gives the designers insights which allow engineers to incorporate many factors that are not easily incorporated into mathematical programs. However, so far a typical GT is essentially a targeting method to find the minimum fresh usage rather than an implementation method for network design. Normally, heuristic rules were used to generate one or more network configurations. On the other hand, MPTs offer the powerful capability to solve complex system with high number of unit operations (e.g., Savelski and Bagajewicz, 2000), including multicomponent systems (e.g., Alva-Argaez et al.,1999; Benko et al., 2000; and Dunn et al., 2001a, 2001b), and unsteady-state and batch systems (e.g., Wang and smith, 1995; Almato et al., 1997; and Zhou et al., 2001). Various methods for solving water network problems have been reviewed by Bagajewicz (2000). Notwithstanding the capability of MPTs, they give only one solution at a time. To get alternative solutions with various network implementations, the designer has to add some constraints (typically, integer cuts) to avoid repeating previous solution. Successive solutions generate alternate configurations. For systems with numerous (or infinite) solutions, the MPTs become cumbersome or even ineffective. Therefore, given the current limitations of GTs and MPTs, it is highly desirable to develop a systematic approach for identifying alternate configurations for recycle/reuse process network systems. In particular, we focus on systems with one dominant property with the objective of addressing the following questions:

1. How many configurations are there for the direct recycle network system?
2. Under what conditions does this system have unique versus infinite solutions?

3. If there are infinite solutions, are there any relations among them? If yes, what are those relations?

4.2 Problem Statement

Consider the material recycle problem described as follows:

Given is a set of process sinks (units) which is designated by SINKS (U) = {j = 1, 2, ..., n, ...N_{sinks}}. Each sink requires a feed with a given flow rate, G_j, and the value of a single targeted composition, z_j, must satisfy the following constraint

$$z_j^{sinkmin} \leq z_j^{\text{sink}} \leq z_j^{sinkmax} \qquad j \in SINKS \qquad (4.1)$$

where $z_j^{sinkmin}$ and $z_j^{sinkmax}$ are given lower and upper bounds, respectively, on the admissible value of property of the feed entering unit j and z_j^{sink} is the actual value of the property entering unit j.

Given also is the set SOURCES which is a set of streams or sources. The sources include fresh (or external) streams and process sources. A fresh (external) resource purchased or synthesized to supplement the use of process sources in sinks and a set of process sources that can be recycled/reused in process sinks were designated SOURCES (S) ={i = *1, 2, ..., m,...,* $N_{LAS,}$ ..., N_{sources}}, with i=*1* representing fresh resources. Each process source has a given flow rate, F_i, and a given property, z_i.

The objective is to develop a systematic procedure to:

1. Derive the conditions that determine whether or not there are unique implementation(s) for the recycle-reuse network(s) that feature the minimum usage of fresh resource.
2. For the case of infinite implementations, determine a parametric method to guide the assignment of sources to sinks

4.3 Theoretical Analysis

The analysis is based on setting up the algebraic equations that correspond to the optimum allocation of sources to sinks then identifying the mathematical conditions for

unique solutions. Next, an approach will be developed to describe the source-sink assignment in terms of parameters whose values can be bounded.

4.3.1 Insights from Pinch Analysis

In order to determine minimum fresh usage for recycle/reuse problems, El-Halwagi et al. (2003) developed the material recovery pinch analysis. This is a non-iterative graphical approach which determines the targets for minimum fresh usage, maximum recycle of process sources, and minimum waste discharge. These targets are determined without commitment to any network configuration. This pinch analysis utilizes two optimality criteria: the source prioritization rule and the sink maximization rule. The source prioritization rule implies that process sources must be used in ascending order of the impurity composition. The sink maximization rule indicates that when a fresh source is used in a sink, its composition must be set to the maximum.

After targeting the system, the next task is to configure the network system, primarily assigning sources to sinks. So far, this task has been carried out subjectively. Also, since there may be infinite feasible implementations, there is a need to determine whether or not there are unique solutions.

In order to develop an implementation for the identified target, it is useful to identify the following insights from the pinch diagram (as shown by Fig. 4.1):

1. The pinch diagram may be classified into two regions: one below the pinch and one above the pinch. It is worth noting that below the pinch, there is complete closure of balances for flowrates and for loads. In other words, below the pinch, the sum of flowrates of used sources equals the sum of flowrate demands of sinks. Also, below the pinch, the sum of impurity loads of used sources equals the sum of the maximum admissible loads of impurities of the sinks. Therefore, the region below the pinch will be referred to as a closed system. In some cases, there may be more than one pinch point. If there are multiple pinches, then the region between each two consecutive pinches will be referred to as a closed system. Above the pinch (or above the

highest pinch in case of multiple pinches), while there is balance for flowrates of sources and demands of sinks, there is no balance for the loads. In other words, above the pinch, the sum of impurity loads of used sources is less than the sum of the maximum admissible loads of impurities of the sinks. Therefore, the region above the pinch will be referred to as an open system.

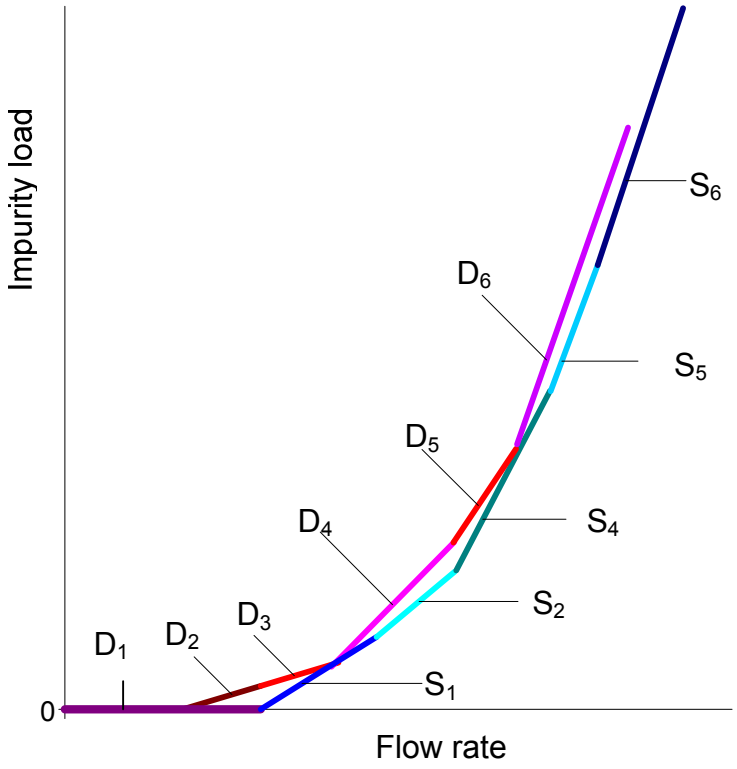

Figure 4.1 Schematic representation for material recovery pinch analysis

Next, we describe the abovementioned observations mathematically.

2. For a closed system,

a. Total flow rate of sinks and sources are equal, i.e.

$$\sum_{j=1}^{n} G_j = \sum_{i=1}^{m_1} F_i \tag{4.2}$$

b. Total property load of sinks and sources are equal, i.e.

$$\sum_{j=1}^{n} G_j z_j^{\text{sink}} = \sum_{i=1}^{m_1} F_i z_i \tag{4.3}$$

where n is the number of sinks involved in the closed system, and source *m* is the pinched source which was split into two substreams: one below the pinch (given an index m_1) and one above the pinch (given an index m_2),

3. For an open system,

a. Equality of total flow rate of sinks and active sources

$$\sum_{j=n+1}^{N_{\text{sinks}}} G_j = \sum_{i=m_2}^{N_{LAS1}} F_i \tag{4.4}$$

b. Total property load of sinks (maximal capability) is larger than that of the total sources used

$$\sum_{j=n+1}^{N_{\text{sinks}}} G_j z_j^{\text{sink}} > \sum_{i=m_2}^{N_{LAS1}} F_i z_i \tag{4.5}$$

where N_{LAS} is the last active (recycled/reused) source. This source is split into N_{LAS1} (which is recycled/reused) and N_{LAS2} (which is discharged as waste).

4.3.2 Analyzing the Set of Linear Algebraic Equations

In this section, the set of equations corresponding to the pinch diagram and the optimality criteria will be analyzed for both a closed system and an open system.

1. Analysis of a Closed System

First, the recycle/reuse network is schematically described through a source-sink mapping representation as shown by Figure 4.1. Consider source i below the pinch. The source is split into n fractions. Each fraction ($x_{i,j}$) is assigned to sink j. Based on the observations from the pinch diagram, the following flow and load balances may be written:

$$G_j = \sum_{i=1}^{m_1} F_i x_{i,j} \qquad j=1, 2, \ldots, n \tag{4.6}$$

where $x_{i,j}$ is the fraction of source *i* flowing into sink *j*.

The load balance is written as follows:

$$G_j z_j^{\text{sink}} = \sum_{i=1}^{m_1} x_{i,j} F_i z_i \qquad j=1, 2, \ldots, n \tag{4.7}$$

By definition, the sum of fractions is one, i.e.

$$\sum_{j=1}^{n} x_{i,j} = 1 \qquad i=1, 2, \ldots, m_1 \tag{4.8}$$

where

$$0 \le x_{i,j} \le 1 \tag{4.9}$$

The set of equations (4.7) - (4.9) are $2n + m_1$ linear equations which can be represented by the general form **AX=B**, The following representation is based on listing the load balance then the flow balance for each sink then listing the set of equations (4.8) for all the sources, i.e.,

$$\begin{bmatrix}
F_1 z_1 & 0 & \cdots & \cdots & 0 & \cdots & F_i z_i & 0 & \cdots & \cdots & 0 & \cdots & F_{m_1} z_{m_1} & 0 & \cdots & \cdots & 0 \\
F_1 & 0 & \cdots & \cdots & 0 & \cdots & F_i & 0 & \cdots & \cdots & 0 & \cdots & F_{m_1} & 0 & \cdots & \cdots & 0 \\
\vdots & & & & & \vdots & & & & & & \vdots & & & & & \vdots \\
0 & \cdots & F_1 z_1 & \cdots & 0 & \cdots & 0 & \cdots & F_i z_i & \cdots & 0 & \cdots & 0 & \cdots & F_{m_1} z_{m_1} & \cdots & 0 \\
0 & \cdots & F_1 & \cdots & 0 & \cdots & 0 & \cdots & F_i & \cdots & 0 & \cdots & 0 & \cdots & F_{m_1} & \cdots & 0 \\
\vdots & & & & & \vdots & & & & & & \vdots & & & & & \vdots \\
0 & \cdots & \cdots & 0 & F_1 z_1 & \cdots & 0 & \cdots & \cdots & 0 & F_i z_i & \cdots & 0 & \cdots & \cdots & 0 & F_{m_1} z_{m_1} \\
0 & \cdots & \cdots & 0 & F_1 & \cdots & 0 & \cdots & \cdots & 0 & F_i & \cdots & 0 & \cdots & \cdots & 0 & F_{m_1} \\
1 & \cdots & \cdots & \cdots & 1 & \cdots & 0 & \cdots & & & & & & & & & 0 \\
\vdots & & & & & \vdots & & & & & & \vdots & & & & & \vdots \\
0 & \cdots & & & 0 & \cdots & 1 & \cdots & \cdots & \cdots & 1 & \cdots & 0 & \cdots & & & 0 \\
\vdots & & & & & \vdots & & & & & & \vdots & & & & & \vdots \\
0 & \cdots & & & 0 & \cdots & 0 & \cdots & & & 0 & \cdots & 1 & \cdots & & & 1
\end{bmatrix}
\begin{bmatrix}
x_{1,1} \\ x_{1,2} \\ \vdots \\ \vdots \\ x_{1,n} \\ \vdots \\ x_{i,1} \\ x_{i,2} \\ \vdots \\ \vdots \\ x_{i,n} \\ \vdots \\ x_{m_1,1} \\ x_{m_1,2} \\ \vdots \\ \vdots \\ x_{m_1,n}
\end{bmatrix}
=
\begin{bmatrix}
G_1 z_1^{\text{sink}} \\ G_1 \\ \vdots \\ G_j z_j^{\text{sink}} \\ F_j \\ \vdots \\ G_n z_n^{\text{sink}} \\ G_n \\ 1 \\ \vdots \\ 1 \\ \vdots \\ 1
\end{bmatrix}$$

(4.10)

The general solution of this set of linear equations system and the rank of the matrix A can be determined by the Gaussian elimination methods. This method forms an augmented matrix and reduces it to a row canonical form (also known as the reduced row echelon form "RREF"). The procedure determines the number of non-zero rows in

the RREF, referred to as *w*. To have a solution, *w* must be less than or equal to the number of unknowns (which is given by $m_1 n$). Therefore, we have the following two cases:

a. If $w < m_1 n$, then the closed system will give a number equal to $m_1 n$-w parameteric families of solutions.

b. If $w = m_1 n$, then the closed system will have a unique solution.

By recalling the insights from the pinch diagram given by Eqs. (4.2) and (4.3), we deduce that there are two linearly dependent equations in the aforementioned set of equations: **AX=B**. This observation can be mathematically shown by taking impurity load balances for example as follows:

For the first n-1 sink, we have:

$$\sum_{i=1}^{m_1} x_{i,1} F_i z_i = G_1 z_1^{\text{sink}} \tag{4.11}$$

$$\vdots$$

$$\sum_{i=1}^{m_1} x_{i,n-1} F_i z_i = G_{n-1} z_{n-1}^{\text{sink}} \tag{4.12}$$

The summation of these first *n-1* linear equations is

$$\sum_{i=1}^{m_1} \sum_{j=1}^{n-1} x_{i,j} F_i z_i = \sum_{j=1}^{n-1} G_j z_j^{\text{sink}} \tag{4.13}$$

which can be rewritten as

$$\sum_{i=1}^{m_1} F_i z_i \sum_{j=1}^{n-1} x_{i,j} = \sum_{j=1}^{n-1} G_j z_j^{\text{sink}} \tag{4.14}$$

Plugging Eq. (4.8) into Eq. (4.14), we have

$$\sum_{i=1}^{m_1} F_i z_i (1 - x_{i,n}) = \sum_{j=1}^{n-1} G_j z_j^{\text{sink}} \tag{4.15}$$

Rearranging, Eq. (4.15) becomes

$$\sum_{i=1}^{m_1} x_{i,n} F_i z_i = \sum_{i=1}^{m_1} F_i z_i - \sum_{j=1}^{n-1} G_j z_j^{\text{sink}} \tag{4.16}$$

Put Eq. (4.3) into Eq. (4.16), it turns out Eq. (4.17)

$$\sum_{i=1}^{m_1} x_{i,n} F_i z_i = G_n z_n^{\text{sink}} \tag{4.17}$$

which is the equation representing load balance of sink *n* in the system **AX=B**. Similarly, if *n-2* sinks are taken into consideration, it is impossible to derive the equations expressing flow rate balance for sink *n-1* and *n*. Therefore, among the *n* equations based on load balance, there is one linearly dependent equation. In another words, there are *n-1* linearly independent equations based on property load balance in **AX=B**.

The same procedure can be used for identifying the other linearly dependent equation derived from the flow balance.

The above analysis indicates that there are $2n+m_1-2$ linearly independent equations while the number of variables in this system is nm_1.

The condition for unique solution in the closed system is given by:

$$2n+m_1-2 = nm_1 \tag{4.18a}$$

Rearranging and simplifying this equation, we get:

$$(n-1)(m_1-2) = 0 \tag{4.18b}$$

Therefore, to have a unique solution of implementing the minimum fresh network, the following conditions must hold below the pinch:

$$m_1=2 \text{ and/or } n=1 \tag{4.18c}$$

On the other hand, the condition for infinite solutions is given by:

$$2n+m_1-2 < nm_1$$

i.e.

$$m_1 > 2 \text{ while } n>1 \tag{4.19}$$

2. Parametric Characterization of Infinite Solutions

In the case of having infinite solutions, it is useful to have a way of characterizing all possible implementations. First, the degrees of freedom for the equations below the pinch are given by the difference between the number unknowns and the number of independent equations, i.e.

$$\text{Degrees of freedom} = nm_1 - 2n+m_1-2$$

$$= (n-1)(m_1-2) \tag{4.20}$$

Therefore, if the number of degrees of freedom are parametrically fixed, i.e.,

$N_{parameter}=(n-1)(m_1-2)$ (4.21)

then, the solution can be fully characterized. Hence,

$$x_{i,j} = a_{1i,j} + b_{1i,j}P_1 + b_{2i,j}P_2 + \cdots + b_{(n-1)(m_1-2)i,j}P_{(n-1)(m_1-2)} \quad (4.22)$$

where $a_{1i,j}, b_{1i,j}, b_{2i,j}, \cdots, b_{(n-1)(m_1-2)i,j}$ are coefficient and $P_1, P_2, \ldots, P_{(n-1)(m1-2)}$ are parameters which can be chosen from $x_{i,j}$ where i is from 1 to m_1 and j is from 1 to n. Each parameter will satisfy the physical constraints of inequality (4.8) and their values can be further confined through the relations of variables, because every variable $x_{i,j}$ should also satisfy the inequality (4.8). For systems with one degree of freedom, the exact range for the values of the parameter can be easily solved (see example 4.1). On the other hand, if the system has several degrees of freedom, the range of the value of individual parameter can be determined by linear programming. However, because of the strong interaction among these parameters, when one or some parameters take certain values, the ranges of other parameters may be narrower than the individual range given by linear programming. To address this problem, the lexicographical concept (i.e. choosing a priority sequence of the parameters) is invoked to build a tower structure used for parameter-value determination. For example, we choose a priority sequence of the parameters as $P_1, P_2, \ldots, P_{(n-1)(m1-2)}$. Linear programming will give the maximum and minimum value of P_1. Choosing one value for P_1, the maximum and minimum value of P2 under this specific P1 value can be acquired. The range of successive parameter is determined under the condition of the chosen previous parameter values. This procedure can be illustrated through a tower structure (named as Tower Model) in Figure 4.2.

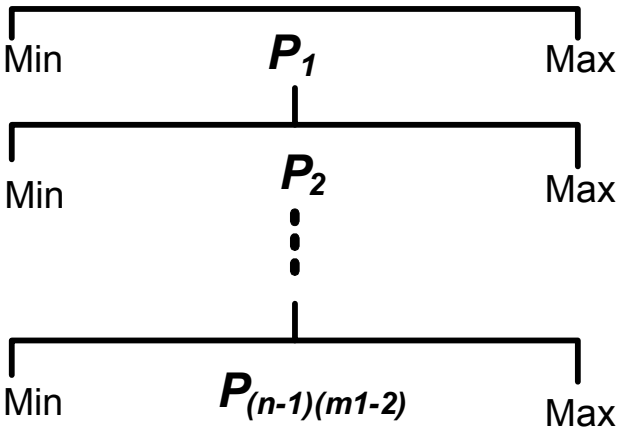

Figure 4.2 Tower Model for parameter value determination

3. Open System

An open system is not as rigorous as the closed system, because of the inequality (4.5). This gives the designers some flexibility to configure the network. However, it may approach the rigor of closed system when the last active source (m_{LAS}) approaches the ending point of the sink composite. In this case, a guideline is desired to ensure appropriate design. Here, we introduce a proxy source m_{proxy} for m_{LAS1} (the part of the last active source flow into sinks). Source m_{proxy} is formed by connecting the tail of m_{LAS} (head of source m_{LAS}-*1*) and the head of sink N_{sinks} as shown in Figure 4.3 (the closed system is omitted from this figure for simplification).

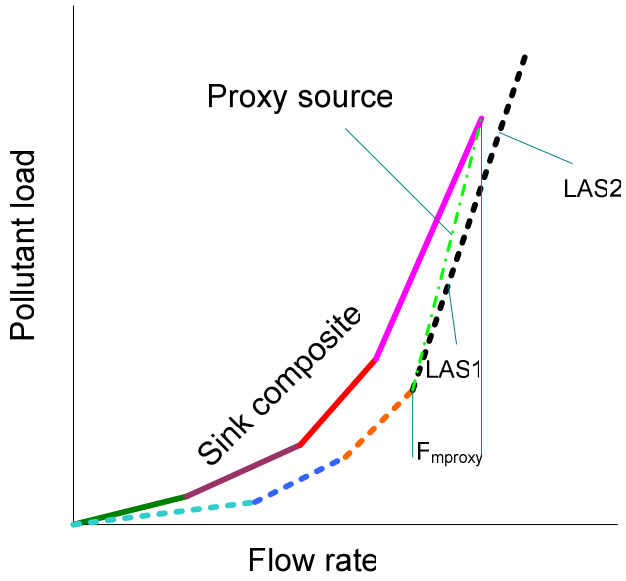

Figure 4.3 Schematic representation of an open system

For the proxy source, there are the following equations

$$F_{m_{proxy}} = F_{m_{LAS1}} = \sum_{j=n+1}^{N_{sinks}} G_j - \sum_{i=m_2}^{m_{LAS1}-1} F_i \tag{4.23}$$

and

$$z_{m_{proxy}} = \left(\sum_{j=n+1}^{N_{sinks}} G_j z_j^{sink} - \sum_{i=m_2}^{m_{LAS1}-1} F_i z_i \right) / F_{m_{Proxy}} \tag{4.24}$$

with

$$z_{m_{proxy}} > z_{m_{LAS1}} \tag{4.25}$$

With the proxy stream, a closed system is constructed. Applying the exact same procedure for the closed system developed above, one can get solutions of the proxy closed system. Designs based on the relations used for the proxy closed system are also applicable for the open system. The applicability is justified below.

According to the problem statement, for every sink of the network system, it is required that

$$G_j z_j^{sink} \geq \sum_{i=1}^{m_{LAS1}} x_{i,j} F_i z_i \tag{4.26}$$

For a closed system, the corresponding formula is Eq. (4.6) whereas for an open system, the formula is

$$G_j z_j^{\text{sink}} \geq \sum_{i=m_2}^{m_{LAS1}} x_{i,j} F_i z_i \tag{4.27}$$

Using source m_{LAS1} instead of the proxy source to configure the open system, i.e. $x_{m_{LAS1},j} = x_{m_{proxy},j}$, we have

$$\begin{aligned} G_j z_j^{\text{sink}} &= \sum_{i=m_2}^{m_{procy}} x_{i,j} F_i z_i = \sum_{i=m_2}^{m_{proxy}-1} x_{i,j} F_i z_i + x_{m_{proxy},j} F_{m_{proxy}} z_{m_{proxy}} \\ &> \sum_{i=m_2}^{m_{LAS1}-1} x_{i,j} F_i z_i + x_{m_{LAS1},j} F_{m_{LAS1}} Z_{m_{LAS1}} = \sum_{i=m_2}^{m_{LAS1}} x_{i,j} F_i z_i \end{aligned} \tag{4.28}$$

which is

$$G_j z_j^{\text{sink}} > \sum_{i=m_2}^{m_{LAS1}} x_{i,j} F_i z_i \tag{4.29}$$

where both m_{proxy}-*1* and m_{LAS1}-*1* have the same meaning for indicating the number of sources involved in the system.

Comparing inequalities (4.27) and (4.29), we notice that inequality (4.29) fully satisfy the constraints expressed by inequality (4.27). Therefore, designs based on the relations used for the proxy closed system are always applicable for the open system in which the last active source is used instead of proxy source. We name the solutions given by this method quasi-general solution of an open system.

In summary, the implementation for a recycle/reuse network design can be carried out using the following procedure:

(1) Develop a material recovery pinch analysis for the whole recycle/reuse network; divide the network into closed systems and an open system.

(2) Formulate linear algebraic equations for closed systems

(3) Identify the general solutions for closed systems through RREF of the augmented matrix formed upon the linear algebraic equations.

(4) Determine the ranges of the parameters in the general solution

(5) Design the closed systems with the solutions attained from step 2 and 3.

(6) Design the open system. If it is very relaxed system, design the open system by simple inspection; if it is very complex and/or it approaches the closed system, use the method for proxy closed system, which is very similar to closed system design, to get the quasi-general solutions.

(7) Integrate the closed systems and open system into a whole network.

4.4 Case Study

To show the significance of this approach, we address two case studies from literature.

4.4.1 Example 4.1: Water Minimization

This case study is taken from Sorin and Bedard (1999). El-Halwagi et al. (2003) and Aly et al. (2005) restudied it by pinch analysis approaches. The data for the problem are shown in Table 4.1.

Table 4.1 Data for example 4.1

Sink (S)	Flow (tonne/h)	Maximum inlet impurity (ppm)	Load (kg/h)
1	120	0	0
2	80	50	4
3	80	50	4
4	140	140	19.6
5	80	170	13.6
6	195	240	46.8
Source (D)	Flow (tonne/h)	Impurity (ppm)	Load (kg/h)
Fresh	?	0	0
1	120	100	12
2	80	140	11.2
3	-	-	-
4	140	180	25.2
5	80	230	18.4
6	195	250	48.75

The pinch analysis shows that this system has three closed systems and one open system (Figure 4.1).

In the first closed system, because sink 1 can only accept fresh water, no recycled source is accepted. The demand of the fresh water is 120 tonne/h.

The second closed system includes two sources: fresh water with F_{fresh}= 80 tonne/h and S_{11} with F_{11}=80 tonne/h (S_1 was split into two parts S_{11} and S_{12}. In the case study, the first digit of the two digit subscript denotes original stream number and the second digit denotes substream number from stream splitting) and two sinks: D_2 and D_3.

According to the develop procedure and conditions, the linear equation system is

$$\begin{bmatrix} 80*0 & 0 & 80*100 & 0 \\ 80 & 0 & 80 & 0 \\ 0 & 80*0 & 0 & 80*100 \\ 0 & 80 & 0 & 80 \\ 1 & 1 & 0 & 0 \\ 0 & 0 & 1 & 1 \end{bmatrix} \begin{bmatrix} x_{fresh,2} \\ x_{fresh,3} \\ x_{11,2}^2 \\ x_{11,3} \end{bmatrix} = \begin{bmatrix} 80*50 \\ 80 \\ 80*50 \\ 80 \\ 1 \\ 1 \end{bmatrix}$$

The augmented matrix is formed and reduced RREF: $\begin{bmatrix} 1 & 0 & 0 & 0 & 0.5 \\ 0 & 1 & 0 & 0 & 0.5 \\ 0 & 0 & 1 & 0 & 0.5 \\ 0 & 0 & 0 & 1 & 0.5 \\ 0 & 0 & 0 & 0 & 0 \\ 0 & 0 & 0 & 0 & 0 \end{bmatrix}$

Consequently, there is unique solution for the first closed system which is given by $(x_{fresh,2}, x_{fresh,3}, x_{11,2}, x_{11,3}) = (0.5,0.5,0.5,0.5)$.

Next, we move to the third closed system which includes three sources S_{12}, $S_{2,}$ and S_{41} (S_4 was split into two parts S_{41} and S_{42}) with flow rates of 40, 80, and 100 tonnes/h respectively, and two sinks D_4 and D_5.

According to Eq. (4.20), the solution for this closed system has one parametric family of solutions. The linear equations for this system are

$$\begin{bmatrix} 40*100 & 0 & 80*140 & 0 & 100*180 & 0 \\ 40 & 0 & 80 & 0 & 100 & 0 \\ 0 & 40*100 & 0 & 80*140 & 0 & 100*180 \\ 0 & 40 & 0 & 80 & 0 & 100 \\ 1 & 1 & 0 & 0 & 0 & 0 \\ 0 & 0 & 1 & 1 & 0 & 0 \\ 0 & 0 & 0 & 0 & 1 & 1 \end{bmatrix} \begin{bmatrix} x_{12,4} \\ x_{12,5} \\ x_{2,4} \\ x_{2,5} \\ x_{41,4} \\ x_{41,5} \end{bmatrix} = \begin{bmatrix} 140*140 \\ 140 \\ 80*80 \\ 80 \\ 1 \\ 1 \\ 1 \end{bmatrix}$$

The RREF for the corresponding augmented matrix is $\begin{bmatrix} 1 & 0 & 0 & 0 & 0 & 2.5 & 2.5 \\ 0 & 1 & 0 & 0 & 0 & -2.5 & -1.5 \\ 0 & 0 & 1 & 0 & 0 & -2.5 & -0.75 \\ 0 & 0 & 0 & 1 & 0 & 2.5 & 1.75 \\ 0 & 0 & 0 & 0 & 1 & 1 & 1 \\ 0 & 0 & 0 & 0 & 0 & 0 & 0 \\ 0 & 0 & 0 & 0 & 0 & 0 & 0 \end{bmatrix}$

Taking $x_{41,5}$ as the parameter, then

$x_{41,4} = 1 - x_{41,5}$

$x_{2,5} = 1.75 - 2.5x_{41,5}$

$x_{2,4} = 2.5x_{41,5} - 0.75$

$x_{12,5} = 2.5x_{41,5} - 1.5$

$x_{12,4} = 2.5 - 2.5x_{41,5}$

Applying physical constraints, i.e. $0 \le x_{i,j} \le 1$ to this solution, we have

$0 \le x_{41,5} \le 1$

$0.3 \le x_{41,5} \le 0.7$

$0.5 \le x_{41,5} \le 0.7$

$0.6 \le x_{41,5} \le 1$

$0.6 \le x_{41,5} \le 1$

Hence, the range for parameter $x_{41,5}$ is [0.6, 0.7].

In summary, for this example, the following guidelines must be used in designing the network:

F_{fresh}=120 tonne/h for D_1,

F_{fresh}=80 tonne/h for D_2 and D_3 with each one have 50%,

F_1 = 80 tonne/h for D_2 and D_3 with each one have 50%,

F_1, F_2, and F_4 for D_4 and D_5 based on the relations of

$$f_{41,4} = 100(1 - x_{41,5})$$

$$f_{2,5} = 80(1.75 - 2.5x_{41,5})$$

$$f_{2,4} = 80(2.5x_{41,5} - 0.75)$$

$$f_{12,5} = 40(2.5x_{41,5} - 1.5)$$

$$f_{12,4} = 40(2.5 - 2.5x_{41,5})$$

where $0.6 \leq x_{41,5} \leq 0.7$.

The general network configuration is illustrated in Figure 4.5.

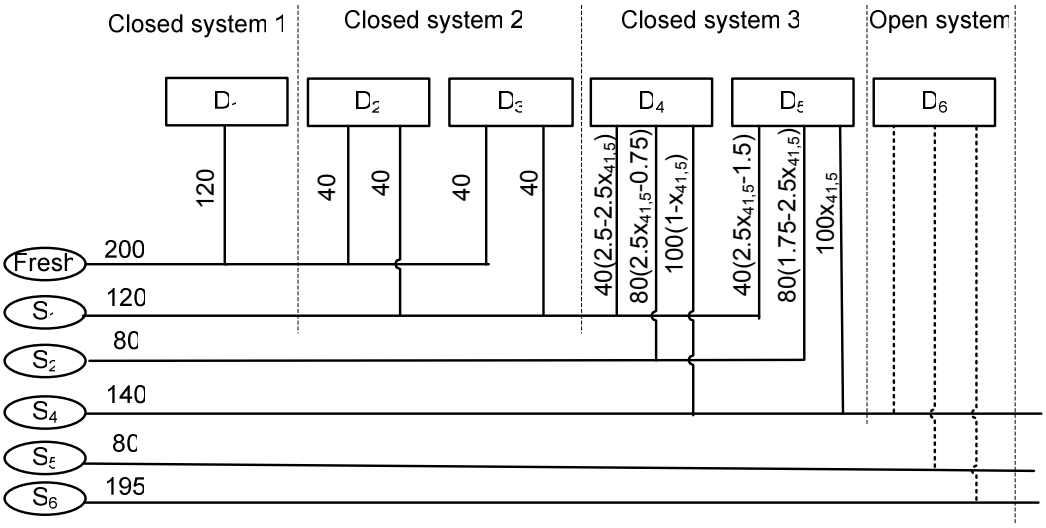

Figure 4.4 General network configuration for example 4.1

When the value of $x_{41,5}$ is selected to be 0.7, the solution configurations match those given by Sorin and Bedard (1999) and Aly et al. (2005) .

4.4.2 Example 4.2: Water Recycle

This example is taken from Polley and Polley (2000). It was also restudied by El-Halwagi et al. (2004) and Aly et al. (2005). The source and sink data are shown in Table 4.2.

Table 4.2 Process information for example 4.2

Sink (U)	Flow (tonne/h)	Maximum inlet impurity (ppm)	Load (kg/h)
1	50	20	1
2	100	50	5
3	80	100	8
4	70	200	14
Source (S)	Flow (tonne/h)	Impurity (ppm)	Load (kg/h)
Fresh	Fresh water	0	0
1	50	50	2.5
2	100	100	10
3	70	150	10.5
4	60	250	15

The pinch analysis (Figure 4.5) shows that this network has one closed system and one open system. The closed system consists of four sources: fresh water, S_1, S_2, and S_3 with the flow rate of 70, 50, 100, and 10 tonne/h respectively, and three sinks D_1, D_2 and D_3.

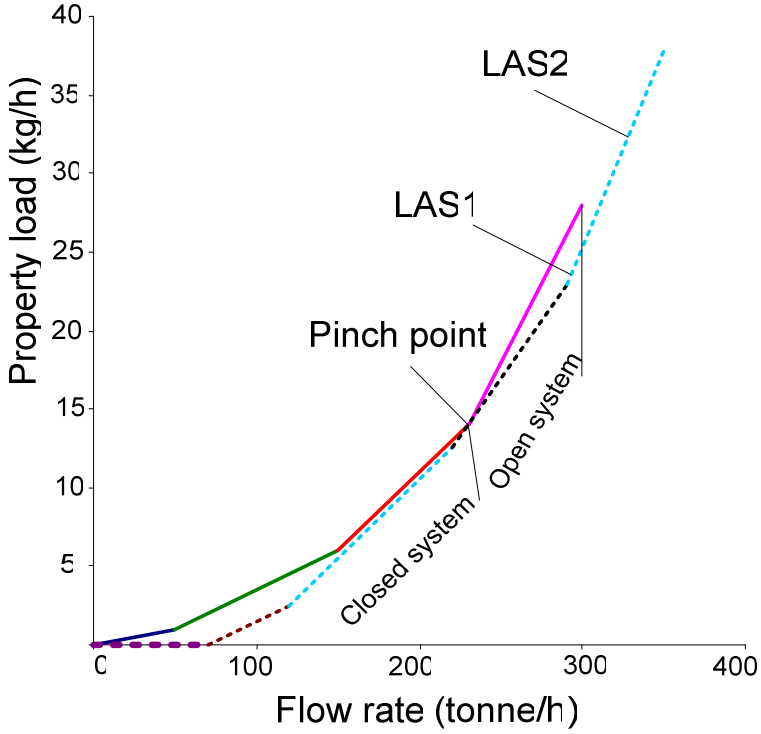

Figure 4.5 Pinch diagram of example 4.2

According to Eq. (4.20), this closed system should have four parametric family of solutions. The linear equations are formed as

$$\begin{bmatrix} 2500 & 0 & 0 & 10000 & 0 & 0 & 1500 & 0 & 0 & 0 & 0 & 0 \\ 50 & 0 & 0 & 100 & 0 & 0 & 10 & 0 & 0 & 70 & 0 & 0 \\ 0 & 2500 & 0 & 0 & 10000 & 0 & 0 & 1500 & 0 & 0 & 0 & 0 \\ 0 & 50 & 0 & 0 & 100 & 0 & 0 & 10 & 0 & 0 & 70 & 0 \\ 0 & 0 & 2500 & 0 & 0 & 10000 & 0 & 0 & 1500 & 0 & 0 & 0 \\ 0 & 0 & 50 & 0 & 0 & 100 & 0 & 0 & 10 & 0 & 0 & 70 \\ 1 & 1 & 1 & 0 & 0 & 0 & 0 & 0 & 0 & 0 & 0 & 0 \\ 0 & 0 & 0 & 1 & 1 & 1 & 0 & 0 & 0 & 0 & 0 & 0 \\ 0 & 0 & 0 & 0 & 0 & 0 & 1 & 1 & 1 & 0 & 0 & 0 \\ 0 & 0 & 0 & 0 & 0 & 0 & 0 & 0 & 0 & 1 & 1 & 1 \end{bmatrix} \begin{bmatrix} x_{1,1} \\ x_{1,2} \\ x_{1,3} \\ x_{2,1} \\ x_{2,2} \\ x_{2,3} \\ x_{31,1} \\ x_{31,2} \\ x_{31,3} \\ x_{fresh1} \\ x_{fresh2} \\ x_{fresh3} \end{bmatrix} = \begin{bmatrix} 1000 \\ 50 \\ 5000 \\ 100 \\ 8000 \\ 80 \\ 1 \\ 1 \\ 1 \\ 1 \end{bmatrix}$$

and the RREF of the augmented matrix is shown as

$$\begin{bmatrix} 1 & 0 & 0 & 0 & 0 & 0 & 0 & 1/5 & 1/5 & 0 & -14/5 & -14/5 & -1 \\ 0 & 1 & 0 & 0 & 0 & 0 & 0 & -1/5 & 0 & 0 & 14/5 & 0 & 2 \\ 0 & 0 & 1 & 0 & 0 & 0 & 0 & 0 & -1/5 & 0 & 0 & 14/5 & 0 \\ 0 & 0 & 0 & 1 & 0 & 0 & 0 & -1/5 & -1/5 & 0 & 7/10 & 7/10 & 1/5 \\ 0 & 0 & 0 & 0 & 1 & 0 & 0 & 1/5 & 0 & 0 & -7/10 & 0 & 0 \\ 0 & 0 & 0 & 0 & 0 & 1 & 0 & 0 & 1/5 & 0 & 0 & -7/10 & 4/5 \\ 0 & 0 & 0 & 0 & 0 & 0 & 1 & 1 & 1 & 0 & 0 & 0 & 1 \\ 0 & 0 & 0 & 0 & 0 & 0 & 0 & 0 & 0 & 1 & 1 & 1 & 1 \\ 0 & 0 & 0 & 0 & 0 & 0 & 0 & 0 & 0 & 0 & 0 & 0 & 0 \\ 0 & 0 & 0 & 0 & 0 & 0 & 0 & 0 & 0 & 0 & 0 & 0 & 0 \end{bmatrix}$$

Taking $x_{31,2}$, $x_{31,3}$, $x_{fresh,2}$, and $x_{fresh,3}$ as the parameters, the general solutions have the following relations:

$$x_{fresh,1} = 1 - x_{fresh,2} - x_{fresh,3}$$

$$x_{31,1} = 1 - x_{31,2} - x_{31,3}$$

$$x_{2,3} = 0.8 + 0.7x_{fresh,3} - 0.2x_{31,3}$$

$$x_{2,2} = 0.7x_{fresh,2} - 0.2x_{31,2}$$

$$x_{2,1} = 0.2 - 0.7(x_{fresh,2} + x_{fresh,3}) + 0.2(x_{31,2} + x_{31,3})$$

$$x_{1,3} = -2.8x_{fresh,3} + 0.2x_{31,3}$$

$$x_{1,2} = 2 - 2.8x_{fresh,2} + 0.2x_{31,2}$$

$$x_{1,1} = -1 + 2.8(x_{fresh,2} + x_{fresh,2}) - 0.2(x_{31,2} + x_{31,3})$$

All the variables and parameters are subject to the physical constraints, i.e. $0 \le x_{i,j} \le 1$. These simple linear functions can be easily solved by linear programming. The range for individual parameter of these parameters are given by

$5/14 \le x_{fresh,2} \le 4/7$,

$0 \le x_{fresh,3} \le 1/14$,

$0 \le x_{31,2} \le 1$,

and $0 \le x_{31,3} \le 1$.

To address the interaction among these parameters, Tower Model is used for parameter-value determination. For illustration, we chose the mean value of the minimum and maximum value of the parameters as the preference (see Figure 4.6).

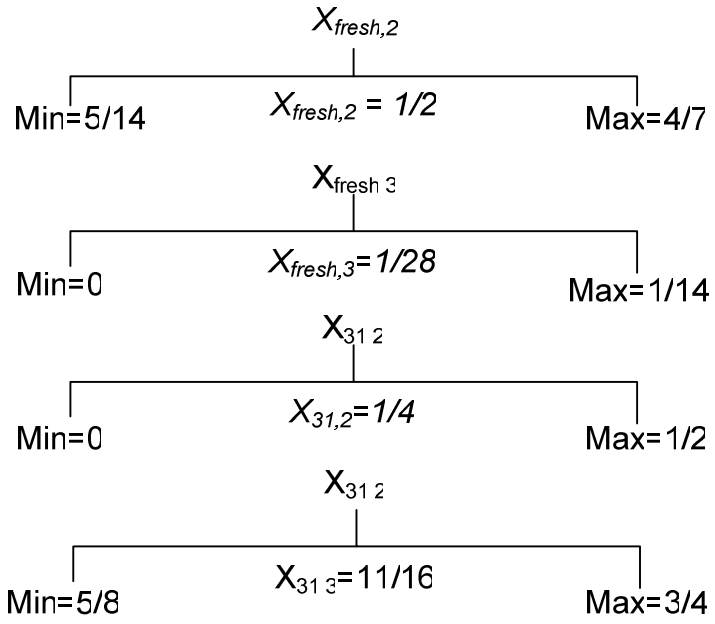

Figure 4.6 Tower Model for example 4.2

The corresponding network configuration is illustrated in Figure 4.7.

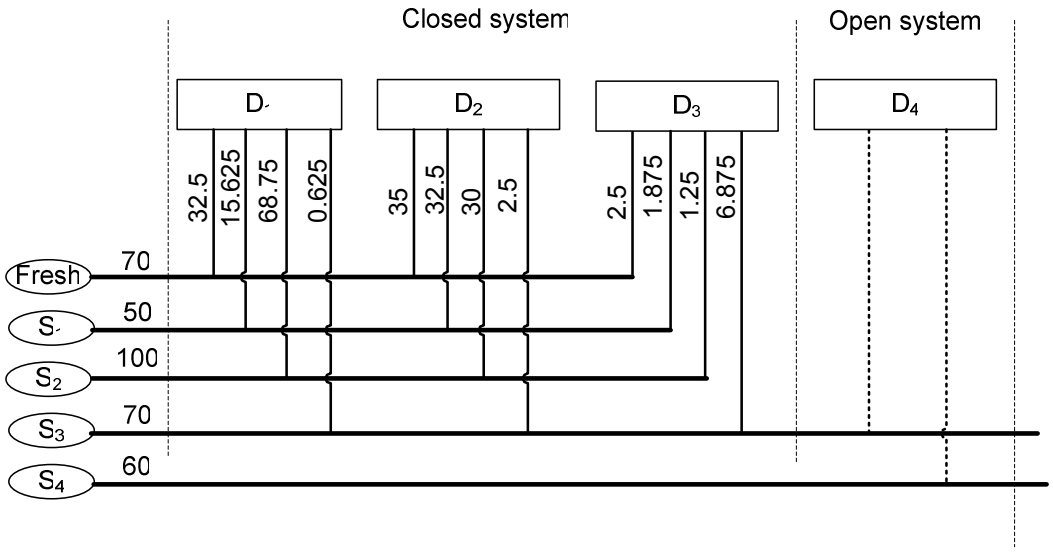

Figure 4.7 Network configuration for example 4.2 corresponding to the Tower Model with mean value

The configuration of the closed system can be developed to feature eight pipelines similar to the solution give by Aly et al. One can also get various configurations with 7 pipelines for this network system, such as ($x_{fresh,1}$, $x_{fresh,2}$, $x_{1,1}$, $x_{1,2}$, $x_{2,2}$, $x_{2,3}$, $x_{31,2}$)=(3/7, 4/7, 2/5, 3/5, 1/5, 4/5, 1), and ($x_{fresh,1}$, $x_{fresh,2}$, $x_{1,2}$, $x_{2,1}$, $x_{2,2}$, $x_{2,3}$, $x_{31,2}$)=(4/7, 3/7, 1, 1/10, 1/10, 4/5, 1) by choosing ($x_{fresh,2}$, $x_{fresh,3}$, $x_{31,2}$, $x_{31,3}$)=(4/7, 0, 1, 0) and ($x_{fresh,2}$, $x_{fresh,3}$, $x_{31,2}$, $x_{31,3}$)=(3/7, 0, 1, 0) respectively.

4.5 Conclusions

This work has developed a systematic implementation approach for process network design to achieve minimum fresh source usage and maximum process source recycle/reuse. Based on analyzing the set of equations, it has been shown that a closed system has a unique solution when there are two sources or one sink. Otherwise, it has infinite solutions. The degrees of freedom for the system needed to transform infinite

solutions into a unique solution is given by *(n-1)(m-2)* where *n* and *m* are the numbers of sinks and sources involved in the closed system. A bounding technique was used to determine the values of the parameters if necessary. Comparisons with published case studies confirm the validity and usefulness of the developed approach.

CHAPTER V
SYNTHESIS, ANALYSIS AND OPTIMIZATION OF BIOMASS-TO-ENERGY SYSTEM

5.1 Introduction

Greenhouse gases (GHGs) from energy-related activities accounted for 86 percent of total U.S. anthropogenic GHG emissions on a carbon equivalent basis in 2004. Of the energy-related emissions, GHGs from fossil fuel combustion are the major portion, 5656.6 Tg CO_2 Equivalent (CO_2-Eq.). More specifically, coal related GHG emissions, 2028 Tg CO_2-Eq., were 35.8 percent of total fossil fuel emissions. Overall, total U.S. GHG emissions have risen by 15.8 percent from 1990 to 2004 (USEPA 2006). Trends show that in the near term GHG emissions will continue to rise, potentially increasing global warming. The Intergovernmental Panel on Climate Change (IPCC) indicates that continued emissions could lead to a temperature increase of between 1.4°C to 5.8°C over the period 1990 to 2100, projecting a decadal increase of between 0.15°C and 0.35°C. This estimated maximum average temperature increase is above the estimated rate that the environment can withstand without damage (0.1°C per decade). The IPCC and others suggest that CO_2 emissions should be decreased (Watson and Albritton 2002).

Several policies and energy consumption related actions have been proposed to limit net GHG emissions. A key example is the Kyoto Protocol. In the US, despite rejecting ratification of the Kyoto protocol, the “Clear Skies Initiative”, announced by President Bush, calls for an 18% reduction in the intensity of GHG emissions per unit gross domestic product (Winters 2002). One mechanism that can be used to mitigate GHG emissions is substitution of less emission intensive alternative fuels for fossil fuels. One such source is biomass. When biomass is used in place of fossil fuel, net carbon emissions decrease because carbon is withdrawn from the atmosphere via photosynthesis during feedstock growth and GHG emissions are avoided from normal routes of biomass disposal (Mann and Spath 2001).

Biomass conversion into forms of energy is receiving increasing attention largely because of environmental, energy supply and agricultural market condition concerns (McCarl and Schneider 2001). In general, biomass can be divided into three categories: crop and wood residues, industrial waste or byproducts, and energy crops.

Researchers at Princeton University showed that half of the total U.S. crop and wood residues could be economically used as fuel. Among the estimated 5 exajoules of recoverable residues per year, one third are made up of agricultural residues and two thirds composed of forestry products and industry residues (60% of which are mill residues). Urban wood and paper waste, another important source of biomass, are recoverable in the amount of 0.56EJ per year (USDOE and EPRI 1997).

There are numerous examples in the agriculture and the pulp and paper industries that illustrate the feasible size of sustainable commercial biomass operations. Over fifty pulp and paper mills in the U.S. use byproducts and waste for internal power and heat generation. U.S. sugar mills have a processing capacity over 1.3 million tons of cane per year. Most of bagasse produced from these plants is used to supply internal energy (USDOE and EPRI 1997).

The price and supply of residues and byproducts can be volatile, so development of dedicated supplies for power generation is believed the best way to ensure a relatively stable price. Although no large scale dedicated feedstock supply systems designed solely for use by biomass power plants exists in the U.S. today, a number of commercial demonstration programs have been launched by the U.S.

Potential energy crops such as switchgrass, willow, poplar and alfalfa are receiving extensive study from their economical, energy and environmental potential (USDOE and EPRI 1997).

At present, the cost difference between using biomass versus coal as a power plant feedstock is generally not enough to cover the capital cost of plant conversion and still generate adequate profit. This cost disadvantage is preventing the adoption of biomass as an energy feedstock. To overcome this disadvantage, appropriate research for biomass production and processing enhancement as well as policies to promote

environmentally sound emission practices and biomass feedstock use should be conducted.

Several types of policy options are currently being considered that could promote biomass as an energy feedstock. One of those involves the use of markets for GHG emission credits as a vehicle for reducing GHG emissions as manifest in the Kyoto Protocol. Such a market would improve biomass competitiveness because biomass has a large GHG offset relative to coal use. This would, in effect, create subsidies for biomass production and use and should enhance biomass penetration in energy feedstock market.

To facilitate biomass market penetration, several biomass-to-electricity techniques have been demonstrated. One technology is biomass gasification and subsequent electricity generation in combustion-turbine or combined-cycle plants. High thermal efficiency, high performance in a wide range of power plant size, and the increased fuel flexibility make this mode very attractive. However, cleanup biogas is needed to prevent damage to the turbine. Also, the capital and maintenance expense of a new boiler and a gasification/combined-cycle system can be excessive. Another technology is direct combustion of biomass that requires much lower capital and maintenance expenditures. Currently the supply of biomass as a sole source of large capacity power plant feedstock is not reliable or economical. The biomass also has some technical problems and considerations such as (Sami et al. 2001):

- The high moisture and ash contents in biomass fuel can cause ignition and combustion problems in power plants;
- The low melting point of the dissolved ash can cause fouling and slagging problems;
- The low heating value of biomass accompanied with flame instability causes burning problem;
- The comparatively large bulk volume of biomass causes feeding problems; and
- The relatively lower heat rate decreases the electricity productivity.

Recent studies have proven that co-firing biomass and coal mitigates these problems. Most co-firing studies have been conducted with biomass percentage of less than 20% by mass of the total fuel. Within this range, the problems incurred when using biomass as a sole fuel are not significant and there are some benefits. The synergetic effects of co-firing on emission reduction of SO_2 and NO_x are quite effective (Tillman 2000). Also, co-firing can improve the heat rate of co-fired biomass. When the heat input of biomass is in the range of 7-10% of the total heat input, the overall boiler efficiency only drops 0.3-1.0 percent compared to a coal fired boiler with an 85-90% efficiency. While there is a large difference between burning biomass alone and burning coal alone, the efficiency of biomass in co-firing is relatively high (Hughes 2000).

These biomass combustion issues have been receiving extensive theoretical and experimental research. However, the issue of process optimization of the biomass-to-energy system has received little attention. Biomass-to-energy is a very complex system that includes many factors, such as biomass supply and power plant operation. An optimized system can greatly reduce energy cost and facilitate biomass usage. Different biomasses have different supply considerations. Biomass supply can be year round or seasonal, such as bagasse from the seasonal sugarcane crush or the summer or fall harvest of switchgrass. To use biomass for co-firing, biomass storage and supply management is necessary. Selecting biomasses and coordinating their supply and storage are key reducing costs. Other factors, such as transport costs, the co-firing ratio, and power plant maintenance scheduling can reduce biomass costs potentially spurring increased biomass use. A comprehensive model, that optimizes power plant feedstock (biomass and fossil fuel) selection and allocation while maximizing power generation industry profits in light of governmental regulations and laws for GHG mitigation, is highly desirable.

The objective of this chapter is to build a framework to synthesize, analyze and optimize the biomass-to-energy (power) system.

5.2 Problem Statement

A given power generation process has a number of power generators previously designated for coal firing only gen1, gen2,…, genN, with their effective power generation capacities of CAP_1, CAP_2, …, CAP_N, thermal efficiencies (coal burning only) of η_1 , η_2 , …, η_n , and mandatory maintenance times.

A given number of biomass resources ($N_{biomass}$) exist with their specific characteristics including high heating value (HHV) and composition of ultimate chemical analysis (e.g. carbon content (C %), hydrogen content (H %), etc). Each kind of biomass has its own supply process that could include crop establishment, crop growing, harvest (collection), processing, transportation, and supply time.

Biomass GHG mitigating effects should be accounted for in the power generation system. To reflect an economic value for these mitigating effects, a GHG discharge permit price (GHG price) is introduced.

The overall objective is to minimize the cost of a power generation system fed with both biomass and coal. More specifically, the following questions should be answered:

- How competitive are the various biomasses as alternative fuels to coal?
- What is the optimal annual biomass supply for a power generation system?
- What is the optimal annual allocation of feedstocks (biomasses and coal) for each generator in the system?
- What is the optimal maintenance schedule for each generator?

To answer these questions, several factors need to be taken into account. Cost of biomasses with no markets, such as energy crops or forest logging residues, should be determined from their supply processes. Different transport technology should be considered because GHG emissions and biomass cost are affected by transport distance and road conditions. Costs of biomass storage and power plant retrofitting for co-firing must be included in energy costing. Biomass supply time and generator maintenance scheduling will affect the storage and consumption of biomass. The co-firing ratio alters the power plant thermal efficiency and determines power plant retrofitting cost.

5.3 Problem Solving Techniques

The problem solving techniques used in this paper include process synthesis, analysis and optimization.

5.3.1 Process Synthesis

"Process synthesis is concerned with the activities in which the various process elements are integrated to provide an improved process flowsheet" (EL-Halwagi 1997). The biomass-to-energy system has many activities and interactive factors. The following steps are used to guide the synthesis of the biomass-to-energy process:

- Define the boundary of the process. A proper boundary should facilitate the problem solving without losing the generality of the problem.
- Determine the major activities of the process. The connection of the major activities should give a complete structure of the process. Very small or insignificant activities may be ignored for easing problem solving.
- Identify the operations and their alternatives that constitute the above activities. This step will identify opportunities for the process optimization. If one operation is qualitatively advantageous over all alternatives, this operation can be selected without proceeding through process analysis.
- Determine and quantify elements of each operation. These elements may include equipment used and various operating conditions and characteristics. This will provide the detailed parameters and data for process analysis and process optimization.
- Generate the complete process by integrate all the elements

5.3.2 Process Analysis

Once the process is synthesized, a process analysis technique is used to predict or depict detailed process characteristics and performance. Process analysis techniques include mathematical models, empirical correlations, and computer-aided process

simulation tools. Figure 5.1 illustrates the process analysis algorithm used for this research.

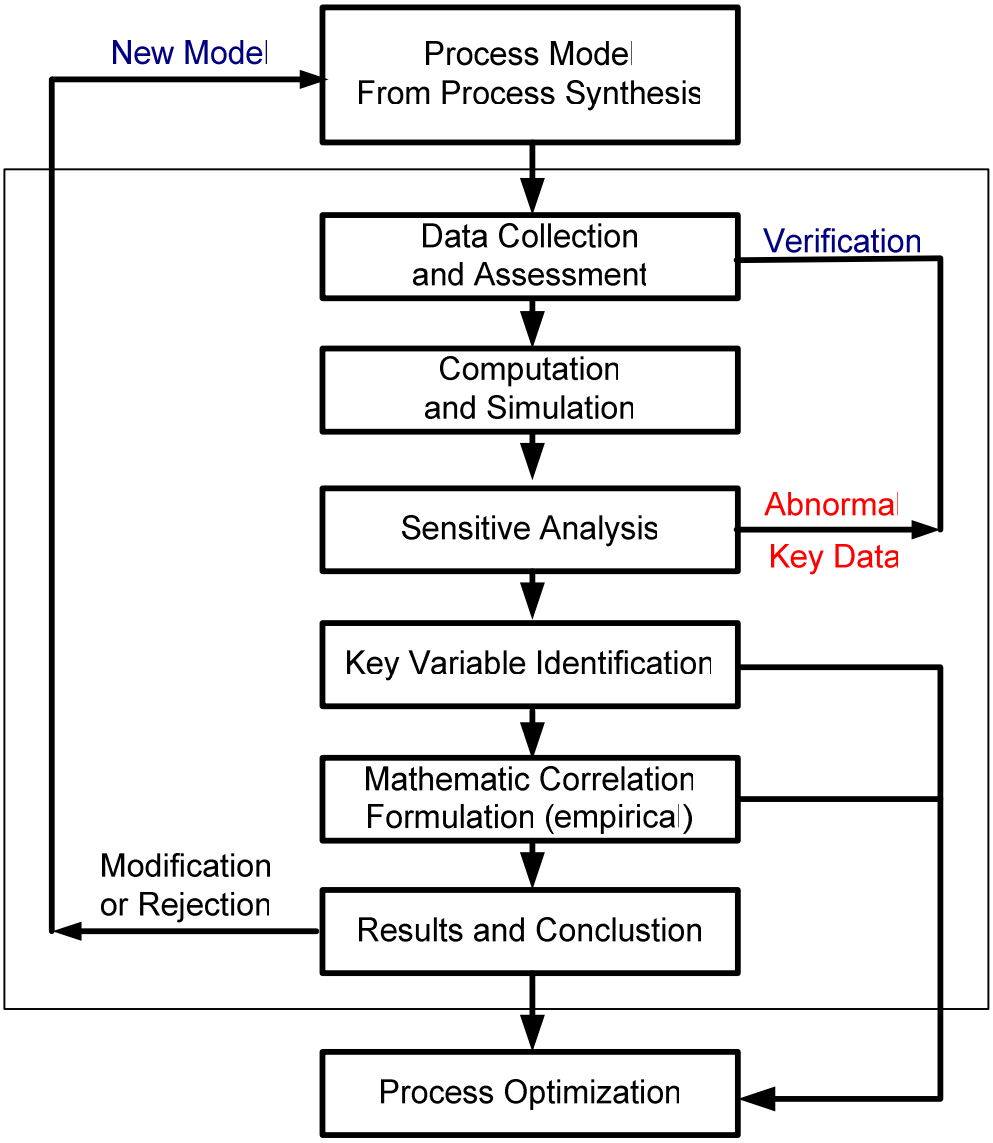

Figure 5.1 Process analysis flow diagram

In process analysis, relationships can be generated as the function of key variables only with all other variables taking typical values. If necessary, subproblem

optimization may be used. Subproblem optimization can mitigate the complexity of the overall problem.

5.3.3 Process Optimization

Process optimization is a process to select the best solution among the set of candidate solutions each comprising a best set of alternative operations. An objective function is quantified to measure the desirability of each problem solution. Having expressed GHG emission reductions from biomasses as an economic value, the GHG price, the objective function can be stated as a cost function of the biomass-to-energy system. Constraints on the objective function were developed based on the process analysis and expressed as equalities and inequalities including an energy balance.

Optimization software like LINGO® or GAMS® can solve relatively complex mixed integer nonlinear programming (MINLP). Based on interval analysis, some MINLP systems, such as a dual-feedstock system, can be effectively solved to acquire global optimization by algebraic methods using a computer spreadsheet such as Excel®. Also, algebraic analysis can be used to help to understand the global optimal solution given by LINGO® for complex systems, such as a multi-feedstock system. These tools were used in this study of the biomass-to-energy system model.

5.4 Problem Solving

5.4.1 Definition of Process Boundary and Process Activities

GHG emissions and cost are two primary elements of the biomass-to-energy system. In quantifying and analyzing the environmental and cost aspects of the biomass-to-energy system, the process boundary should be defined as broad as possible. However, a broad boundary will lead to the inclusion of almost every industrial process because all industrial operations work within a complex network. This is impractical. Therefore, two rules will be applied in the definition of the process boundary and process activities (Kadam 2000).

Rule 1: The constituents and ancillary materials whose impacts are estimated to be negligible should be excluded from the system.

Rule 2: Activities functionally equivalent in products or facilities, materials shared by the compared products, and activities for which allocating shared products is difficult should be excluded from the system.

Based on these rules, the process boundary for different feedstocks and power plants are defined as follows.

For the coal feedstock, coal costs are taken directly from the market. GHG emissions are evaluated for all major activities such as material and energy consumption during coal mining, mining gas recovery and emission, coal combustion, postmining activities and process related transportation.

For the residue feedstock, such as logging residue, the cost and GHG emissions are evaluated for the processing cycle including collection, processing, combustion, transportation and storage.

For the byproduct feedstock, such as bagasse, cost is contingent on process plant and storage, and GHG emissions are evaluated for combustion and landfilling.

For the energy crop feedstock, such as switchgrass, lifecycle analysis is used to evaluate both cost and GHG emissions. The boundary covers activities such as seeding, growing, harvesting, processing, transportation, combustion and storage.

For the power plant, maintenance and retrofitting costs are included in the system. Variation of power plant thermal efficiency for various co-firing rates was also included.

5.4.2 Identification of Operations and Alternatives for Process Activities

In each process activity, many operation alternatives can be identified. Activities are linked in the process. One activity may be restricted by the preceding activity and affect the following activity. Figure 5.2 is an example of switchgrass harvesting and transport alternative activities which illustrates this point (Qin et al. 2006).

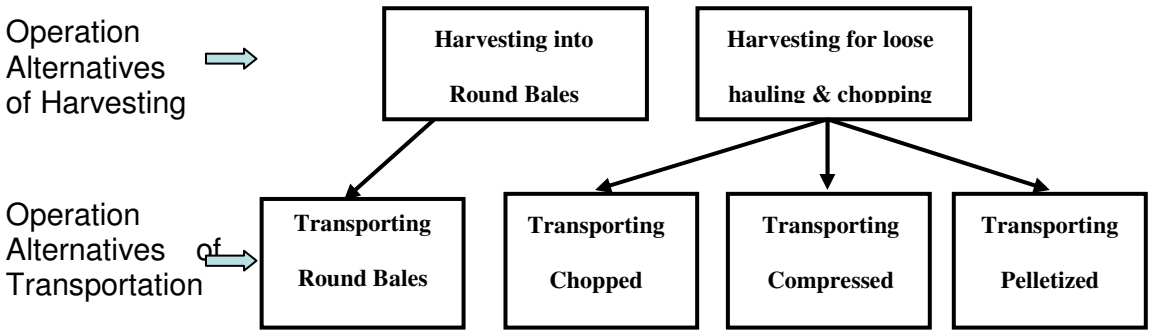

Figure 5.2 Operation alternatives of switchgrass harvesting and transportation

Operational elements were also determined. For example, if the transport method is by truck, then the truck type (heavy duty or light duty), fuel type (gasoline or diesel), payload capacity, and other elements were determined. These elements may be obvious upon observation of current practices. If not, the elements can be determined by process analysis and optimization.

Data processing and computation is conducted in a sequence of elements, operations, activities, and processes in an onion model (Figure 5.3), which is the reverse order of process synthesis.

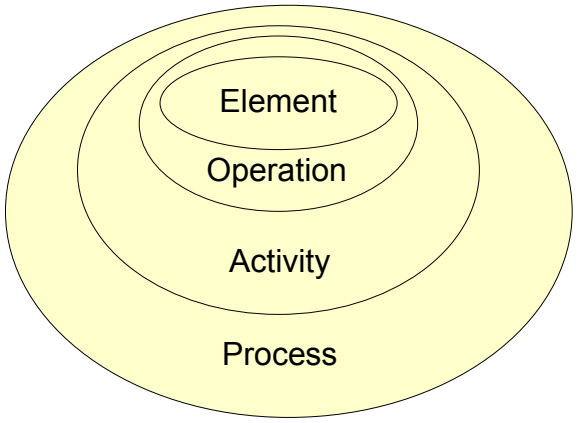

Figure 5.3 Onion model for data processing

5.4.3 Identification of Base Variables

The whole system involves of thousands of variables. The majority of them can be assigned with typical values and become parameters rather than variables. Some variables are a function of other variables. Base variables are not a function of other variables. For example, the acreage of planted crop can be regarded as a base variable because from it the biomass field transport distance, the amount of the crop harvested and used for power generation can be calculated and, thus, GHG emissions from per unit energy crops can be derived.

5.4.4 Process Optimization

1. Objective Function

The objective is to minimize the cost of power generation. Within this cost minimization, the best alternative processes will be determined. The cost minimizing objective function of this system can be expressed with four elemental costs, feedstock cost, GHG price cost, plant retrofitting cost, and storage cost, and specified as:

Min =f(feedstock cost, GHG price cost, plant retrofitting cost, storage cost) (5.1)

2. Constraints and Correlations

The constraints and correlations for this problem include following aspects.

a. Energy balance

$$CAP_{i,j} = \eta_{i,j} * \sum_{k=1}^{N_{feed}} (HHV_k * m_{i,j,k}) \qquad \text{for generator } i \text{ in month } j \tag{5.2}$$

Where $P_{i,j}$ is the power generated by generator i in month j, $m_{i,j,k}$ is the consumption of feedstock k by generator i in month j, N_{feed} is the total number of feedstocks, $\eta_{i,j}$ is thermal efficiency of generator i in month j, and N_{feed} is the number of different feedstocks.

b. Mass balance

$$m_{i,k} = \sum_{j=1}^{12} m_{i,j,k} \tag{5.3a}$$

$$m_{j,k} = \sum_{i=gen1}^{genN} m_{i,j,k} \tag{5.3b}$$

$$m_k = \sum_{i=gen1}^{genN} \sum_{j=1}^{12} m_{i,j,k} \tag{5.3c}$$

where $m_{i,k}$, is annual consumption of feedstock k in generator i, $m_{i,j,k}$ is the monthly consumption of feedstock k in generator i in month j, $m_{j,k}$, is the monthly consumption of feedstock k in month j for all generators, m_k is the annual consumption of feedstock k in all generators, and $genN$ is the number of generators.

c. Energy efficiency

Co-firing biomass with coal can improve the heat rate of co-fired biomass. In general energy efficiency can be expressed as the function of energy efficiency of burning coal alone and the biomass co-firing ratio,

$$\eta_{i,j} = f(\eta_{i,coal}, R_{cofiring,i,j}) \tag{5.4}$$

Where $\eta_{i,j}$ is the energy efficiency of generator i in month j, $\eta_{i,coal}$ is the energy efficiency of generator i burning coal only, and $R_{cofiring,i,j}$ is the co-firing ratio expressed in mass base as

$$R_{cofiring,i,j} = \sum_{k=1}^{Nbiomass} m_{i,j,k} / (\sum_{k=1}^{Nbiomass} m_{i,j,k} + m_{i,j,coal}) \tag{5.5}$$

and in thermal base as

$$R_{cofiring\_th,i,j} = \sum_{k=1}^{Nbiomass} (m_{i,j,k} HHV_k) / (\sum_{k=1}^{Nbiomass} (m_{i,j,k} HHV_k) + m_{i,j,coal} HHV_{coal}) \tag{5.6}$$

where $N_{biomass}$ the number of biomass involved in the cofiring system, and $m_{i,j,coal}$ is the coal consumption of generator i in month j.

d. Storage

$$St_{j,k} = Rd_{j,k} = Rd_{j-1,k} + Su_{j,k} - \sum_{i=gen1}^{genN} m_{i,j,k} \tag{5.7}$$

where $St_{j,k}$ and $Rd_{j,k}$ is the storage and residual of feedstock k in month j, and $Su_{j,k}$ is the supply of feedstock k in month j.

e. Retrofitting cost

Cost of power plant retrofitting is a function of co-firing ratio. The cost of power plant retrofitting should be expressed as the function of maximum co-firing ratio ($R_{cofiring,max,i}$) because retrofitting is a long term decision.

$$C_{retrofitting,i}=f(R_{cofiring,max,i}) \quad (5.8)$$

where $R_{cofiring,max,i}=Max\{R_{cofiring,\ i,j}\}$

f. GHG emissions

Biomass combustion affects GHG emissions in three ways. The first is from feedstock preparation such as fertilizer used to grow energy crops and fossil fuels use in supplying the biomass. The second is from combustion during power generation which is a function of the carbon content of the feedstock and the amount of feedstock combusted. The third is from GHG mitigation, such as photosynthesis, soil CO_2 sequestration, or, reduced landfilling (reduced CO_2 and CH_4 emissions). The net GHG emissions effect is expressed as,

$$E_{GHG\,k} = E_{GHG\ prep,k} + E_{GHG\,comb,k} - E_{GHG\,miti,k} \quad (5.9)$$

where $E_{GHG\,k}, E_{GHG\ prep,k}, E_{GHG\,comb,k}$, and $E_{GHG\,miti,k}$ are net GHG emissions, GHG emissions from preparation, GHG emissions from combustion, and GHG emissions from mitigation of biomass k respectively.

5.5. Case Study

This case study is for a biomass-to-power generation system with three power generators. The operating calendar for the system is 30 days per month and 12 month per year with a 15-day mandatory maintenance for each generator occurring in different months. The specifications are listed in Table 5.1.

Table 5.1 Specifications of the power generation system

	Effective operating capacity (MW)	Thermal efficiency (coal burning alone)	Maintenance time (days)
Generator 1	200	0.3413	15
Generator 2	150	0.3413	15
Generator 3	100	0.3413	15

Three types of biomass, bagasse (a sugar cane processing byproduct), switchgrass (an energy crop), and forest logging residue are considered as potential feedstocks. The specifications of all feedstocks are shown in Table 5.2.

Table 5.2 Specifications of feedstocks for power generation

	Coal	Bagasse	Switchgrass	Logging residue
HHV (kJ/kg)	23552.12	14141.79	15591.00	20307.34
Thermal efficiency	0.3413	0.1846	0.2069	0.24
Ash %	8.64	2.76	4.61	0.63
C%	57.49	33.78	42.04	46.85
H_2O%	10.80	25.37	11.99	7.30
Cellulose%	N/A	50.0 (bone dry)	37.1 (bone dry)	N/A
Hemicellulose%	N/A	27.9 (bone dry)	32.1 (bone dry)	N/A

It is assumed the sugar cane plant is next to the power plant. Therefore, bagasse supply costs and GHG emissions are not significant. Logging residue is assumed to be collected from a 40 year rotational forest with even annual timber harvest and 25 highway miles away from the closest processing point to the power plant. The switchgrass collection points are assumed to be an average of 15 highway miles away from the power plant. The GHG emission discharge permit price is assumed to be \$30/tonne CO_2-Eq. Storage costs for all biomass feedstocks are assumed \$1/tonne. To reduce the disturbance to power plant operation, it was assumed each generator has a uniform annual co-firing ratio.

5.5.1. Feedstock and Power Plant Analysis

1. Coal

The average 2004 delivered coal price for electric utility plants was \$27.30/ton, i.e. \$30.10/tonne (EIA 2006). Coal delivery is upon request, so no storage cost for coal was used in the analysis.

The GHG emissions associated with burning coal was determined from lifecycle analysis of coal including fuel and material consumption during coal mining, mining gas emissions and recovery, postmining activities, transportation, and coal combustion. The boundary of coal analysis was illustrated by Figure 5.4. Lifecycle coal GHG emissions are 2225.5471 kg CO_2-Eq. /tonne coal.

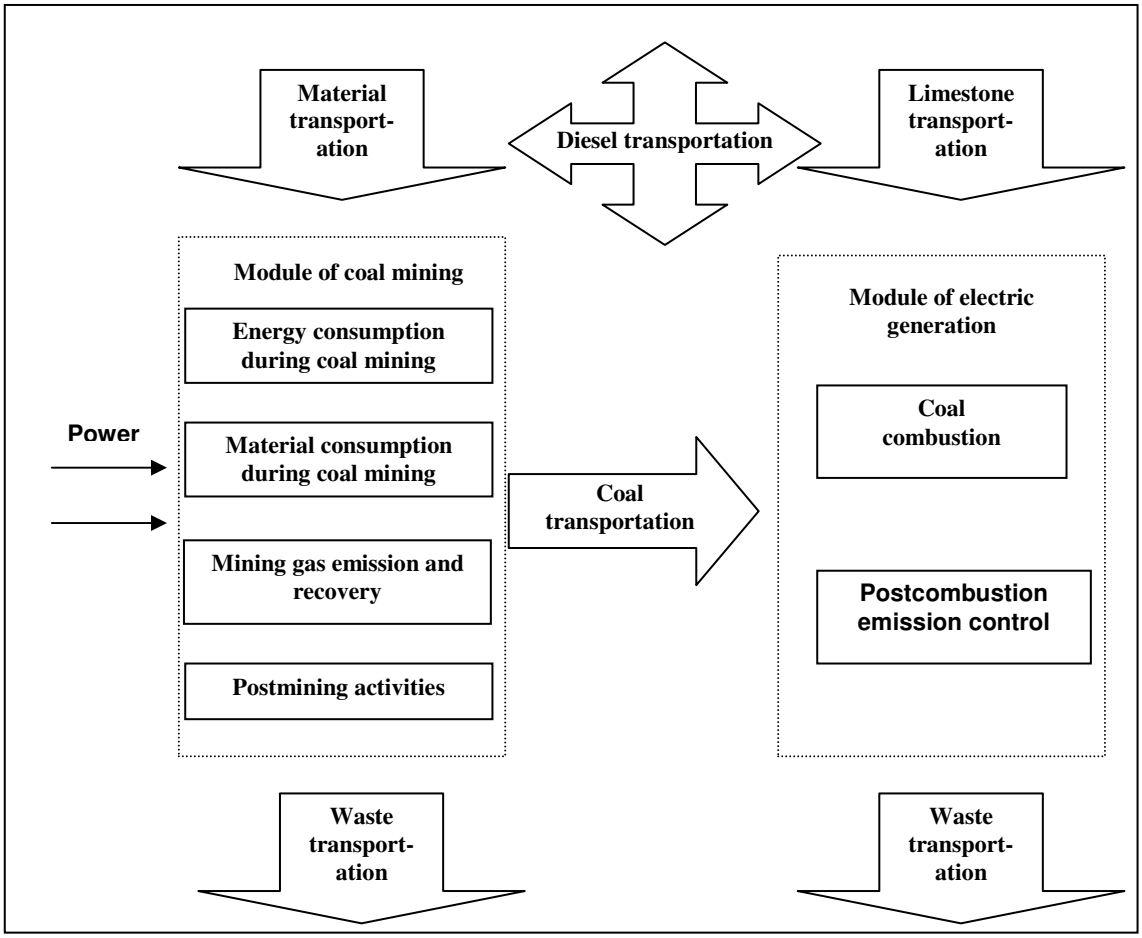

Figure 5. 4 Boundary of coal lifecycle analysis

2. Bagasse

The supply of bagasse is assumed to be 21,649 tonne/month from October to May (240 days). The annual weighted-average moisture is 34% on oven dry basis, i.e. 25.37% on a wet basis (Kadam 2000). The price is assumed to be $20/tonne. Storage is required for year round bagasse use.

The primary GHG mitigation mechanism of biomass is CO_2 intake through photosynthesis during plant growth. 1237.7351 kg of CO_2/tonne of bagasse is taken in during sugarcane growth. Because sugarcane is grown for purposes other than bagasse production, a reduction in CO2 emissions from plant growth should not be considered for bagasse power generation use (Mann and Spath 2001). Instead, the reduced GHG

emissions from not disposing of bagasse in a landfill should be used to determine bagasse GHG mitigation. The degradation mechanism is illustrated in Figure 5.5. This GHG mitigation is 1.36 tonne CO_2-Eq./tonne of bagasse resulting in a net GHG emission of -107.4106 kg CO_2-Eq/tonne of bagasse.

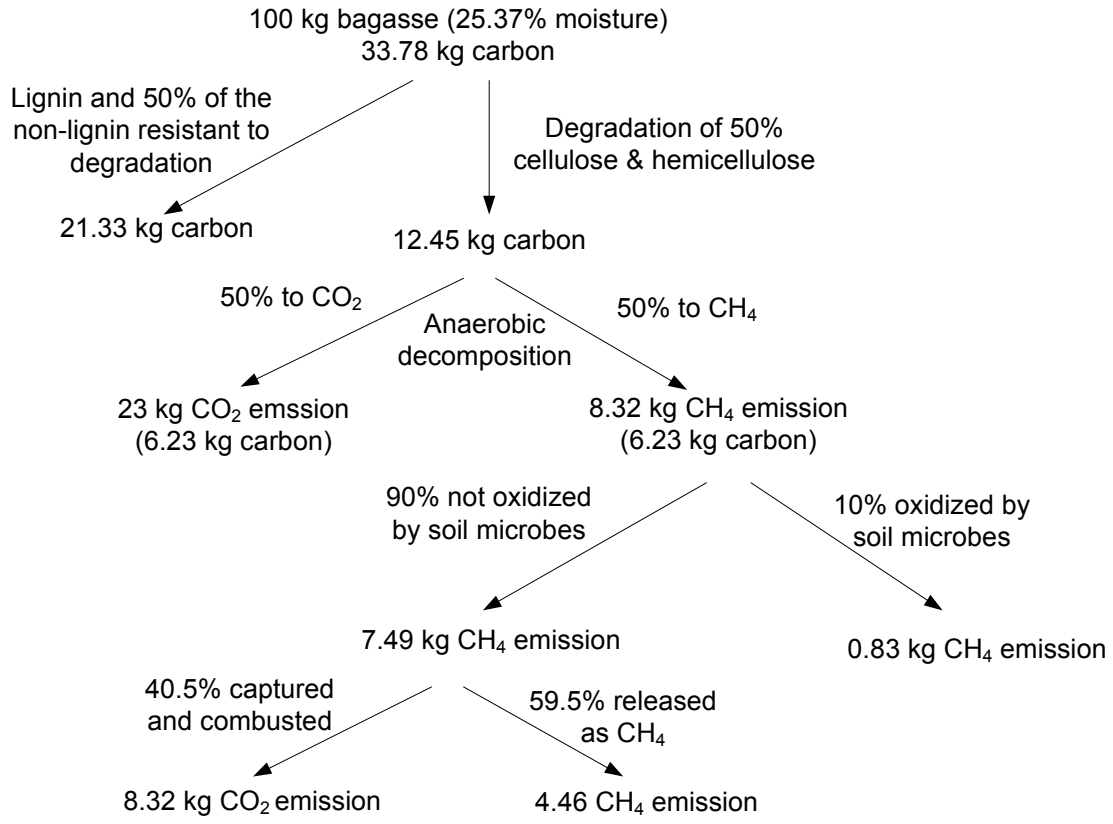

Figure 5.5 The degradation mechanism of bagasse in a landfill

3. Switchgrass

Switchgrass is one of the most promising energy crops. In this case study, harvesting switchgrass is assumed once a year in September. The cost and GHG emissions evaluation of switchgrass is based on (Qin et al. 2006). Figure 5.6 shows the boundary and activities of switchgrass supply. The optimal combination of activities, establishing switchgrass on cropped land, harvesting loose for chopping, and

transporting after compression into modules is taken from Qin et al. (2006). In this study, switchgrass transportation is divided into growing area and highway transportation. Highway transport distances are assumed to be known. Field transportation distances will vary with the growing area size determined by annual switchgrass use. To minimize the field transportation distances, hence reduce cost and GHG emissions, the geographic shape of the growing area was optimized and the relationship between field transportation distances and growing area established.

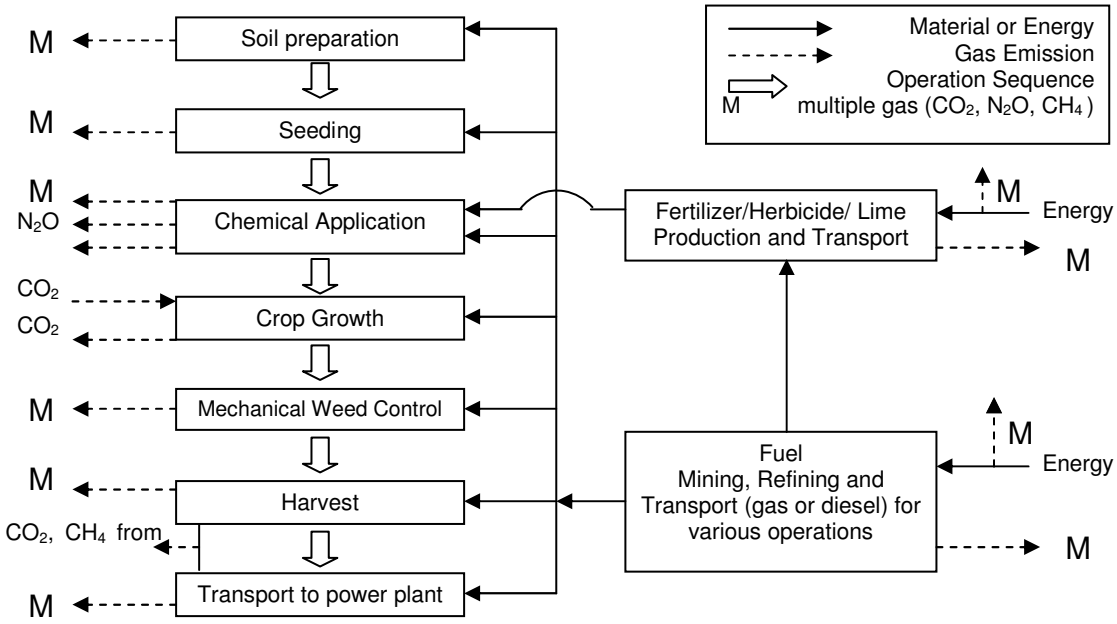

Figure 5.6 Boundary and activities of switchgrass supply (Qin, et al. 2006)

Assume the growing area is a rectangle which is expandable along two dimensions with a highway connecting to the growing area at one corner of the rectangle. The field transportation vehicles are assumed to go through the growing area in grid mode. The situation is schematically illustrated in Figure 5.7.

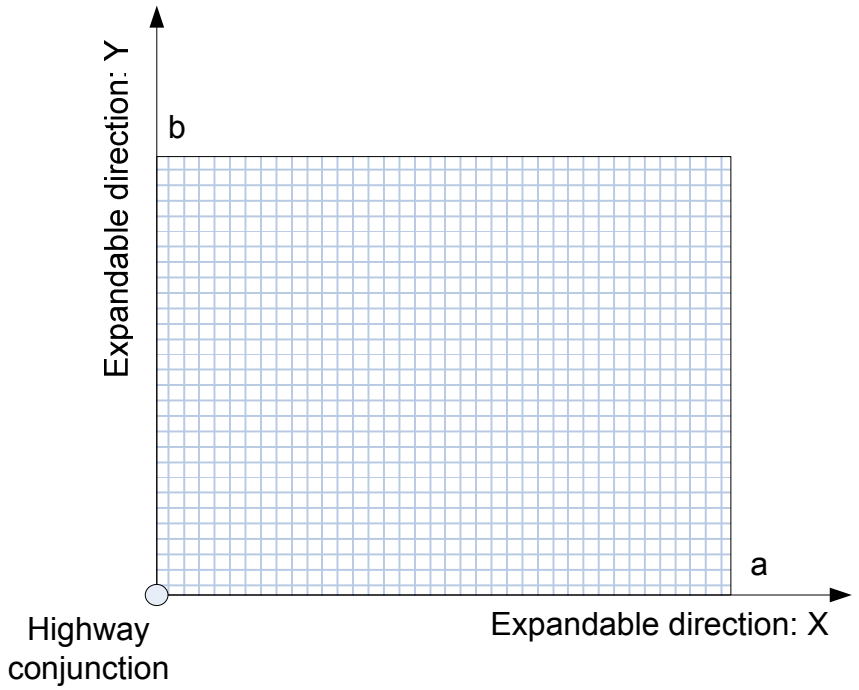

Figure 5.7 Schematic illustration of switchgrass growing area and field transportation

Minimizing the field transportation distance (L_{in_land}) requires determining the growing area shape. Assume the required area is A, and the side lengths of the rectangle are a and b, then we have following relations:

$$L_{in\_land} = \frac{1}{ab}\int_0^b \int_0^a (x+y)dxdy = \frac{a+b}{2} \tag{5.10}$$

Hence, the optimization model in parameter can be written as

$$\min = L_{in\_land} = \frac{a+b}{2} \tag{5.11}$$

s.t.

$$ab=A \tag{5.12}$$

The global optimal solution is

$$L_{in\_land} = a = b = \sqrt{A} \tag{5.13}$$

Furthermore,

$$A = m_{sw} / Y_{sw} \tag{5.14}$$

where m_{sw} is the annual switchgrass consumption and Y_{sw} is the swithgrass yield in unit of mass per unit area.

Thus, the minimum field transportation distance is

$$L_{in\_land} = (m_{sw} / Y_{sw})^{1/2} \tag{5.15}$$

With values from Qin et al. (2006), GHG emissions as the function of field transportation distance (L_{in_land}) and highway transportation distance ($L_{highway}$) were simulated (see Figure 5.8a and 5.8b.).

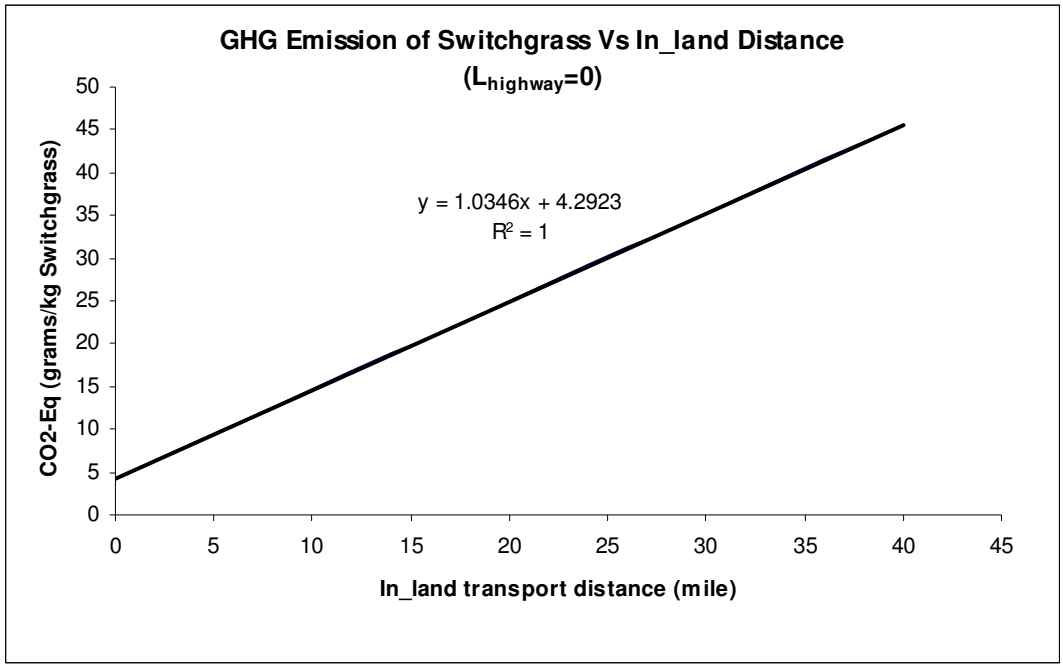

Figure 5.8a Correlation of GHG emissions of switchgrass supply with field transportation distance

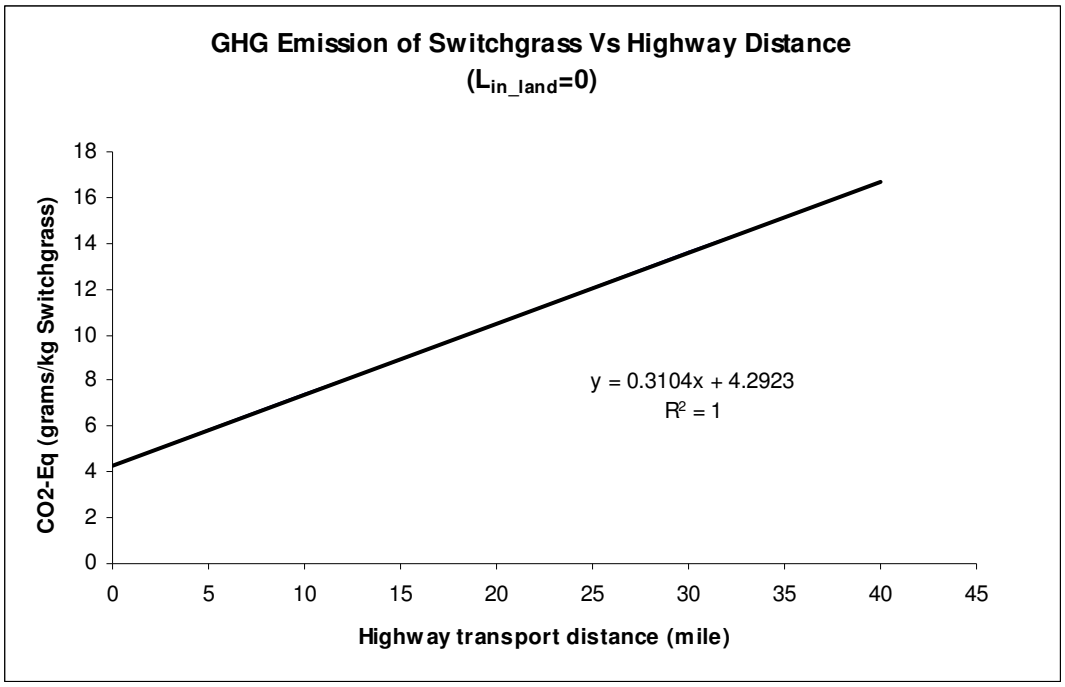

Figure 5.8b Correlation of GHG emissions of switchgrass supply with highway transportation distance

The net lifecycle GHG emissions of switchgrass used as a function of transport distance was expressed as

$$E_{GHG,sw} = 1.0346L_{in\_land,sw} + 0.3104L_{highway,sw} + 4.2923 \quad (5.16)$$

Similarly, the cost function of switchgrass supply was expressed as

$$C_{sw} = 0.7353L_{in\_land,sw} + 0.2206L_{highway,sw} + 32.49 \quad (5.17)$$

4. Logging Residue

Logging residues are left in the forest after timber harvest. CO_2 intake during photosynthesis in the forest is already occurring, therefore, there is no GHG mitigation effect from this process. However, the avoided GHG emissions from ongoing logging residue decomposition are the GHG mitigation effects. Assuming 90% of the carbon in logging residue is aerobically decomposed to CO_2 and 10% of the carbon is anaerobically decomposed to CH_4 (Mann and Spath 2001), the total GHG mitigation is 2985.1369 kg CO_2-Eq./tonne of logging residue. The price of logging residue in the

forest is assumed to be $2/ton (50% moisture oven dry basis), the price paid to forest landowners for stumpage (USDA 2004). The overall GHG emissions and cost of delivered logging residue are calculated from a modified processing model from FoRTSv4 (USDA 2005). The optimal combination of operations, loading with knuckleboom loader, forest transport with RO container, processing with disk chipper, and highway transport with 120 yard chip van, was used in this study.

In order to establish the GHG emissions and cost for logging residue, the shape-distance logic used for switchgrass was applied. It is assumed that the 40 year rotational forest is harvested in 5 mile by 5 mile squares arranged in a rectangular shape. The schematic layout of the forest is illustrated in Figure 5.9, in which the period on the grid represents the wood chipping location for each year. It is further assumed that the power plant to forest (point O) distance is 30 miles by highway. Thus, the average highway distance would be 57.5 miles.

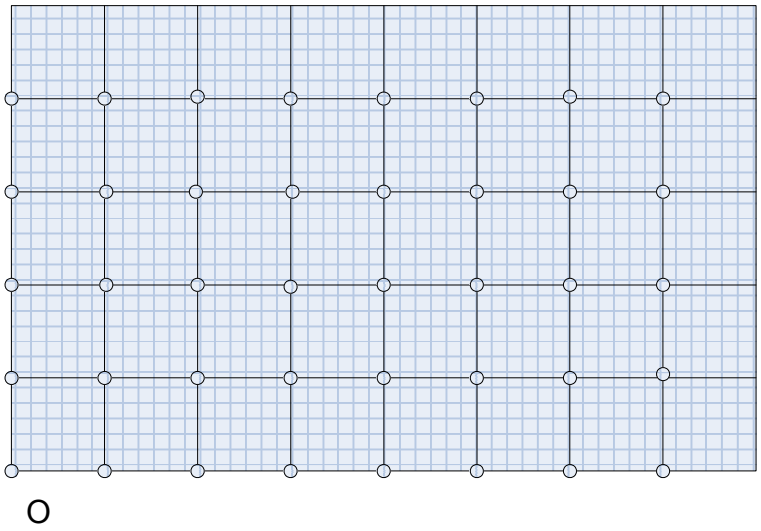

Figure 5.9 Schematic layout of 40 year rotational forest

With these assumptions and taking values for other variables from FoRTSv4, the net processing cycle GHG emissions ($E_{GHG,logging}$) and cost of delivered logging residue ($C_{logging}$) can be expressed as functions of transport distance as follows:

$$E_{GHG,\text{logging}} = 13.446L_{in\_wood,\text{logging}} + 0.586L_{highway,\text{logging}} - 1237.9806 \quad (5.18)$$

$$C_{\text{logging}} = 5.337L_{in\_wood,\text{logging}} + 0.225L_{highway,\text{logging}} + 9.946 \quad (5.19)$$

5. Power Plant

Co-firing can effectively increase the thermal efficiency of biomass. However, the overall power plant thermal efficiency decreases with the increase of biomass co-firing ratio. The empirical boiler efficiency loss of biomass co-firing can be expressed by the following formula (Plasynski et al. 1999)

$$\eta_{loss} = 0.45R_{biomass}^2 + 0.0005R_{biomass} - 0.000044 \quad (5.20)$$

where R_{biomass} is biomass co-firing ratio on a mass basis.

If the mechanical efficiency is 0.3969 and coal only fired boiler efficiency is 0.86, the overall thermal efficiency is 0.3413. The power plant thermal efficiency of biomass co-firing can be expressed as

$$\eta_{cofiring} = 0.3969(0.860044 - 0.45R_{biomass}^2 - 0.0005R_{biomass}) \quad (5.21)$$

To co-fire, a facility will need to be retrofitted. Cost of retrofitting is in a order of \$50-\$100/Kw for biomass for blending feed and \$175-\$200/kW for biomass for separated feed (Hughes 2000). If a 10-year straight line depreciation method without salvage value is assumed, then the average annual retrofitting cost of *i* generator ($C_{\text{retrofitting,i}}$) can be expressed as

$$C_{retrofitting,i} = CAP_i * 200 * R_{th\_cofiring,\max,i} / 10 \quad (5.22)$$

where $R_{\text{th\_cofiring,max,i}}$ is the maximum biomass co-firing ratio on a thermal basis for generator *i*, which can be calculated from Eq. (5.6),and a \$200/kW retrofitting cost was used.

5.5.2 Competitiveness of Biomass Feedstocks

To determine the GHG prices for each co-firing ratio for each feedstock, the optimization model was solved with an objective function minimizing the GHG price. The relations and constraints were formed with Eq. (5.2) –Eq. (5.9) with specific

feedstock parameters and relations from Eq. (5.14) –Eq. (5.22). The cost balance equation was included as

$$\sum C_{feedstocks,cofiring} + \sum C_{GHG,cofiring} + C_{storage} + C_{retrofitting} = C_{coal,coalonly} + C_{GHG,coalonly} \qquad (5.23)$$

which links two cases, co-firing and coal firing alone, to determine GHG price.

Although the model is a MINLP, with the global solver of LINGO, global optimal solution for each cofiring ratio can be acquired. The algebraic method can also be used in this situation. With each given annual biomass consumption, coal consumption and the co-firing ratio are defined. Minimizing total cost (hence, minimizing the GHG price) is minimizing storage cost. Minimizing storage cost is a matter optimizing the generator maintenance schedule. For switchgrass, the harvest time is September, thus, by arranging the generator maintenance time in June for gen3, July for gen2 and August for gen1, the storage cost is minimized. For bagasse, the maintenance schedule should be July for gen3, August for gen2, and September for gen3. For logging residue, the maintenance schedule is insignificant because the supply is year around. The procedure is illustrated in Figure 5.10.

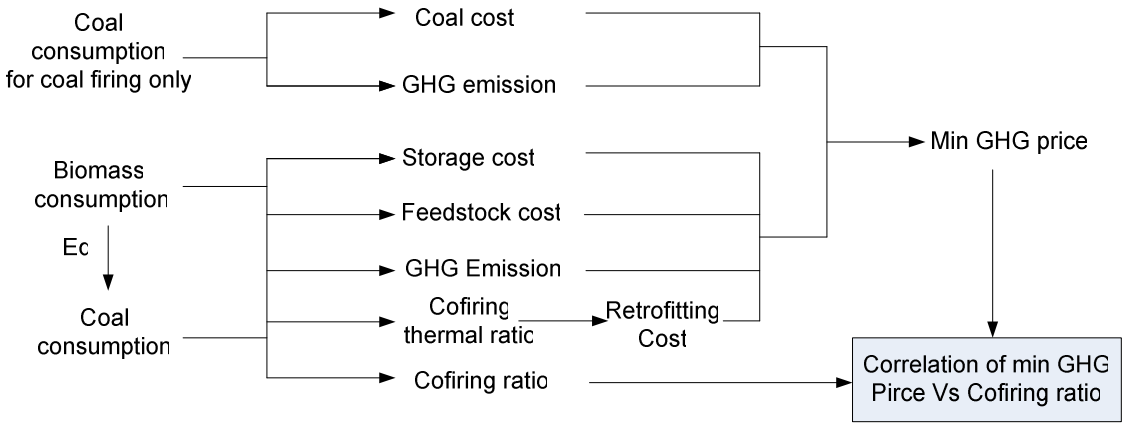

Figure 5.10 Flowchart of algebraic method for identifying minimum GHG price at each co-firing ratio

The relation of the global minimum GHG price to the biomass co-firing ratio for individual feedstocks is shown in Figure 5.11.

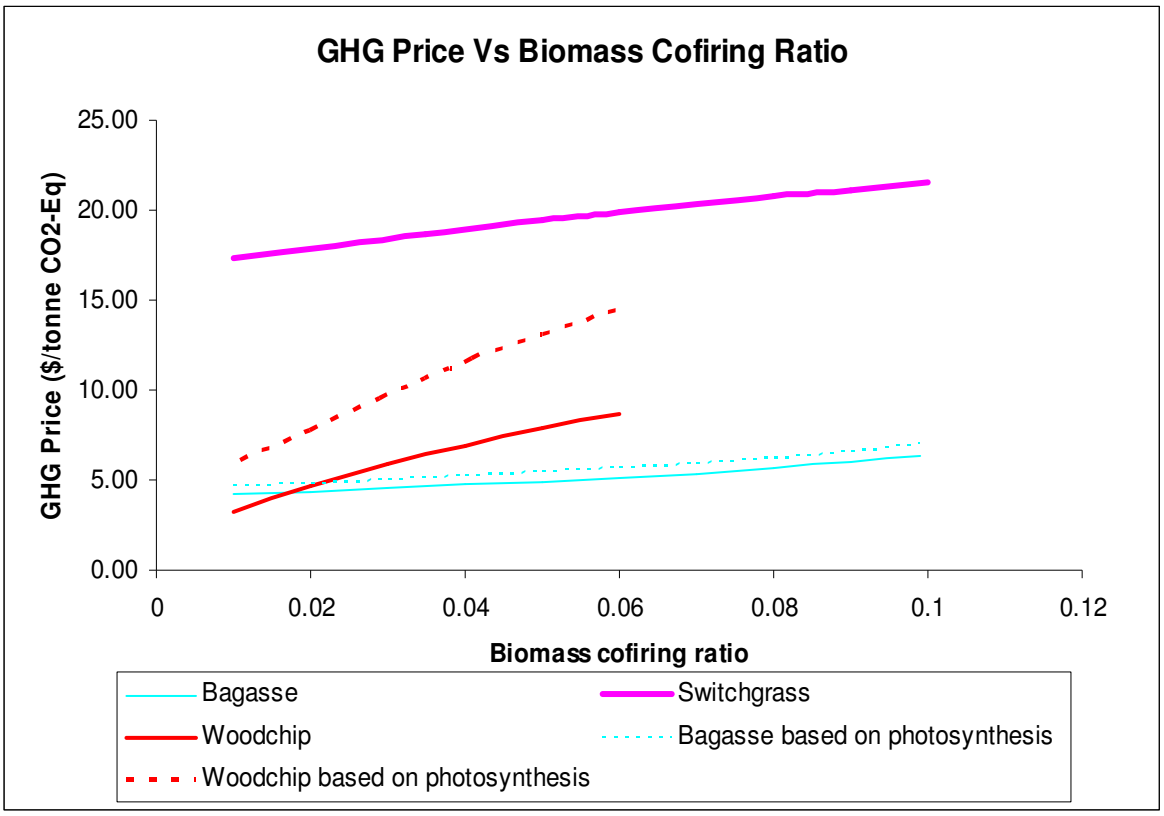

Figure 5.11 Relation of minimum GHG price and co-firing ratio for different biomass feedstocks

If the GHG price is below \$17/tonne CO_2-Eq, no switchgrass will be used by the power generation system. Bagasse and logging residue only need an incentive CO_2 price less than \$5/tonne to be used by the system, and with less than \$10/tonne CO_2, all of them will be used up in this case study. One can also see that different reference for GHG emission calculation, i.e. avoided GHG emission and CO_2 intake from photosynthesis will definitely affect the GHG price for co-firing logging residue and bagasse, with the effect for logging residue even more obvious.

5.5.3 Global Optimization of Dual Feedstock Cofiring System

The GHG price of \$30/tonne CO_2-Eq. was set as a base to compare the global optimal solution for three dual feedstock co-firing systems, i.e. coal-bagasse, coal-logging residue and coal-switchgrass. The mathematical models for these three systems are very similar. The objective function is minimizing total cost. Constraints and correlations are different only in cost and GHG emission functions for individual biomasses. Both LINGO and the algebraic method were used to solve these models globally, Figure 5.12. The generator maintenance schedules for co-firing coal-switchgrass and coal-bagasse system are same as discussed earlier. Based on the analysis above, the coal-logging residue co-firing system would use all available logging residues. A uniform co-firing ratio will result in a monthly logging residue consumption of $m_{wood}/11.5$ when all generators are in full operation, but, the supply, limited by the collection capacity, is only $m_{wood}/12$. Thus, one generator would need to be scheduled for maintenance in the first month. There are six generator maintenance sequences, 1-2-3, 1-3-2, 2-1-3, 2-3-1, 3-1-2, and 3-2-1. By comparison, the scenarios for global minimum total cost of coal-logging residue co-firing system was identified. Figure 5.12 schematically represents the algebraic method for the system

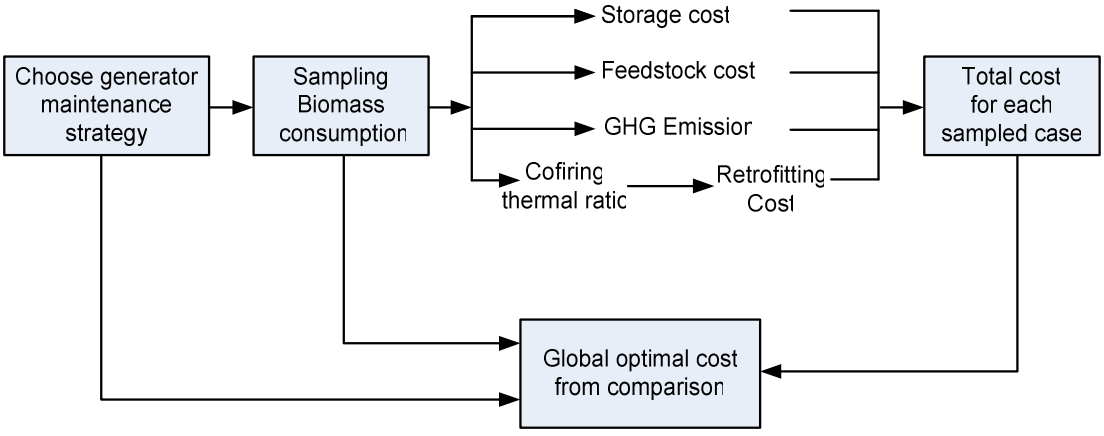

Figure 5.12 Flowchart of algebraic method for identifying minimum total cost for dual feedstock co-firing system

Although the maintenance schedule for coal-switchgrass co-firing system is logically straight forward, because the growing area is unknown, it would need to be optimized along with total cost. Figure 5.13 shows the result calculated by the algebraic method which is identical to the global optimal solution given by LINGO.

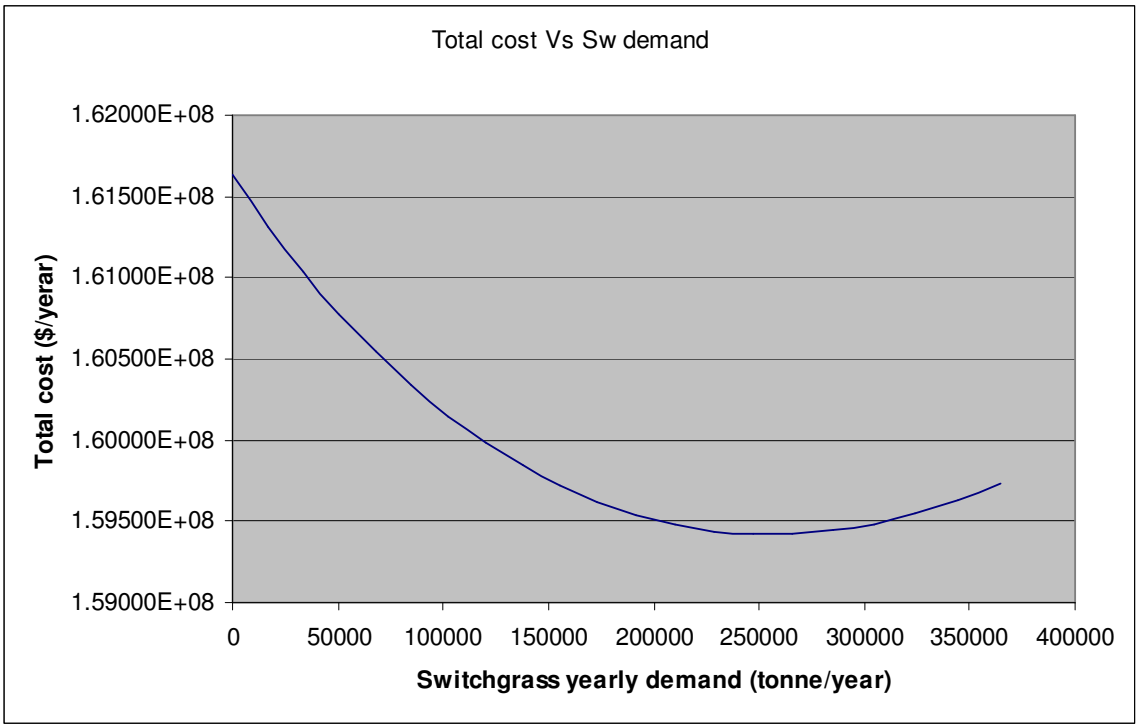

Figure 5.13 Total cost versus switchgrass consumption (demand) for coal-switchgrass co-firing system

The global optimal solutions for the three systems are summarized in Table 5.3.

Table 5.3 Summary of global optimization solutions for three co-firing systems at \$30/tonne CO_2-Eq

	Coal-bagasse	Coal-logging residue	Coal-Switchgrass
Minimum total cost (\$/year)	1.5618E08	1.5462E08	1.5942E08
Annual demand (tonne/year)	1.7319E05	1.0854E05	2.4715E05
Optimal co-firing ratio	9.92% (limited by supply)	6.43% (limited by supply)	14% (global optimal)
Generator maintenance schedule	gen1(Sep), gen2(Aug), G3(July)	gen1(Jan),gen2(Sep),gen3(June) or gen1(Jan),gen2(May),gen3(Oct)	gen1(Aug), gen2(July), gen3(June)

5.5.4 Optimization of Multifeedstocks System

The multifeedstock system is the incorporation of the three individual co-firing systems. The generator maintenance scheduling for individual co-firing systems is logically determinable, but, this can not be done for the multifeedstock system. Therefore, generator maintenance scheduling was included in the optimization. The global optimal solution is summarized in Table 5.4.

Table 5.4 Brief report of global optimal solution of multifeedstock system from LINGO under optimality tolerance of 1E-06

	Generator 1	Generator 2	Generator 3
Co-firing ratio	0.1986	0.1918	0.1836
Efficiency	0.3342	0.3347	0.3352
Retrofitting Cost ($)	518290	444146	324963
Coal (tonne/month)	57322	42019	27493
Bagasse (tonne/month)	14211	849	0
Switchgrass (tonne/month)	0	5873	0
Wood (tonne/month)	0	3252	6186
Maintenance (month)	September	August	February

1. Discussion 1: Global Optimal Switchgrass Consumption

Figure 5.14a, b, and c generated from analysis for individual power generator system may help in understanding the global optimal amount of switchgrass consumption results. Figure 5.14 shows that both increasing and decreasing switchgrass usage will increase the cost of the whole system.

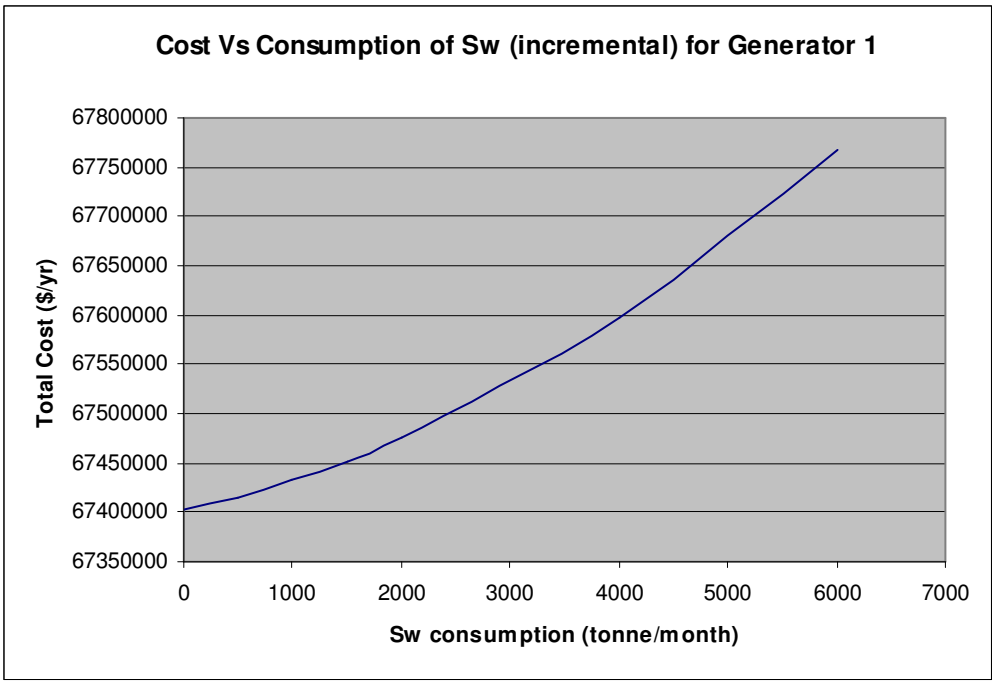

Figure 5.14a Total cost versus switchgrass consumption for generator 1

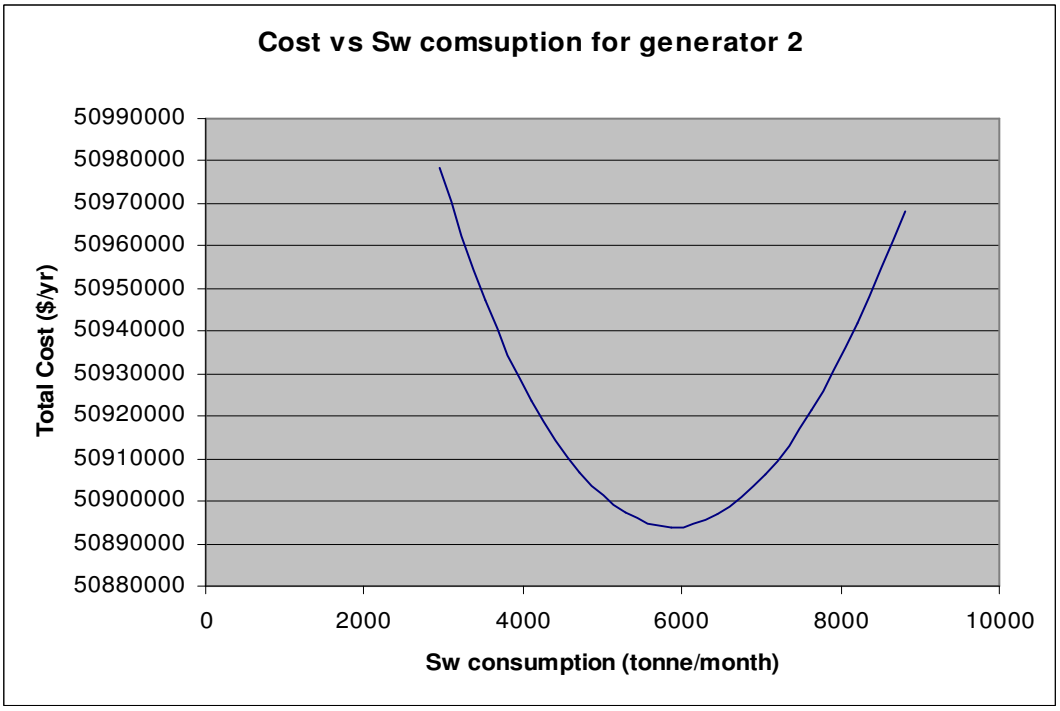

Figure 5.14b Total cost versus switchgrass consumption for generator 2

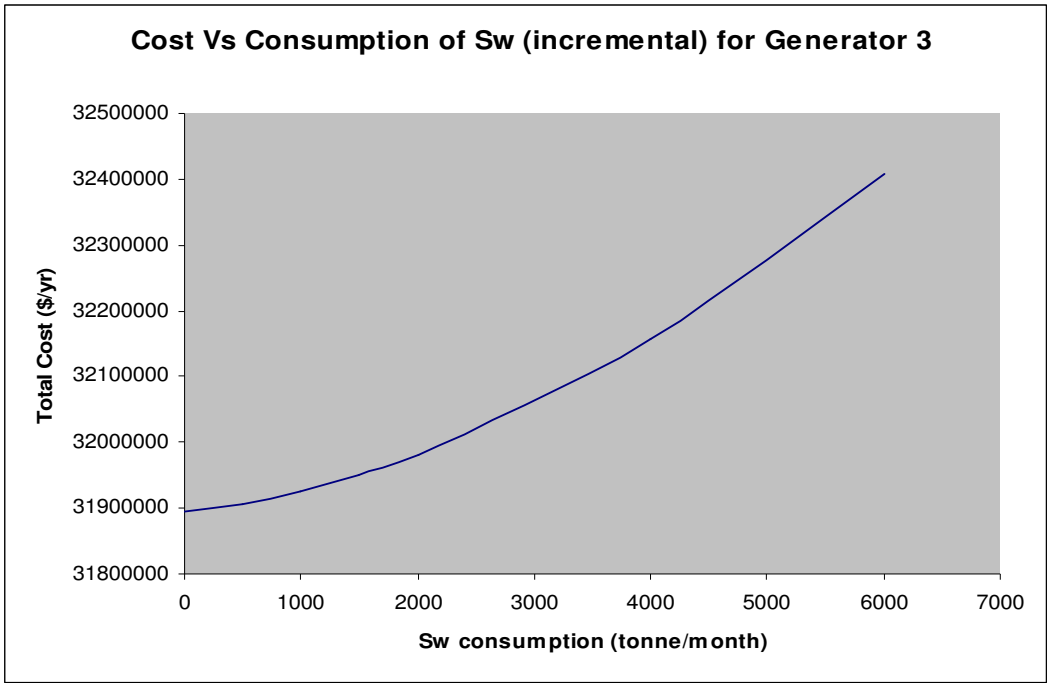

Figure 5.14c Total cost versus switchgrass consumption for generator 3

2. Discussion 2: Uniform Annual Co-firing Ratio (R_{year}) versus Uniform Monthly Co-firing Ratio (R_{month})

The constraint of a uniform annual co-firing ratio for each generator provides a constant feed of biomass for power generation. However, this constraint limits the flexibility of system configuration, and results in a higher total cost than allowing a uniform monthly co-firing ratio for each generator. Allowing a uniform monthly co-firing ratio for the system results in a cost reduction of $289,140/year, even though the result for R_{month} system can not be claimed to be global optimal. Figure 5.15 shows the monthly consumption of coal (nest), bagasse (ball), switchgrass (dot) and logging residue (solid) for generator 1. The consumption of coal is relatively stable, whereas, consumptions of all other feedstocks fluctuate greatly month by month which may be harmful to system stability.

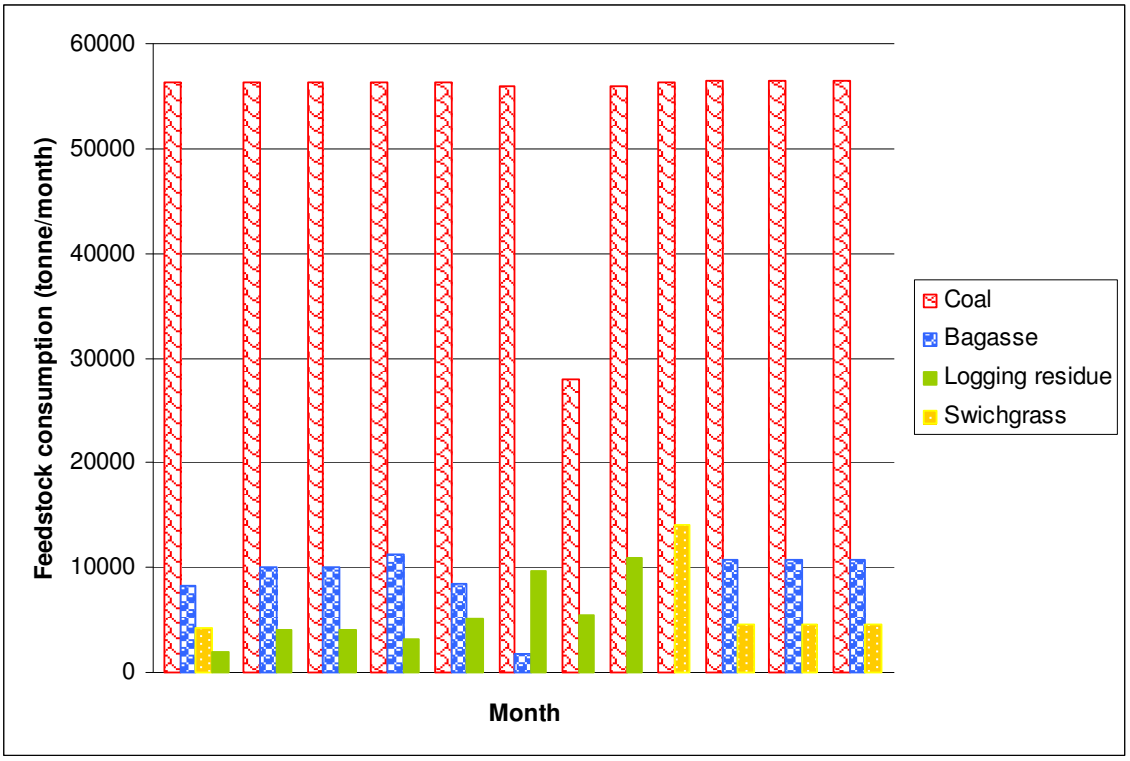

Figure 5.15 Monthly feedstock consumptions for generator 1 with uniform monthly co-firing ratio

5.6. Conclusions

A generic model and approach for synthesizing, analyzing, and optimizing the biomass-to-power system was created. Process synthesis incorporated all major activities and identified alternative operations in the system boundary. Process analysis established the values and constraints for process parameters and variables and determined the correlations of cost and GHG emissions with biomass usage. Process optimization identified the optimal feedstock consumption and allocation, and power plant operation. Mathematic programming models were created as an open framework for biomass-to-energy systems. Global optimal solutions of dual-feedstock co-firing systems were determined using both the global solver of LINGO® and the algebraic method. For the multifeedstock co-firing system, the global optimal solution was derived by LINGO. The optimal feedstock supplies, allocation to different generators, and the optimal generator

maintenance scheduling were identified. This work shows that bagasse and logging residue are more competitive than switchgrass as an alternative energy feedstock to coal. In our case study, no biomass is viable as a replacement for coal as a feedstock unless there is a realized value for the biomass GHG mitigating effect. Uniform monthly co-firing ratio (R_{month}) system results in a cost reduction when comparing with uniform annual co-firing ratio (R_{year}), but the latter is easier to operate.

CHAPTER VI
CONCLUSIONS AND FUTURE WORK

6.1 Conclusions

This work has systematically developed a holistic approach for simultaneous process and molecular (material) design/selection through property integration. For the problem with one dominant property, a new graphical approach for material targeting and substitution has been introduced. Property operators for mixing streams and GCM have been used to consistently represent process sources, sinks, and different functional groups on the same property-based pinch diagram. Representation of the candidate molecules has been obtained by adding up their functional groups represented as property vectors on the pinch diagram. This graphical approach offers a starting point for new methodological approaches such as mathematical programming techniques for designing and optimizing property-oriented processes upon material information and process objectives. This is significant in designing new molecules or selecting existing molecules that are best suited for process utilization. Compared to earlier work, this research provides a simultaneous approach which balances process and molecular needs. To determine specific design realization for material-recovery networks, an implementation approach has been developed. This approach identifies the criteria for feasible implementation networks. Compared to earlier works, this work embeds all possible configurations and gives criteria for generating alternatives.

For systems with multiple properties, a mathematical programming technique has been developed to address the simultaneous process and molecular design. A global solution procedure has been devised. This approach is based on decomposing the problem into a number of interconnected and tractable tasks. Each task is globally solvable.

A particularly important application of the property integration methodology in the selection of biomass feedstocks for energy generation has been explored. The problem entails the screening of different feedstocks including fossil fuel and biomass. A

generic model has been developed to optimize the types and quantities of the feedstocks used to maximize the profit of the power generation industry while complying with the governmental regulations and laws. The devised tool also allows the determination of reasonable GHG discharge permit price. It also determines conditions fro which a certain biomass feedstock becomes economically competitive. For instance, in our case study, when bagasse co-firing with coal at co-firing ratio of 5%, baggase becomes competitive at $4.92/tonne of GHG price; for logging residue and switchgrass at the same co-firing ratio, the GHG prices are $7.84 and $19.39/tonne GHG.

6.2 Future Work

The following topics are recommended for future research:

- The recycle/reuse process network design is based on the condition of steady state. Future work can be extended into dynamic systems.
- The devised approach has focused on continuous processes. There is a need to address batch systems.
- This dissertation has focused on design problems. Future work can simultaneously address design and operation problems.
- The biomass-to-energy system is mainly focused on power generation with direct burning. In the future work, more process operations such as gasification and biological pathway manufacturing process can be incorporated into the system.
- Biomass utilization in this work has been limited to energy generation. In the future, the more general issue of a bioerfinery can be addressed in a systematic manner. A biorefinery may involve multiple pathways to transform biomass into useful products (e.g., power, biofuel, chemicals, additives, etc.).
- Instead of “nominal-case design” adopted in this work, it is recommended that design under uncertainty be considered. The objective is to generalize the techniques developed in this work by accounting for uncertainties in data

(feedstocks, economic, performance, etc.) as well as design and operating parameters.

REFERENCES

Achenie, L.E.K., Gani R., Venkatasubramanian V., 2003. Computer aided molecular design: theory and practice. Vol.12, Elsevier, Amsterdam.

Almato, M., Sanmarti, E., Espuna, A., Puigjaner, L., 1997. Rationalizing the water use in the batch process industry. Computers & Chemical Engineering 21, S971-S976.

Alva-Argeaz, A., Vallianatos, A., Kokossis, A. A., 1999. Multicontaminant transshipment model for mass exchange networks and wastewater minimization problems. Computers & Chemical Engineering 23, 1439-1453.

Aly, S., Abeer, S., Awad, M., (2005). A new systematic approach for water network design. Clean Technology Environmental Policy 7(3), 154-161.

Bagajewicz, M., (2000). A review of recent design procedures for water network in refineries and process plants. Computers and Chemical Engineering 24, 2093-2113

Benko, N., Rev, E., Fonyo, Z., 2000. The use of nonlinear programming to optimal water allocation. Chemical Engineering Communications 178, 67-101.

Buxton, A., Livingston, A.G., Pistikopoulos, E.N., 1999. Optimal design of solvent blends for environmental impact minimization. AIChE Journal 45, 817-843.

Constantinou, L., Gani, R., 1994. New group contribution method for estimating properties of pure compounds. AIChE Journal 40, 1697-1710.

Derringer, G.C., Markham, R.L., 1985. A computer-based methodology for matching polymer structure and required properties. Journal of Applied Polymer Science 30, 4609-4617

Dunn, R. F., Wenzel, H., Overcash, M. R., 2001a. Process integration design methods for water conservation and wastewater reduction in industry: part i design for single contaminants. Clean Products and Processes 3, 307-318.

Dunn, R. F., Wenzel, H., Overcash, M. R., 2001b. Process integration design methods for water conservation and wastewater reduction in industry: part ii design for multiple contaminants. Clean Products and Processes 3, 319-325.

Eden, M. R., Jorgensen, S. B., Gani, R., El-Halwagi, M.M., 2002. Property integration – a new approach for simultaneous solution of process and molecular design problems. Computer Aided Chemical Engineering 10, 79-84.

Eden, M. R., Jørgensen, S. B., Gani, R., El-Halwagi, M. M., 2004. A novel framework for simultaneous separation process and product design. Chemical Engineering and Processing 43(5), 595-608.

United States Department of Energy, Energy Information Administration (USDOE/EIA), 2006. Average price of coal delivered to end use sector by census division and state. http://www.eia.doe.gov/cneaf/coal/page/acr/table34.html accessed 06/15/2006.

El-Halwagi, M. M., 1997. Pollution prevention through process integration. Academic Press, San Diego.

El-Halwagi, M.M., Gabriel, F., Harell, D., 2003. Rigorous graphical targeting for resource conservation via material recycle/reuse networks. Industrial and Chemical Engineering Research 42, 4319-4328.

El-Halwagi, M. M., Glasgow, I. M., Eden, M. R., Qin, X., 2004. Property integration: componentless design techniques and visualization tools. AIChE Journal 50 (8), 1854-1869.

El-Halwagi, M. M., Manousiouthakis, V., 1989. Mass exchanger networks. American Institute of Chemical Engineering Journal 35(8), 1233.

Gani, R., Brignole, E.A., 1983. Molecular design of solvents for liquid extraction based on UNIFAC. Fluid Phase Equilibria 13, 331-340.

Gani, R., Constantinou, L., 1996. Molecular structure based estimation of properties for process design. Fluid Phase Equilibria 116, 75-86.

Gani, R., Pistikopoulos, E., 2002. Property modeling and simulation for product and process design. Fluid Phase Equilibria 194-197, 43-59.

Giovanoglou, A., Barlatier, J., Adjiman, C.S., Pistikopoulos E.N., 2003. Optimal solvent design for batch separation based on economic performance. AIChE Journal 49, 3095-3109.

Horvath, A.L., 1992. Molecular design: chemical structure generation from the properties of pure organic compounds. Elsevier, New York.

Hostrup, M., Harper, P.M., Gani, R., 1999. Design of environmentally benign processes: integration of solvent design and separation process synthesis. Computers and Chemical Engineering 23, 1395-1414.

Hughes, E., 2000. Biomass cofiring: economics, policy and opportunities. Biomass and Bioenergy 19, 457-465.

Jensen, F., 1999. Introduction to computational chemistry. Wiley, New York.

Joback, K.G., Stephanopoulos, G., 1989. Designing molecules possessing desired physical property values. Proceedings of the Third International Conference on Foundations of Computer Aided Design (FOCAPD), Eds. J. J. Siirola, I. E. Grossmann and G. Stephanopoulos, 363-387, CACHE Corp.

Kadam, K. L., 2000. Environmental life cycle implications of using bagasse derived ethanol as a gasoline oxygenate in Mumbai (Bombay). NREL/TP-580-28705.

Karunanithi, A.T, Achenie, L.E.K., Gani, R., 2005. A new decomposition-based computer aided molecular/mixture design methodology for the design of optimal solvents and solvent mixtures. Industrial and Engineering Chemistry Research 44, 4785-4797.

Kazantzi, V., El-Halwagi, M.M., 2005. Targeting material reuse via property integration. Chemical Engineering Progress 101 (8), 28-37.

Kohl, A., Nielsen, R., 1997. Gas purification, 5th edition. Gulf Publishing Co., Houston.

Lehman, A., Maranas, C., 2004. Molecular design using quantum chemical calculations for property estimation. Industrial and Engineering Chemistry Research 43, 3419-3432.

Mann, M. K., Spath, P. L., 2001. A life cycle assessment of biomass cofiring in a coal-fired power plant, Clean Products and Processes 3, 81-91.

Marcoulaki, E.C., Kokossis, A.C., 2000. On the development of novel chemical using a systematic optimization approach. Part II. Solvent design. Chemical Engineering Science 55, 2547-2561.

Marrero, J., Gani, R., 2001. Group-contribution based estimation of pure component properties. Fluid Phase Equilibria 183-184, 183-208.

McCarl B.A., Schneider, U.A., 2001. The cost of greenhouse gas mitigation in u.s. agriculture and forestry. Science 294 , 2481-2482.

Mintzer I., Leonard J.A., Schwartz, P., 2003. U.S. Energy scenarios for the 21st century. Pew Center on Global Climate Change, Arlington, Virginia.

Odele O., Macchietto, S., 1993. Computer-aided molecular design: a novel method for optimal solvent selection. Fluid Phase Equilibria, 82, 47-54.

Pistikopoulos, E.N., Stefanis, S.K., 1998. Optimal solvent design for environmental impact minimization. Computers and Chemical Engineering 22, 717-733.

Plasynski, S. I., Costello, R., Hughes, E., Tillman, D. A., 1999. Biomass cofiring in full-sized coal fired boilers, In : Proceedings of the International Technical Conference on Coal Utilization & Fuel Systems 24, 281-292.

Polley, G. T., Polley, H. L., 2000. Design better water networks. Chemical Engineering Progress 96(2), 47-52.

Pretel, E.J., Lopez, P.A., Bottini, S.B., Brignole, E.A., 1994. Computer-aided molecular design of solvents for separation processes. AIChE Journal 40, 1349-1360.

Qin, X., Gabriel, F., Harell, D., El-Halwagi, M.M., 2004. Algebraic techniques for property integration via componentless design. Industrial and Engineering Chemistry Research 43, 3792-3798.

Qin, X., Mohan, T., El-Halwagi, M.M., Cornforth G., McCarl, B., 2006. Switchgrass as an alternate feedstock for power generation: integrated environmental, energy, and economic life-cycle assessment. Clean Technology and Environment Policy, in press.

Sahinidis, N.V., Tawarmalani, M., Yu, M., 2003. Design of alternative refrigerants via global optimization. AIChE Journal 49, 1761-1775.

Sami, M., Annamalai, K., Wooldrige, M., 2001. Co-firing coal and biomass fuel blends. Progress in Energy and Combustion Science 27, 171-214.

Savelski, M. J., Bagajewicz, M. J., 2000. On the optimality conditions of water utilization systems in process plants with single contaminants. Chemical Engineering Science 55, 5035-5048.

Shelley, M. D., El-Halwagi, M.M., 2000. Componentless design of recovery and allocation systems: a functionality-based clustering approach. Computers and Chemical Engineering 24, 2081-2091.

Sorin M., Bédard, S., 1999. The global pinch point in water reuses networks. Trans. IChemE (Part B). 77, 305–308

Tillman, D. A., 2000. Biomass cofiring: the technology, the experence, the combustion consequences. Biomass & Bioenergy 19, 365-384.

United States Department of Agriculture (USDA), 2004. Turning logging residues into marketable wood products. http://www.na.fs.fed.us/ss/03/ea_logresidue.pdf accessed June 19, 2006. Washington, DC.

United States Department of Agriculture (USDA), 2005. Forest residue trucking model v.4. http://www.srs.fs.usda.gov/forestops/downloads/FoRTSv4.xls accessed June 19, 2006. Washington, DC.

United States Department of Energy, Energy Efficiency and Renewable Energy (USDOE/EERE), Electric Power Research Institute (EPRI), 1997. Renewable energy technology characterizations. TR-109496. Washington, DC.

United States Environmental Protection Agency (USEPA), 2006. Inventory of U.S. greenhouse gas emissions and sinks:1990-2004. Washington, DC.

Vaidyanathan, R., El-Halwagi, M.M., 1994. Compouter-aided design of high performance polymers. Journal of Elastomers and Plastics 26, 277-293.

Vaidyanathan, R., El-Halwagi, M.M., 1996. Compouter-aided synthesis of polymers and blends with target properties. Industrial and Engineering Chemistry Research 35, 627-634.

Venkatasubramanian, V., Chan, K., Caruthers, J.M., 1994. Computer-aided molecular design using genetic algorithms. Computers and Chemical Engineering 18, 833-844.

Wang, Y. P., and Smith, R., 1994. Wastewater minimization. Chemical Engineering Science 49 (7), 981

Wang, Y. P., Smith, R., 1995. Time pinch analysis. IChemE 73, 905-914

Watson, R. T., Albritton, D. L., 2002. Climate Change 2001: Synthesis report, summary for policymakers (Third IPCC assessment report), an assessment of the intergovernmental panel on climate change. Cambridge University Press, Cambridge, United Kingdom.

Winters, T., 2002. Clear skies initiative: new beginning or bait and switch. The Electricity Journal 15(6), 56-66.

Zhou, Q., Lou, H. H., Huang, Y. L., 2001. Design of a switchable water allocation network based on process dynamics. Industrial & Engineering Chemistry Research 40 (22), 4866-4873.

APPENDIX A

PROCESS TARGETING TO IDENTIFY THE QBFR LINGO CODE

```
model:
max=hvf; ! Maximize the value of heat vaporization of fresh source;
sets:
solvent/1,2,3,4/:Hv,F; !1 MDEA, 2 MEA, 3 DEA 4 DGA, F Source flowrate;
unit/1,2,3,4,5/:HVl, !Lower bound of Hv;
            Hvu, !Upper bound of Hv;
            G; ! Sink flowrate;
allocation(solvent,unit):x;
allocationf(unit):xf; ! For fresh;
endsets

Fr=720; !Fresh solvent usage;
! Property constraints for each operating unit;
@for(unit(j):@sum(solvent(i):x(i,j)*F(i)*Hv(i))+Hvf*xf(j)*Fr<=Hvu(j)*G(
j));
@for(unit(j):@sum(solvent(i):x(i,j)*F(i)*Hv(i))+Hvf*xf(j)*Fr>=Hvl(j)*G(
j));
! Flowrate balance for the sources and units;
@for(unit(j):@sum(solvent(i):x(i,j)*F(i))+xf(j)*Fr=G(j));
@for(solvent(i):@sum(unit(j):x(i,j)*F(i))=Us(i));
! Physical constraints;
@for(solvent(i):@sum(unit(j):x(i,j))<=1); ! This is for the solvent;
@for(allocation(i,j):x(i,j)<=1);
@for(allocation(i,j):x(i,j)>=0);
@sum(allocationf(j):xf(j))=1; ! This is for the fresh;
@for(allocationf(j):xf(j)<=1);
@for(allocationf(j):xf(j)>=0);

data:
Hv=95,64,85,82;
F=60,90,70,60;
Hvl=67.5,67.5,70,70,72.5;
Hvu=80,82.5,82.5,85,85;
G=200,210,230,190,170;
enddata
```

APPENDIX B
MOLECULAR DESIGN TO IDENTIFY FEASIBLE MOLECULES
LINGO CODE

```
DATA:
N=20; ! A large number to remove the group number constraint;
enddata

sets:
group /1..16/:covalence,Hv,Tc,Hfus,Tm,Tb;
position /1..N/;
pair (group,position):y;
ndgroup/1..9/:Hv2, Tc2,Hfus2,Tm2,Tb2,N2; ! Second order groups;
rdgroup/1..4/:Hv3,Tc3,Hfus3,Tm3,Tb3,N3; ! Third order groups;
endsets

@for(group(g):@for(position(l):@bin(y(g,l)))); ! Y(g,l) is g group in l position (in finding the feasible group set section, the position is not the rigorous molecule structure position;)

@for( ndgroup(s):@Gin(N2(s)));
@for( rdgroup(t)|R#GE# 2:@Bin(N3(t)));
@Gin(N3(1)); ! For N^{1,4}≥3, and N^{1,4}≥ 2 case, use @Gin(N3(t))only;

@For(position(l):@sum(group(g):y(g,l))=1); ! For every position, there is no more than one group;

@sum(position(l):@sum(group(g):y(g,l)*(2-covalence(g))))=2; ! Octet rule for acyclic molecule;

! Certain groups must have some occurrence in the molecule;
@sum(position(l):y(8,l))+@sum(position(l):y(9,l))+@sum(position(l):y(10
,l))+@sum(position(l):y(11,l))+@sum(position(l):y(12,l))=1; !For amino groups;

@sum(position(l):y(4,l)+y(15,l))=2; ! For group OH; for N^{1,4}≥ 2 case, use >=2; for N^{1,4}≥3 case, use >=3;

! Constraints from 2ndgroup;
@sum(position(l):y(1,l))>=2*N2(1)+3*N2(2); ! For 2ndgroup 21-22, CH3;
@sum(position(l):y(1,l))>=N2(1)+1.05*N2(3); ! For the worst case -CH(CH3)-CH(CH3)-CH(CH3)-CH(CH3)-... for N2(3);
@sum(position(l):y(1,l))>=3*N2(2)+1.05*N2(3); ! For the reason same as above;
@sum(position(l):y(1,l))>=N2(1)+1.75*N2(4); ! If there is only one N2(4), we have @sum(position(l):y(1,l))>=N2(1)+3*N2(4); Instead, to be a little bit conservative, we consider there may exist a worst case with three N2(4)connected consecutively, i.e.CH3-CH(CH3)C(CH3)2-CH(CH3)C(CH3)2-CH(CH3)C(CH3)2-none carbon;
@sum(position(l):y(1,l))>=2*N2(1)+2.4*N2(5); ! If there is only one N2(5), we have @sum(position(l):y(1,l))>=2*N2(1)+4*N2(5);!Instead, we consider there may exist some worst case with
```

three N2(4)connected consecutively, i.e.-C(CH3)2C(CH3)2-C(CH3)2C(CH3)2-C(CH3)2C(CH3)2-none carbon;

```
@sum(position(l):y(3,l)+y(7,l)+y(9,l)+y(12,l))>=N2(1)+N2(6);
```
! For 2ndgroup 21,26, CH;

```
@sum(position(l):y(13,l)+y(14,l))>=N2(2)+N2(7);
```
!For 2ndgroup 22,27, C;

```
@sum(position(l):y(3,l)+y(7,l)+y(9,l)+y(12,l))>=1.01*N2(3);
```
! For 2ngroup 21, CH;!for reason same as above;

```
@sum(position(l):y(13,l)+y(14,l))>=0.6*N2(4);
```
! For 2ndgroup 24, C;

```
@sum(position(l):y(3,l)+y(7,l)+y(9,l)+y(12,l))>=0.6*N2(4);
```
! For 2ndgroup 21, CH;

```
@sum(position(l):y(13,l)+y(14,l))>=1.2*N2(5);
```
! For 2ndgroup 25, C;

```
@sum(position(l):y(4,l))>=N2(6);
```
! For 2ndgroup 26, OH;

```
@sum(position(l):y(4,l))>=N2(7);
```
! For 2ndgroup 27, OH;

```
@sum(position(l):y(4,l))>=2*N2(8);
```
*! For ndgroup 28, OH; @bin(N2(8)); ! for $N^{l,4}\geq 3$, and $N^{l,4}\geq$ 2 case, use @sum(position(l):y(4,l))>=1.1*N2(8) in case of special case CH(OH)CH(OH)CH(OH)...;*

```
@sum(position(l):y(4,l))>=N2(9);
```
! N2(9)<=2; for2 ndgroup 29,OH and N;

! Constraints for 3rdgroup;

```
@sum(position(l):y(4,l))>=2*N3(2);
```
*! For 3rdgroup 32, OH; for $N^{l,4}\geq 3$, and $N^{l,4}\geq$ 2 case, the constraints become insignificant, i.e.>=C_n^2*N3(2);*

```
@sum(position(l):y(6,l)+y(7,l)+y(14,l)+y(15,l))>=N3(3);
```
! For rdgroup 33, O;

```
@sum(position(l):y(4,l))>=2*N3(4);
```
*!For 3rdgroup 34, OH; for $N^{l,4}\geq 3$, and $N^{l,4}\geq$ 2 case, the constraints become insignificant >=C_n^2*N3(2);*

!constraint for some group can not coexist;

```
0.5*N2(6)+N2(8)<=1;
```
! For OH; for $N^{l,4}\geq 3$, and $N^{l,4}\geq$ 2 case, it dosen't valid;

```
0.5*N2(7)+N2(8)<=1;
```
! For OH; $N^{l,4}\geq 3$, and $N^{l,4}\geq$ 2 case, it doesn't valid;

```
N2(8)+N3(2)+N3(3)+N3(4)<=1;
```
! For OH; for $N^{l,4}\geq 3$, and $N^{l,4}\geq$ 2 case, it doesn't valid

```
N2(8)+N2(9)<=2;
```
! For OH and N; for $N^{l,4}\geq 3$, and $N^{l,4}\geq$ 2 case, it doesn't valid

```
2*N2(8)+@sum(position(l):y(15,l))<=2;
```
! For N2(8) and Y(15,l) can not coexist; $N^{l,4}\geq 3$, and $N^{l,4}\geq$ 2 case, it doesn't valid;

! Constraints for Hv;

```
Hv_molecule=@sum(position(l):@sum(group(g):y(g,l)*Hv(g)))+@sum(ndgroup(
s):Hv2(s)*N2(s))+@sum(rdgroup(t):Hv3(t)*N3(t));

@sum(position(l):@sum(group(g):y(g,l)*Hv(g)))+@sum(ndgroup(s):Hv2(s)*N2
(s))+@sum(rdgroup(t):Hv3(t)*N3(t))<=72.392;
@sum(position(l):@sum(group(g):y(g,l)*Hv(g)))+@sum(ndgroup(s):Hv2(s)*N2
(s))+@sum(rdgroup(t):Hv3(t)*N3(t))>=53.642;
```

! Constraints for Tc;

```
Tc_molecule=@sum(position(l):@sum(group(g):y(g,l)*Tc(g)))+@sum(ndgroup(
s):Tc2(s)*N2(s))+@sum(rdgroup(t):Tc3(t)*N3(t));

@sum(position(l):@sum(group(g):y(g,l)*Tc(g)))+@sum(ndgroup(s):Tc2(s)*N2
(s))+@sum(rdgroup(t):Tc3(t)*N3(t))<=22.16;
@sum(position(l):@sum(group(g):y(g,l)*Tc(g)))+@sum(ndgroup(s):Tc2(s)*N2
(s))+@sum(rdgroup(t):Tc3(t)*N3(t))>=19.88;
```

! Constraints for Hfus;

```
Hfus_molecule=@sum(position(l):@sum(group(g):y(g,l)*Hfus(g)))+@sum(ndgr
oup(s):Hfus2(s)*N2(s))+@sum(rdgroup(t):Hfus3(r)*N3(t));

@sum(position(l):@sum(group(g):y(g,l)*Hfus(g)))+@sum(ndgroup(s):Hfus2(s
)*N2(s))+@sum(rdgroup(t):Hfus3(t)*N3(t))<=22.006;
@sum(position(l):@sum(group(g):y(g,l)*Hfus(g)))+@sum(ndgroup(s):Hfus2(s
)*N2(s))+@sum(rdgroup(t):Hfus3(t)*N3(t))>=16.52;
```

! Constraints for Tm;

```
Tm_molecule=@sum(position(l):@sum(group(g):y(g,l)*Tm(g)))+@sum(ndgroup(
s):Tm2(s)*N2(s))+@sum(rdgroup(t):Tm3(t)*N3(t));
@sum(position(l):@sum(group(g):y(g,l)*Tm(g)))+@sum(ndgroup(s):Tm2(s)*N2
(s))+@sum(rdgroup(t):Tm3(t)*N3(t))<=7.3;
```

! Constraints for Tb;

```
Tb_molecule=@sum(position(l):@sum(group(g):y(g,l)*Tb(g)))+@sum(ndgroup(
s):Tb2(s)*N2(s))+@sum(rdgroup(t):Tb3(t)*N3(t));
@sum(position(l):@sum(group(g):y(g,l)*Tb(g)))+@sum(ndgroup(s):Tb2(s)*N2
(s))+@sum(rdgroup(t):Tb3(t)*N3(t))>=8.64;
```

```
DATA:
covalence=1,2,3,1,1,2,3,1,2,1,2,3,4,4,1,2;
Tm=0.6953,  0.2515,  -0.3730,  2.7888,  1.3643,  0.8733,  0.2461,  3.2742,
30.8394, 2.4034, 1.7746, 1.7577, 0.0256, -0.4446, 2.3651, 0;
Tb=0.8491,  0.7141,  0.2925,  2.5670,  1.7703,  1.3368,  0.8924,  2.7987,
2.0948,  2.2514, 1.8750, 1.2317, -0.0671, 0.4983, 4.8721, 0;
Tc=1.7506,  1.3327,  0.5960,  5.2188,  3.4393,  2.4217,  0.7889,  8.1745,
4.2847, 4.5529, 3.2422, 2.0057, 0.0306, 0.2511, 10.4579,0;
Hv=0.217,  4.91,  7.962,  24.241,  5.783,  9.997,  14.62,  15.432,  16.048,
11.831, 13.067, 14.048, 10.73, 13.85, 31.493, 0;
Hfus=1.66,  2.639,  0.134,  4.786,  5.089,  4.891,  4.766,  13.482,  6.283,
4.490, 7.711,   2.561, -1.232,  2.458,   8.454, 0;
Tm2=0.1175, -0.1214, 0.2390, -0.3276, 3.3297, -0.3489, 0.3695,
-0.0414, -0.5941;
Tb2=-0.0035,  0.0072,  0.316,  0.3976,  0.4487,  -0.2825,  -0.5325,  0.8854,
0.5082;
Tc2=-0.0471, -0.1778, 0.5602, 0.8994, 1.5535, -0.6768, -1.5224, 1.9395,
1.2342;
Hv2=-0.399, -0.417, 0.532, 0.623, 5.086, -0.206, -1.579,
-6.611, 0;
Hfus2=0.396, 0.554, -1.766, 0.351, -1.089, -0.599, -0.459,
-0.306, -0.041;
Tm3= 0.7732, 0.6674, -0.1073, -0.0781;
Tb3= 1.075, 0.7193, 1.1867, 0.2991;
Tc3= 0.495, 0.1725, 6.6872, 0;
Hv3= 4.171, 5.411, -8.651, 1.753;
Hfus3=-4.840, -0.272, 1.661, 0.301;
Enddata
```

APPENDIX C

PROCESS DESIGN LINGO CODE

```
model:
sets:
solvent/1,2,3,4/:Hv,Tc,Hfus,F; ! 1 MDEA, 2 MEA, 3 DEA 4 DGA;
unit/1,2,3,4,5/:HVl,Tcl,Hfusl, ! Lower bound;
            Hvu,Tcu,Hfusu, ! Up bound;
            G; ! Demand flowrate;
allocation(solvent,unit):x; ! Allocation fraction of process source m to sink n;
allocationf(unit):xf; ! Allocation fraction of fresh (new molecule) to sink n;
endsets
! Properties of molecule to check;
Tmf=292.9201;
Tbf=518.0995;
Tcf=698.8097;
Hvf=79.76;
Hfusf=18.563;
Fr=720;

! Property constraints for each operating unit;
! Hv constraints for each unit;
@for(unit(j):@sum(solvent(i):x(i,j)*F(i)*Hv(i))+Hvf*xf(j)*Fr<=Hvu(j)*G(
j));
@for(unit(j):@sum(solvent(i):x(i,j)*F(i)*Hv(i))+Hvf*xf(j)*Fr>=Hvl(j)*G(
j));
! Tc constraints for each unit;
@for(unit(j):@sum(solvent(i):x(i,j)*F(i)*Tc(i))+Tcf*xf(j)*Fr<=Tcu(j)*G(
j));
@for(unit(j):@sum(solvent(i):x(i,j)*F(i)*Tc(i))+Tcf*xf(j)*Fr>=Tcl(j)*G(
j));
! Hfus constraints for each unit;
@for(unit(j):@sum(solvent(i):x(i,j)*F(i)*Hfus(i))+Hfusf*xf(j)*Fr<=Hfusu
(j)*G(j));
@for(unit(j):@sum(solvent(i):x(i,j)*F(i)*Hfus(i))+Hfusf*xf(j)*Fr>=Hfusl
(j)*G(j));!
Tmf<=293;
Tbf>=480;
! Flowrate balance for the sources and units;
@for(unit(j):@sum(solvent(i):x(i,j)*F(i))+xf(j)*Fr=G(j)); ! This is equivalent
to n equations;

! Physical constraints;
@for(solvent(i):@sum(unit(j):x(i,j))<=1); ! This is for the solvent;
@for(allocation(i,j):x(i,j)<=1);
@for(allocation(i,j):x(i,j)>=0);
@sum(allocationf(j):xf(j))=1; ! This is for the fresh;
@for(allocationf(j):xf(j)<=1);
@for(allocationf(j):xf(j)>=0);
```

```
@for  (used_solvent_unit(i,j):x(i,j)*F(i)=f(i,j));  ! Calculate the flowrate allocation of process source i to sink j;
@for  (unit(j):Fr*xf(j)=ffresh(j)); ! Calculate the flowrate allocation of fresh (new molecule) to sink j;

data:
Hv=95,64,85,82;
Tc=678,670,715,699;
Hfus=23,18.4,22.1,21.7;
F=60,90,70,60;
Hvl=67.5,67.5,70,70,72.5;
Hvu=80,82.5,82.5,85,85;
Tcl=685,690,690,695,695;
Tcu=705,705,710,710,715;
Hfusu=19,19.5,19.5,20,20;
Hfusl=15,15,16,16,17;
G=200,210,230,190,170;
enddata
```

APPENDIX D

OPTIMIZATION OF BIOMASS-TO-ENERGY SYSTEM LINGO CODE

```
model:
sets:
generator/gen1,gen2,gen3/:capacity,efficiency,efficiency_coal,R_cofirin
g,R_th_cofiring,cost_modification;! i for generator;
month/jan..dec/;!j for month;
feedstock/coal,bagasse,sw,wood/:HHV,
cost,GHG,GHG_year,cost_GHG_year,m_year,cost_year,cost_storage_feedstock
,cost_year_storage_feedstock; !k for feedstock, m_year is yearly
feedstock demand in tonne;
genfeed(generator,feedstock):m;!m is the monthly feedstock demand;
genmon(generator, month):Y;!Y is a binary varialbe for maintenance;
monfeed(month,feedstock):Residual_mon,supply_mon,demand_mon,storage_mon
,cost_mon_storage;
endsets



data:
capacity=200000,150000,100000;!in KW;
efficiency_coal=0.3413,0.3413,0.3413;
HHV=23552120,14141790,15991000,20307340;!in kJ/tonne;
cost_storage_feedstock=0,1,1,1;!in $/tonne/month;
enddata
@for(feedstock(k):@free(GHG));
@for(feedstock(k):@free(GHG_year));
@for(feedstock(k):@free(cost_GHG_year));
!@free(GHG_price);
@free(total_GHG_year_cost);

!coal;
cost(1)=30.10;!in $/tonne coal;
GHG(1)=2225.5471;! in CO2-Eq kg/tonne coal (LCA of GHG emission exclude
post combustion control and ash transport);
!HHV_coal=23552.12;!in kJ/kg coal;

!Bagasse
cost(2)=20;!in $/tonne bagasse;
GHG(2)=-107.4106;!net GHG emission kg co2/tonne bagasse;
!HHV_bagasse=14141.79; !in kJ/kg bagasse;
@for(month(j)|j#LE#5 #or# j#GE#10:supply_mon(j,2)=21649);!in
tonne/month bagasse;
@for(month(j)|j#GT#5 #and# j#LT#10:supply_mon(j,2)=0);! from june to
sep no bagasse supply;


!switchgrass;
```

```
!HHV_sw=15991;!kJ/kg sw;
Y_sw=5806;!yield of sw in tonne/mile2;
L_sw_highway=15;!in miles;
L_in_land^2-m_year(3)/Y_sw<=0;!1-way in miles,m_sw is the yearly demand
for power generation;
L_in_land^2-m_year(3)/Y_sw>=0;! convexiation for nolinear function;
cost(3)=0.7353*L_in_land+0.2206*L_sw_highway+32.49;! in $/tonne
switchgrass;
GHG(3)=1.0346*L_in_land+0.3104*L_sw_highway+4.2923;! GHG effect before
sw combustion in kg CO2-Eq/tonne;
supply_mon(9,3)=m_year(3);!all sw were harvest in sep;
@for(month(j)|j#NE#9:supply_mon(j,3)=0);!monthes other than sep no
harvest;

!Logging residue, Data based on 7.3% moisture in green (as received);
!HHV_wood=20307.34;! in kJ/kg;
M_wood_max=108540;!in tonne/year;
Y_wood=4341.6;!in tonne/mile2;
m_wood_load=3.96;!in tonne;
L_wood_highway=47.50;!in mile;
L_in_wood^2-m_year(4)/Y_wood<=0;!1-way in miles,m_year(wood)in tonne is
the yearly demand for power generation;
L_in_wood^2-m_year(4)/Y_wood>=0;!convexiation for nolinear function;
price_log=3.066; !in $/tonne;
cost(4)=5.337*L_in_wood+0.225*L_wood_highway+6.88+price_log;! in
$/tonne logging residue;
GHG(4)=13.446*L_in_wood+0.586*L_wood_highway-1237.9806;!net GHG
emission after combustion, in kg co2-Eq /tonne logging residue
including avoid CO2 emission;
!!GHG(4)=-1100;
@for(month(j):supply_mon(j,4)<=M_wood_max/12);!monthly supply of wood
can not exceed the collection speed;
!m_year(4)=@sum(month(j):supply_mon(j,4));!yearly demand of wood is the
sumation of month supply;



!combustion and power generation;
@for(genmon(i,j): @bin(Y(i,j)));
@sum(month(j):Y(1,j))=1;
@sum(month(j):Y(2,j))=1;
@sum(month(j):Y(3,j))=1;
@for(month(j):@sum(genmon(i,j):Y(i,j))<=1);

@for(genmon(i,j):capacity(i)*(30-
y(i,j)*15)*24*3600=efficiency(i)*@sum(feedstock(k):HHV(k)*m(i,k)*(1-
0.5*Y(i,j))));!1kwh=3600kJ, energy balance in month j;
@for(generator(i):efficiency(i)=efficiency_coal(i)/0.86*(0.860044-
0.45*R_cofiring(i)^2-0.0005*R_cofiring(i)));!get the monthly thermal
efficiency;
@for(generator(i):R_cofiring(i)*@sum(feedstock(k):m(i,k))=@sum(feedstoc
k(k)|k#GE#2:m(i,k)));!get the monthly cofiring ratio;
!@for(genmon(i,j):R_cofiring=0.06);! to get maximal cofiring ratio
during a year;
```

```
!maximum thermal input;
@for(generator(i):R_th_cofiring(i)*@sum(feedstock(k):HHv(k)*m(i,k))=@su
m(feedstock(k)|k#GE#2:HHV(k)*m(i,k)));!get the thermal cofiring ration
of generator i in month j;
@for(generator(i):cost_modification(i)=capacity(i)*R_th_cofiring(i)*200
/10);!the modification cost of each generator in ten year linear
depriciation with 0 salvage;
total_cost_modification=@sum(generator(i):cost_modification(i));!total
yearly modification cost;


!link the yearly demand to monthly consumption;
@for(feedstock(k):m_year(k)=11.5*@sum(generator(i):m(i,k)));!yearly
demand of feedstock k;
@for(monfeed(j,k):demand_mon(j,k)=@sum(generator(i):m(i,k)*(1-
y(i,j)*0.5)));!in month j, demand of k ;
@for(monfeed(j,k)|k#GE#2:residual_mon(j,k)=supply_mon(j,k)-
demand_mon(j,k)+residual_mon(@wrap(j-1,12),k));!in month j, the
residual of feedstock 2 sw;
!residual_mon(12,2)=0;
@for(month(j):residual_mon(j,1)=0);! no storage for coal;
@for(monfeed(j,k):storage_mon(j,k)=residual_mon(j,k));! in month j, the
storage,i.e.residual of k in tonne;

!storage cost;
@for(monfeed(j,k):cost_mon_storage(j,k)=storage_mon(j,k)*cost_storage_f
eedstock(k));!in month j, the storage cost of k in $;
@for(feedstock(k):cost_year_storage_feedstock(k)=@sum(monfeed(j,k):cost
_mon_storage(j,k)));!the storage cost of k in a year;
total_cost_year_storage=@sum(feedstock(k):cost_year_storage_feedstock(k
));!the storage cost of all feedstocks in a year;


!cost of GHG;
GHG_price=0.03;! in $/kg;
@for(feedstock(k):GHG_year(k)=GHG(k)*m_year(k));! yearly GHG emission
from burning feedstock k;
@for(feedstock(k):cost_GHG_year(k)=GHG_price*GHG_year(k));!yearly GHG
cost for feedstock k;
Total_cost_year_GHG=@sum(feedstock(k):cost_GHG_year(k));! yearly GHG
cost of all feedstocks;

!link cost to feedstock demand;
@for(feedstock(k): cost_year(k)=m_year(k)*cost(k));!yearly cost of
feedstock k;
total_cost_year_feedstock=@sum(feedstock(k):cost_year(k)); !total
yearly cost of all feedstocks;

!total_cost_year_feedstock+Total_cost_year_GHG+total_cost_year_storage+
total_cost_modification=50225390.00+3705082000.00*GHG_price;
```

```
min=total_cost_year_feedstock+Total_cost_year_GHG+total_cost_year_stora
ge+total_cost_modification;

!max=cost(2);
!min=GHG_price;

end
```

VITA

Xiaoyun Qin is the second son of Jinfu Qin and Xuezhu Xiao. He received his B.S. degree in chemical engineering from Nanjing University of Science and Technology in July 1989. He received his M.S. degree in chemical engineering from the Chinese Academy of Forestry Science in August 1994. He worked at the Nanjing Printing Ink General Factory from July 1989 to July 1991. He worked in the Jiangsu Province Department of Petrochemical Industry from August 1994 to December 2001. During this period, he acted as manager of second division of Jiangsu Petrochemical International Exchange and Cooperation Center and vice director of the center for many years. He was at Auburn University as a Research Scholar from December 2001 to July 2002 and at Texas A&M University as a Research Associate from July 2002 to August 2004. He entered the Ph.D. program in chemical engineering at Texas A&M University in August 2004 and received his Ph.D. Degree in December 2006. He has published more than ten papers and made many professional talks. He is a licensed International Business Engineer.

Mr. Qin may be reached at:
Xiaoyun Qin
3122 TAMU
College Station, TX 77843-3122